The molecular origins of life

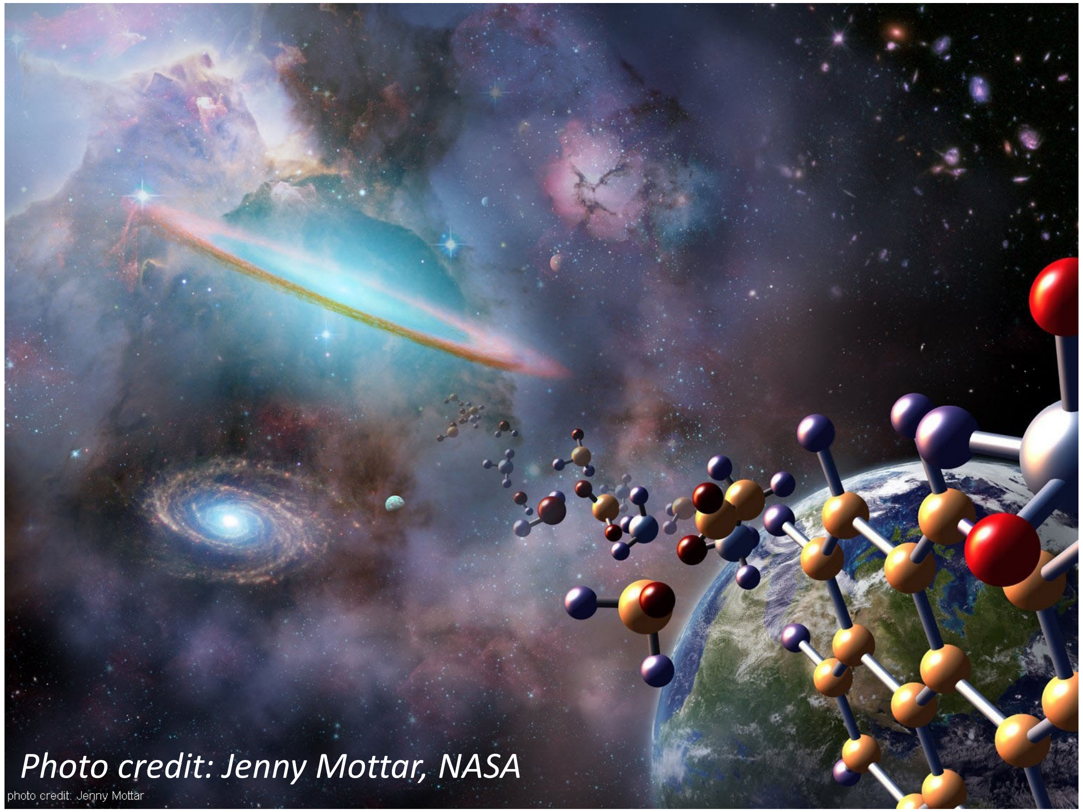

Photo credit: Jenny Mottar, NASA

L3 SoSe 2020

Zbigniew Pianowski

Overview of the course

Origin of the Universe – stars, planets, elements

Origin of biorelevant monomers – primordial soup

Complex chemical processes on the way to living systems

Protocells and LUCA

Basic classes of biomolecules

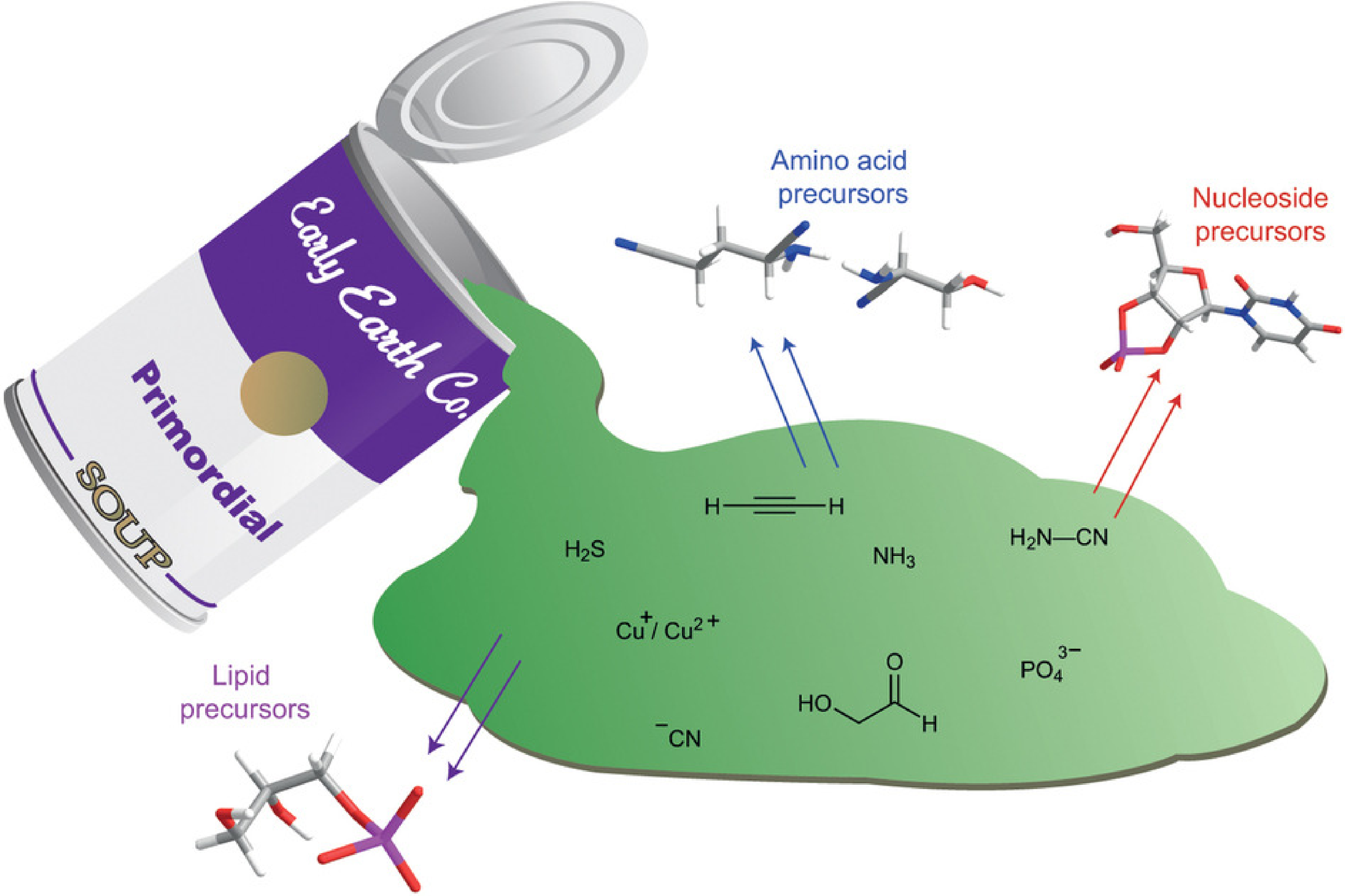

- Aminoacids
- **Lipids**
- **Carbohydrates (sugars)**
- Nucleobase
- Nucleosides (sugar+nucleobase)

Abiotic synthesis of aminoacids

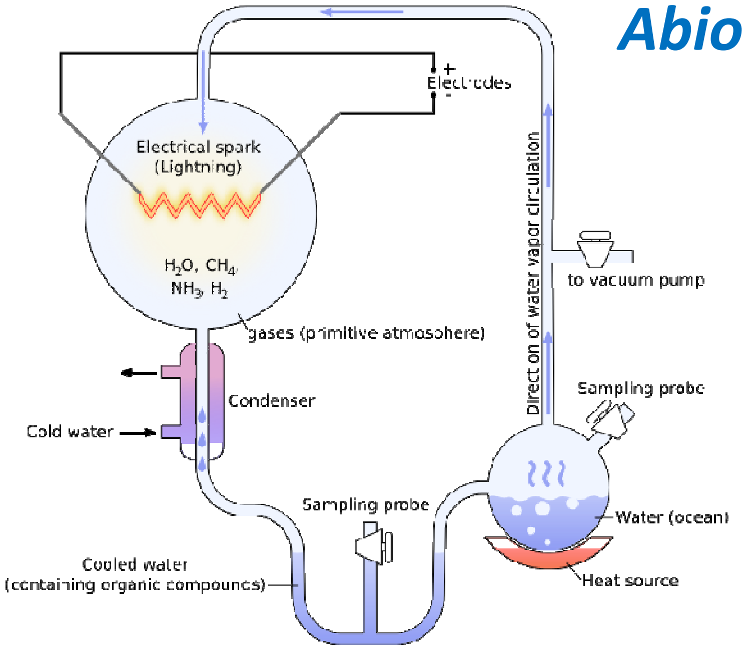

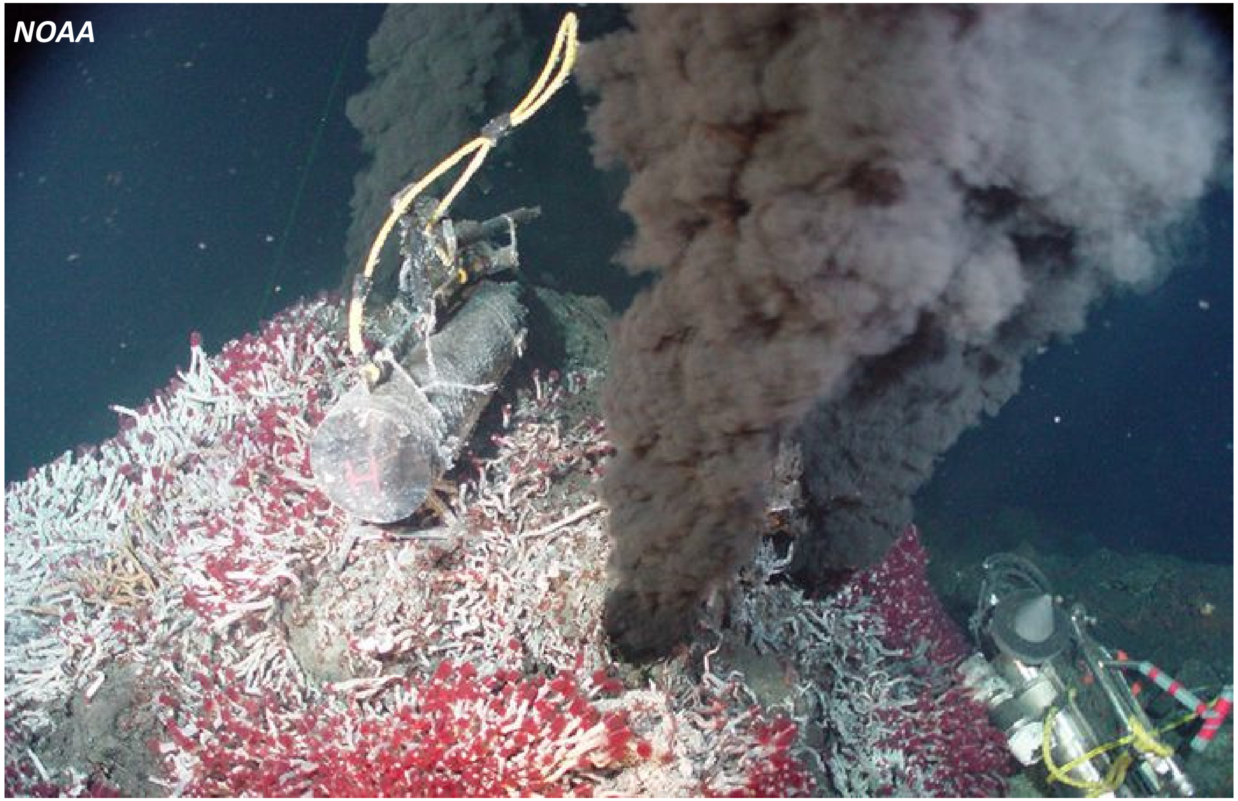

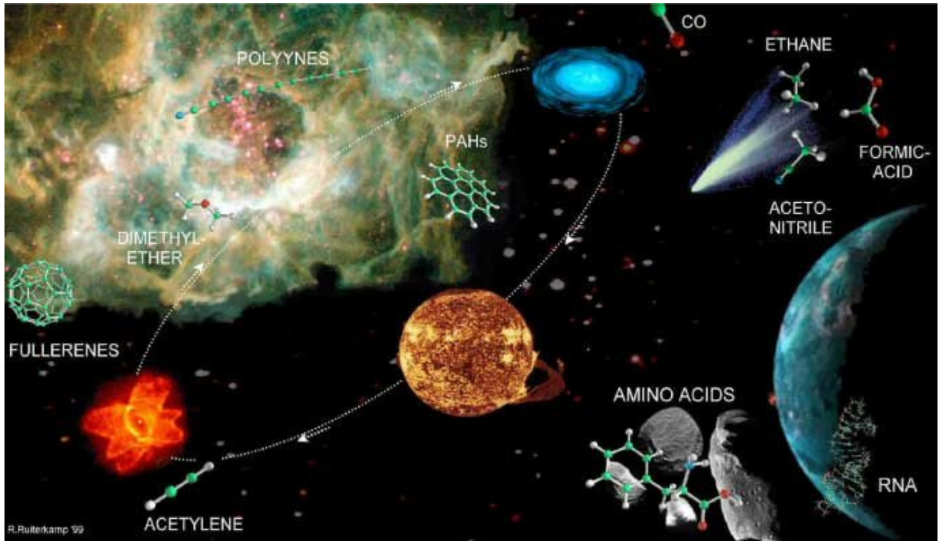

Murchison meteorite
chondrite

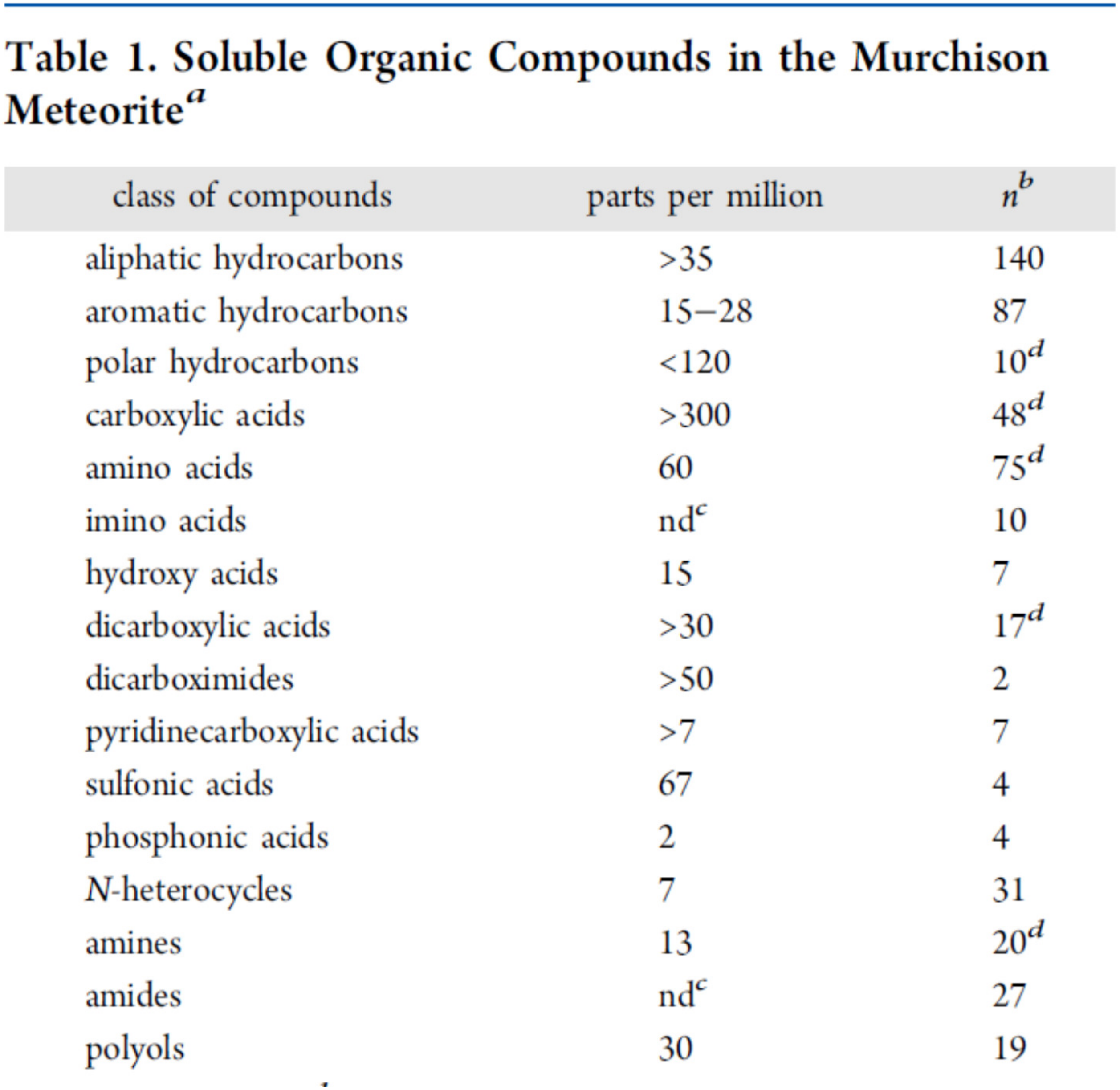

Table 1. Soluble Organic Compounds in the Murchison Meteorite[a]

class of compounds	parts per million	n[b]
aliphatic hydrocarbons	>35	140
aromatic hydrocarbons	15–28	87
polar hydrocarbons	<120	10[d]
carboxylic acids	>300	48[d]
amino acids	60	75[d]
imino acids	nd[c]	10
hydroxy acids	15	7
dicarboxylic acids	>30	17[d]
dicarboximides	>50	2
pyridinecarboxylic acids	>7	7
sulfonic acids	67	4
phosphonic acids	2	4
N-heterocycles	7	31
amines	13	20[d]
amides	nd[c]	27
polyols	30	19

The origins of homochirality

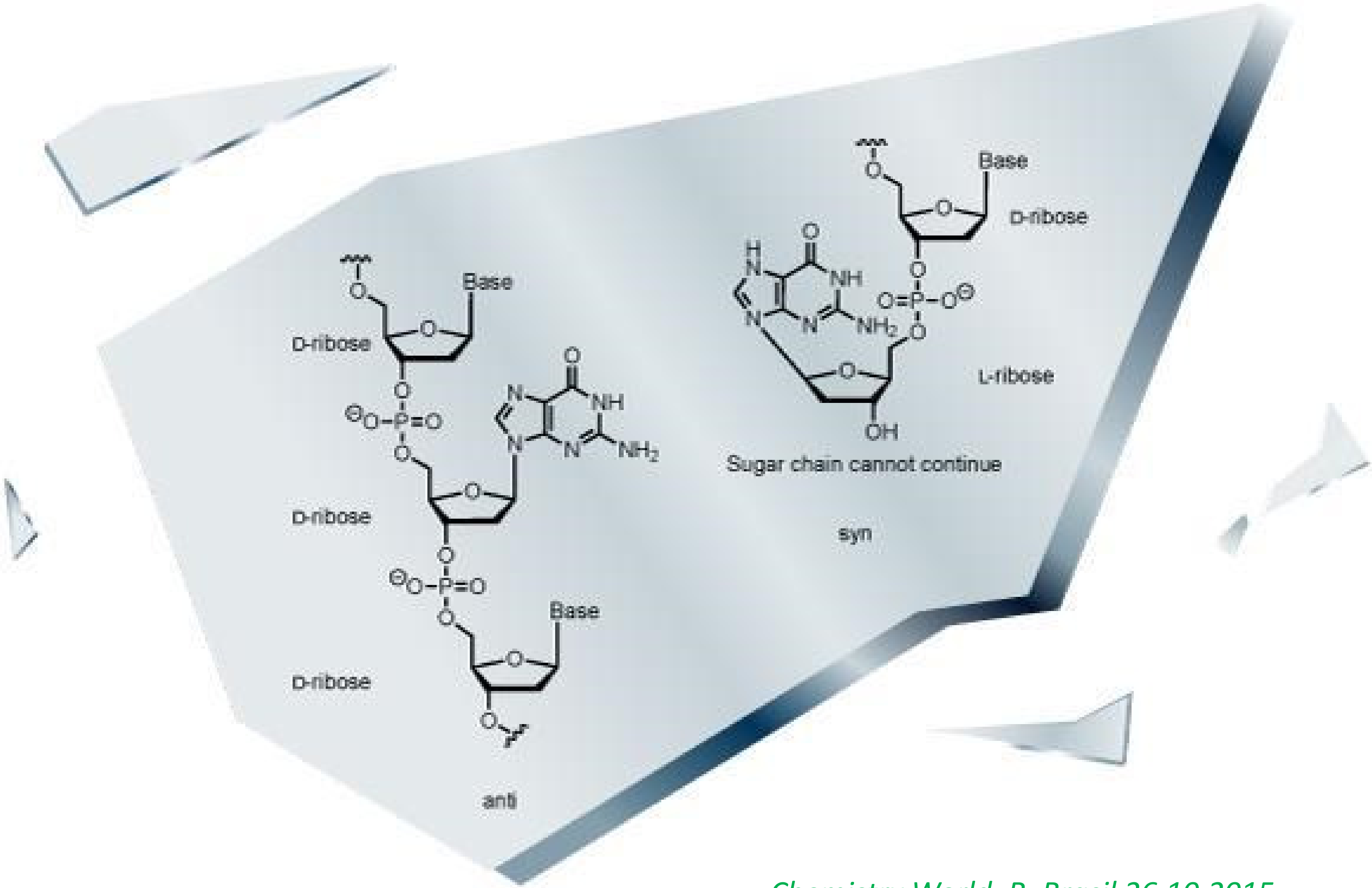

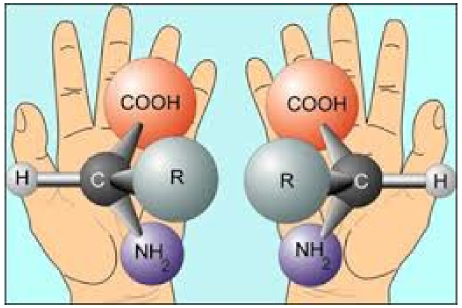

Chemistry World, R. Brasil 26.10.2015

Condensation of aminoacids into peptides

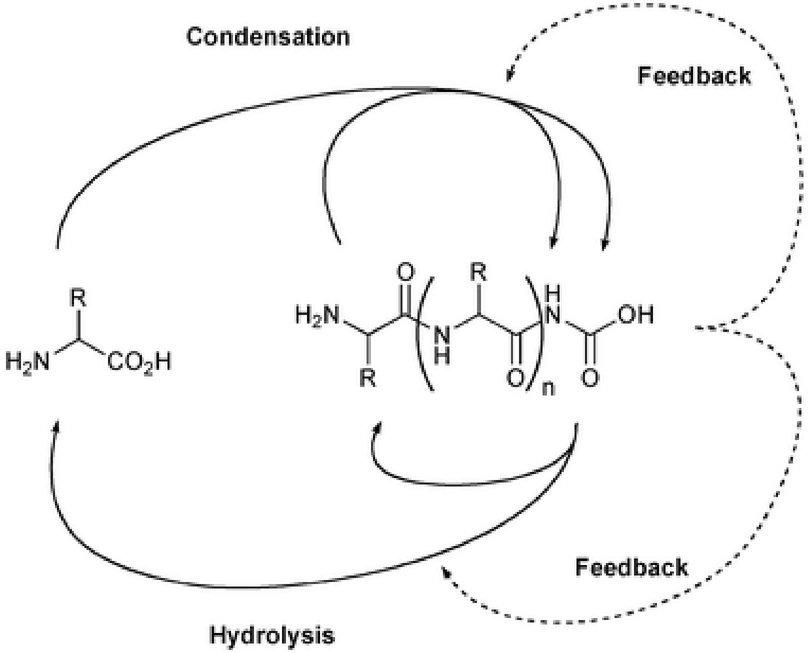

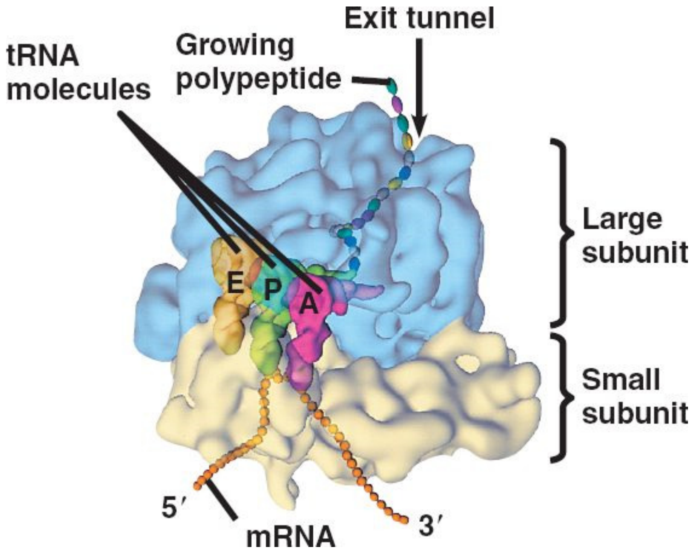

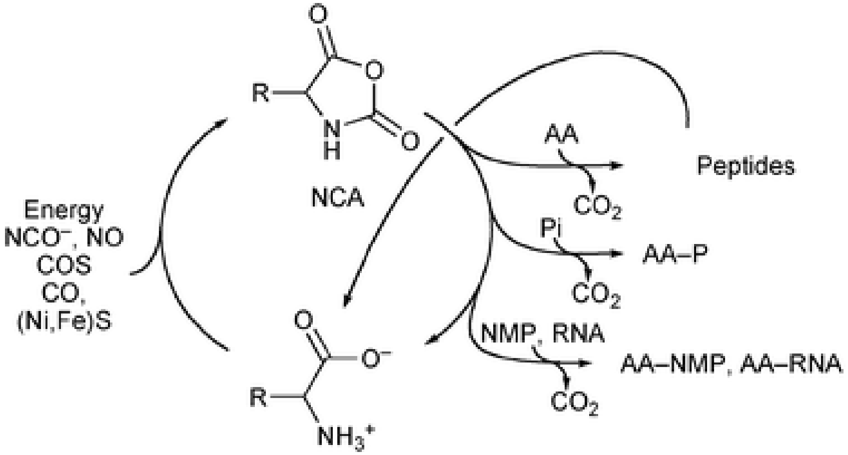

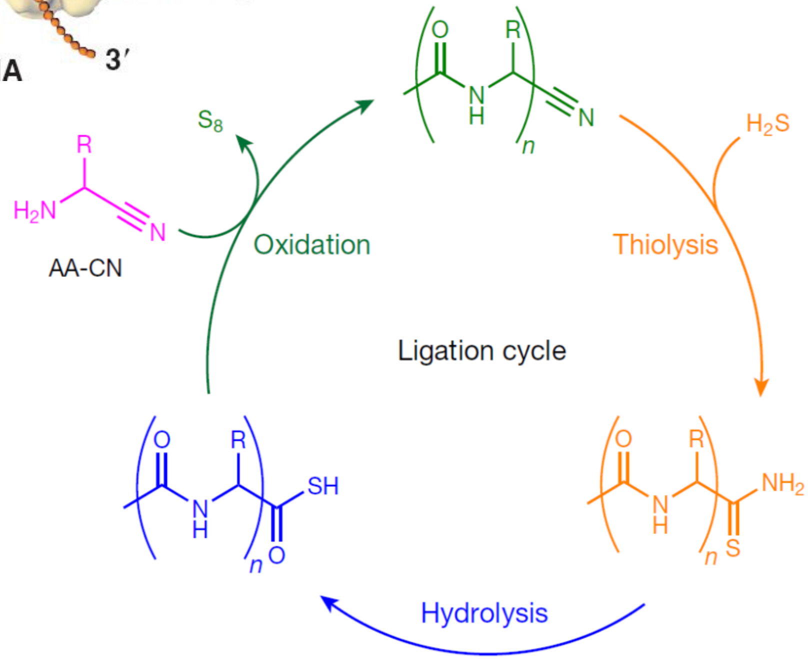

Emerging functions of oligopeptides

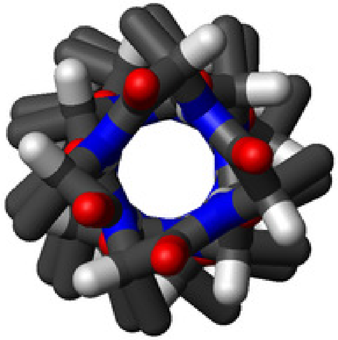

α-helix (Ala)

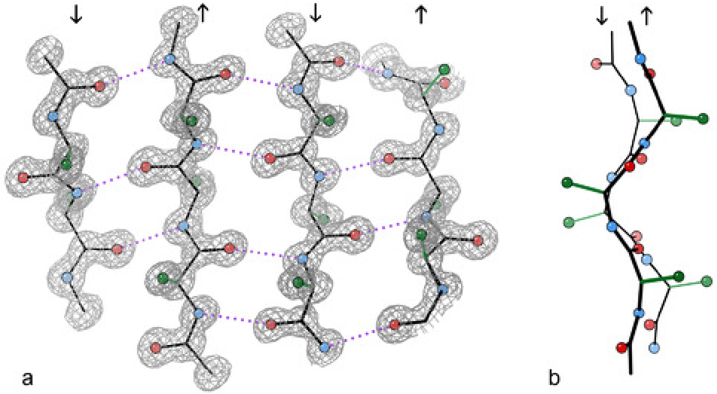

β-sheet (Val)

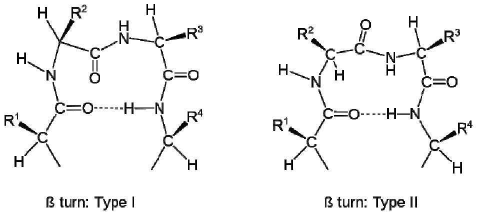

β-turn (coil) (Gly)

Globular, Hydrophilic/ hydrophobic structures

Catalytic (Asp)

Reduced aminoacid alphabet

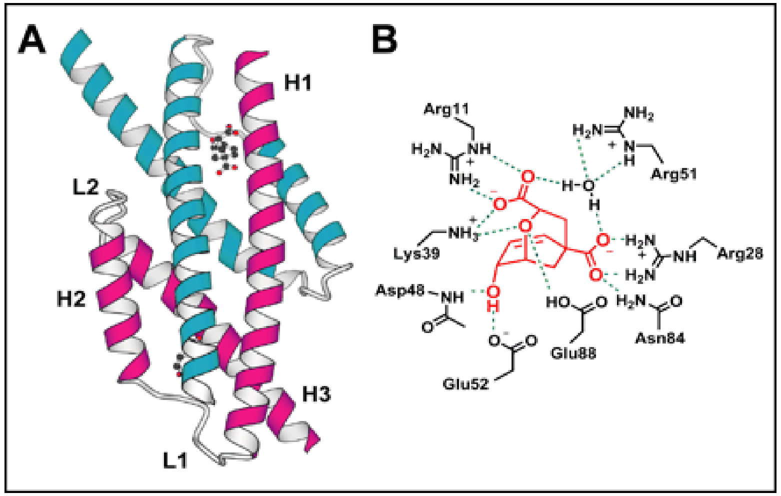

Prebiotic amyloids

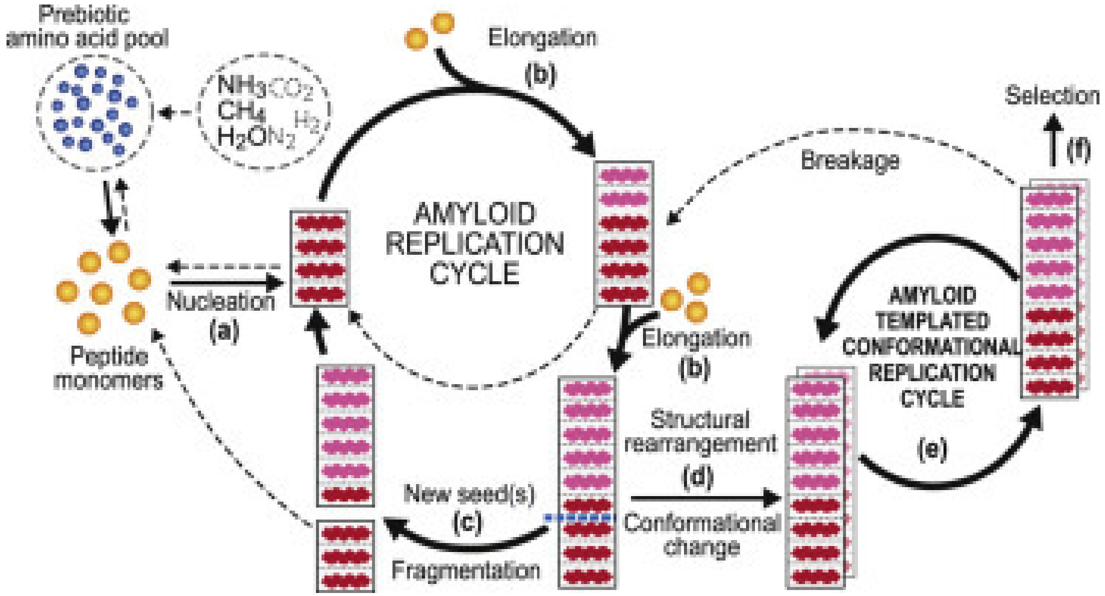

Encapsulation – essential for life

Formation of membranes is most easy to explain among major cellular components of the prebiotic Earth.

Many amphiphilic organic compounds spontaneously form vesicles in water at sufficiently high concentrations

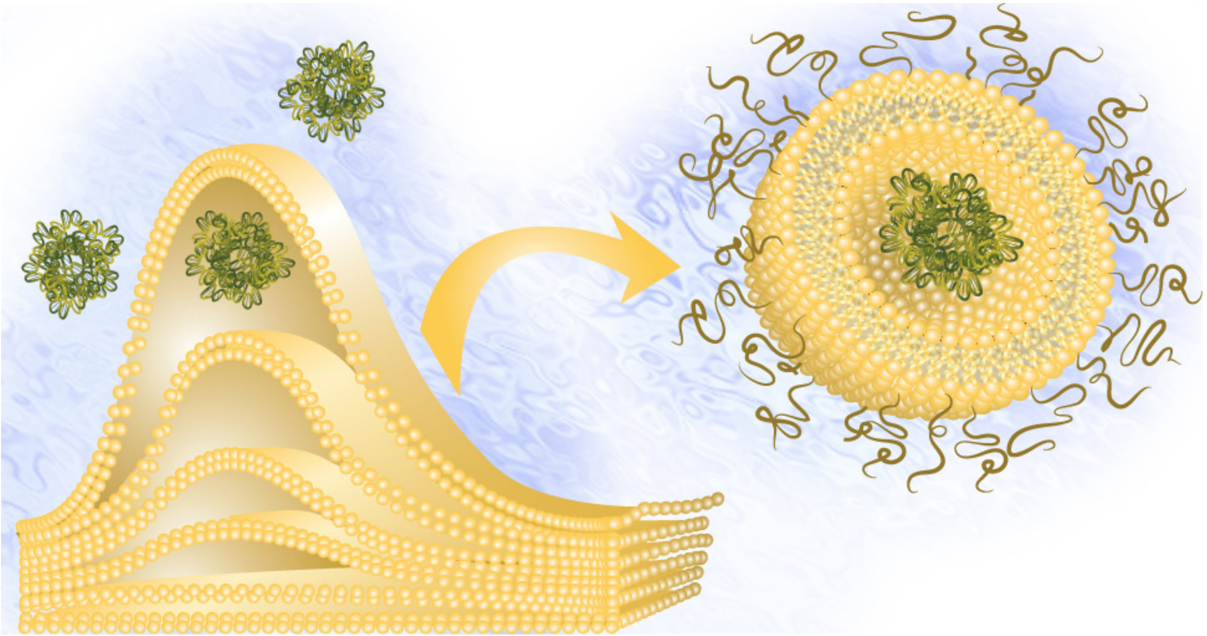

Levine, R.M., Pearce, T.R., Adil, M., Kokkoli, E. Langmuir, 2013, 29 (29): 9208–9215.

The vesicle will encapsulate an aqueous solution inside a thin layer of organic material

Fischer-Tropsch synthesis

Long hydrocarbon chains from CO + H_2 in presence of metal catalysts and high pressure, fatty acids and alcohols are minor by-products

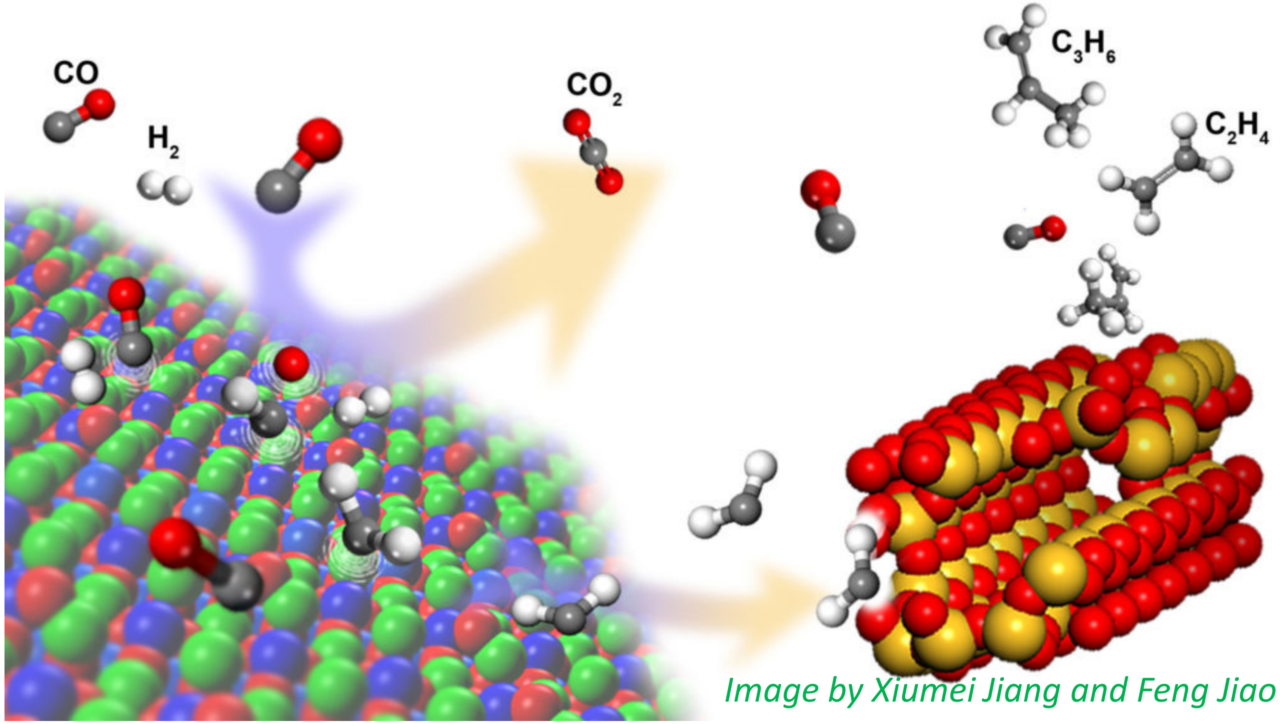

Image by Xiumei Jiang and Feng Jiao

The mixture of D_2 and CO over meteoritic iron or iron ore produced alkanes and n-fatty acids

Oro, J. et al. Geochim. Cosmochim. Acta **1976**, *40,* 915-924.

Hydrothermal Fischer-Tropsch synthesis

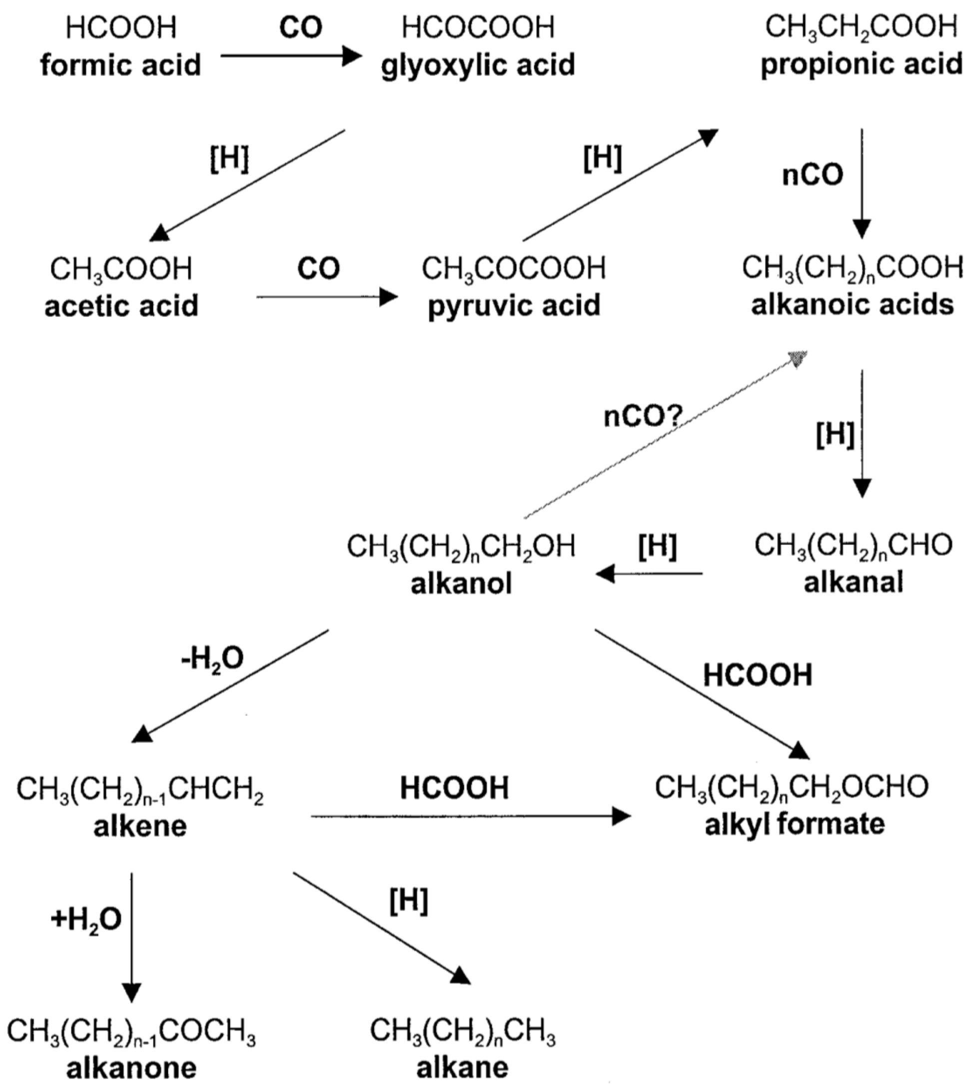

Formic or oxalic acid heated in water at 150-250^{0}C (stainless steel reactor) yielded a mixture of C_{12}-C_{33} lipids

Rushdi, A., Simoneit B. Origins Life Evol. Biospheres **2001**, *31,* 103-118

When CO, H_2 and NH_3 are allowed to react at 200-700^{0}C in presence of Ni, Al, or clay catalysts, aminoacids are detected:
glycine, alanine, sarcosine, aspartic acid, glutamic acid, arginine, histidine, lysine and ornithine

Yoshino, D.; Hayatsu, R.; Anders, E. *Geochim. Cosmochim. Acta* **1971**, *35,* 927-938

Encapsulation – essential for life

Fatty acids have been found in meteorites – plausible prebiotic synthesis pathways existed in the early Solar System

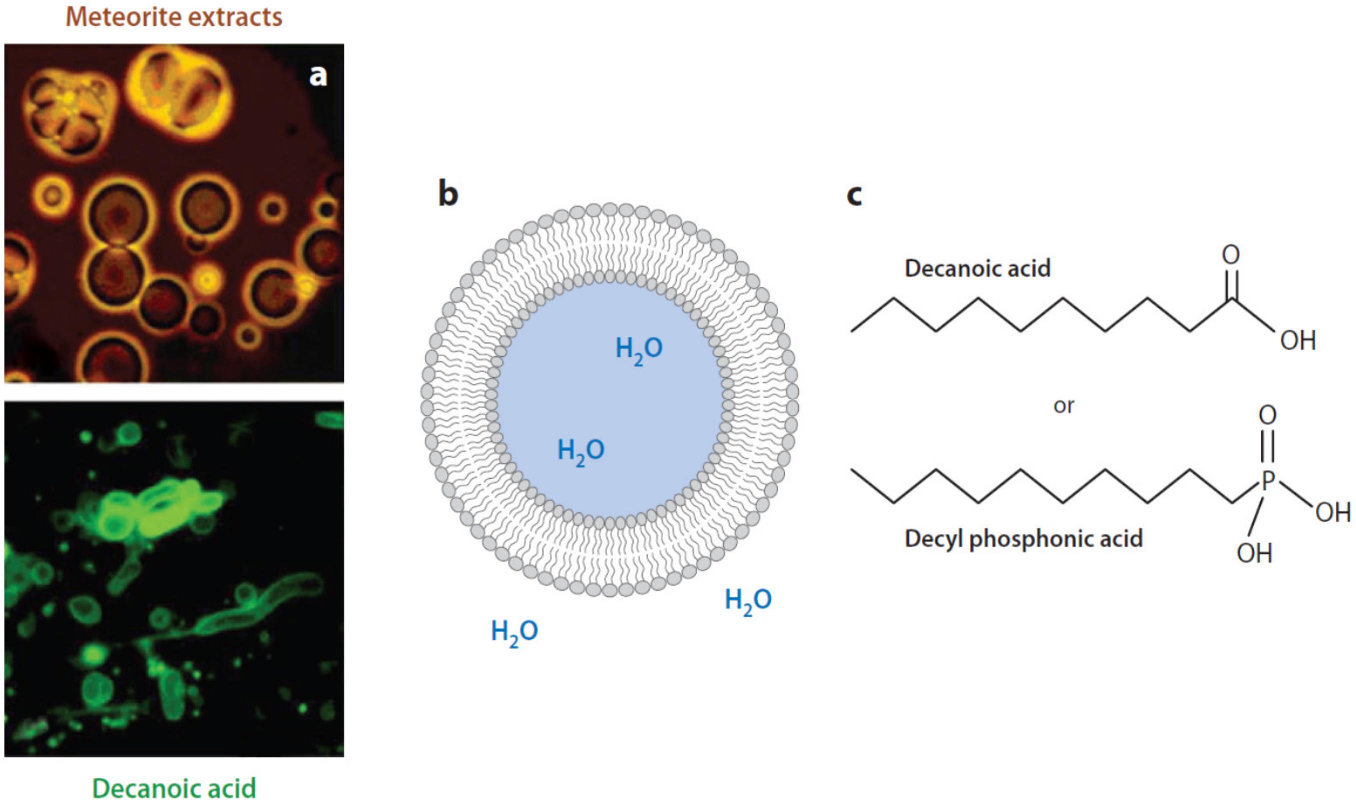

Extracts of meteorites containing these compounds spontaneously form vescicles when hydrated

Spontaneous generation of lipid vesicles

The first protocell membranes may have assembled from fatty acids and related single-chain lipids available in the prebiotic environment.

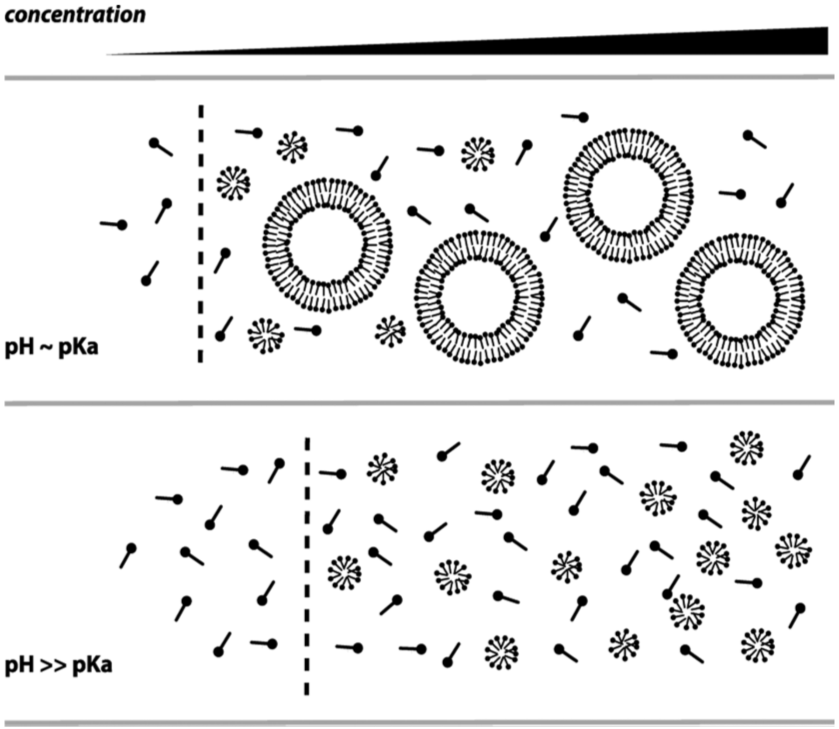

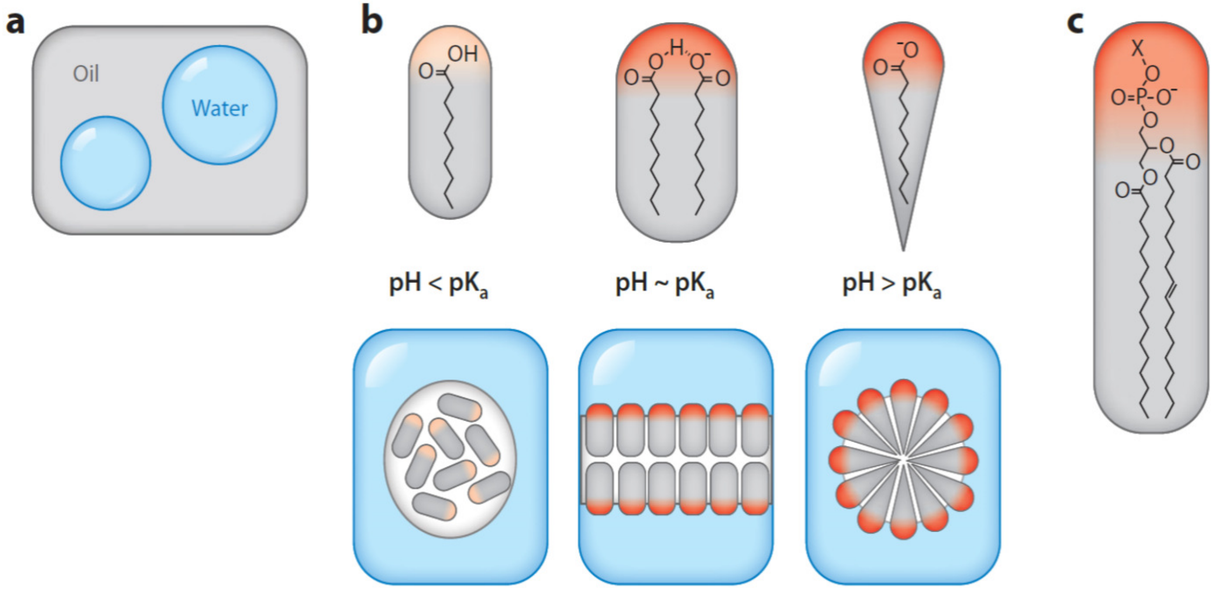

At different concentrations, fatty acids can partition between several different phases, including soluble monomers, micelles, and lamellar vesicles, with higher concentrations favoring larger vesicle aggregates.

I. Budin, A. Debnath, J. W. Szostak *J. Am. Chem. Soc.*, **2012**, 134, 20812-20819

By Markus Pössel (Mapos)

Jack Szostak

(* November 9, 1952) - Canadian American biologist of Polish British descent,

Nobel Prize laureate 2009 for Physiology and Medicine, for the discovery of how chromosomes are protected by telomeres; Professor of Genetics at Harvard Medical School.

Szostak has made significant contributions to the field of genetics. His achievement helped scientists to map the location of genes in mammals and to develop techniques for manipulating genes.

His research findings in this area are also instrumental to the Human Genome Project.

In the early 90s his laboratory shifted its research direction and focused on studying ***RNA enzymes***, which had been recently discovered by Cech and Altman. He developed the technique of ***in vitro evolution of RNA*** (also developed independently by Gerald Joyce) which enables the discovery of RNAs with desired functions through successive cycles of selection, amplification and mutation. He isolated the first ***aptamer*** (term he used for the first time). He isolated ***RNA enzymes with RNA ligase activity*** directly from random sequence (project of David Bartel).

Currently his lab focuses on the challenges of understanding the ***origin of life*** on Earth, and the construction of ***artificial cellular life*** in the laboratory

Coupled growth and division of model protocell membranes

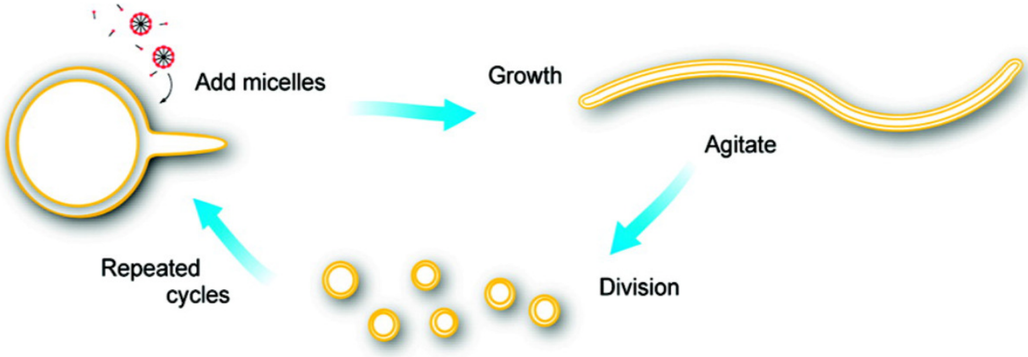

The growth of large multilamellar fatty acid vesicles fed with fatty acid micelles, in a solution where solute permeation across the membranes is slow, results in the transformation of initially spherical vesicles into long thread-like vesicles, a process driven by the transient imbalance between surface area and volume growth. Modest shear forces are then sufficient to cause the thread-like vesicles to divide into multiple daughter vesicles without loss of internal contents.

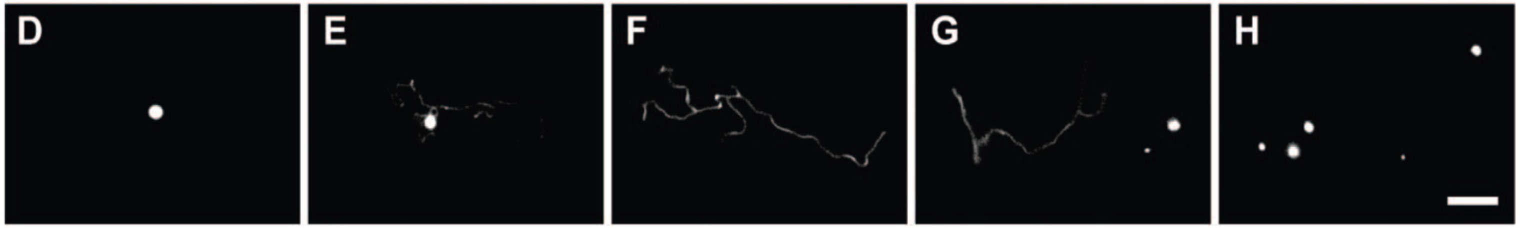

Ting F. Zhu, and Jack W. Szostak *J. Am. Chem. Soc.*, **2009**, 131 (15), 5705-5713

Coupled growth and division of model protocell membranes

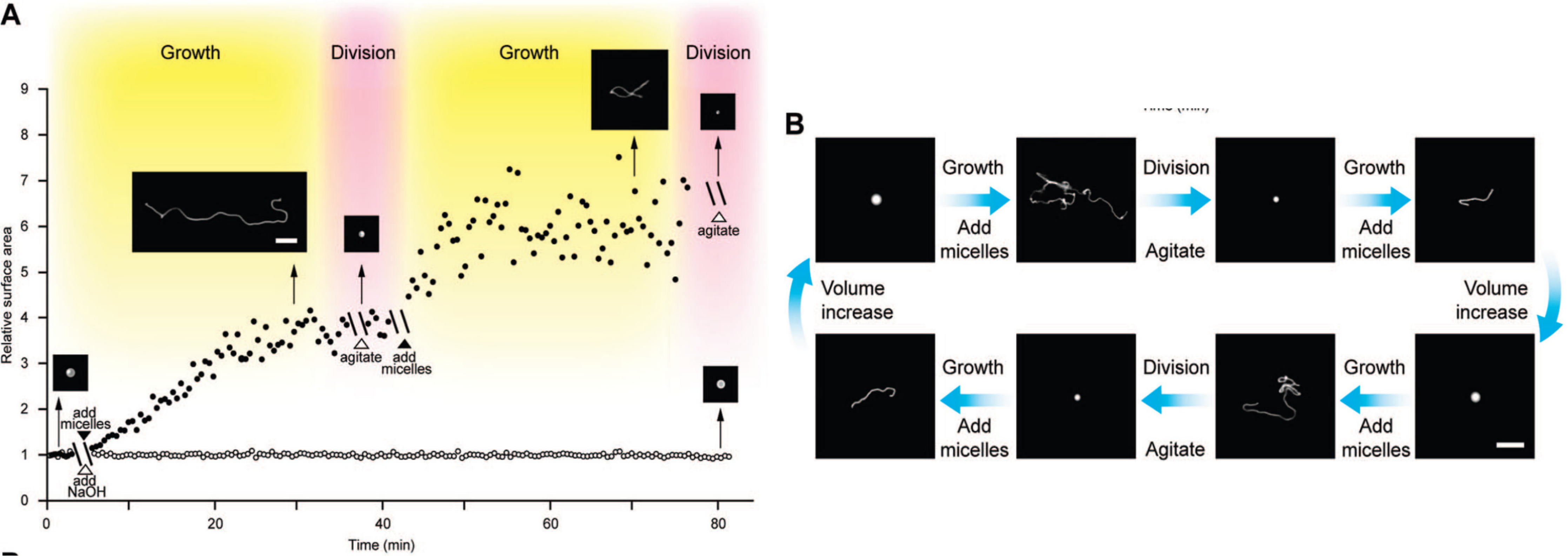

Cycles of vesicle growth and division. (A) Relative surface area after two cycles of addition of 5 equiv of oleate micelles (solid circles) or 5 equiv of NaOH (open circles) to oleate vesicles, each followed by agitation. Inset micrographs show vesicle shapes at indicated times. Scale bar, 10 *μ*m. (B) Vesicle shapes during cycles of growth and division in a model prebiotic buffer (0.2 M Na-glycine, pH 8.5, ~1 mM initial oleic acid, vesicles contain 10 mM HPTS for fluorescence imaging). Scale bar, 20 *μ*m.

Ting F. Zhu, and Jack W. Szostak *J. Am. Chem. Soc.*, **2009**, 131 (15), 5705-5713

Photochemically driven protocell division

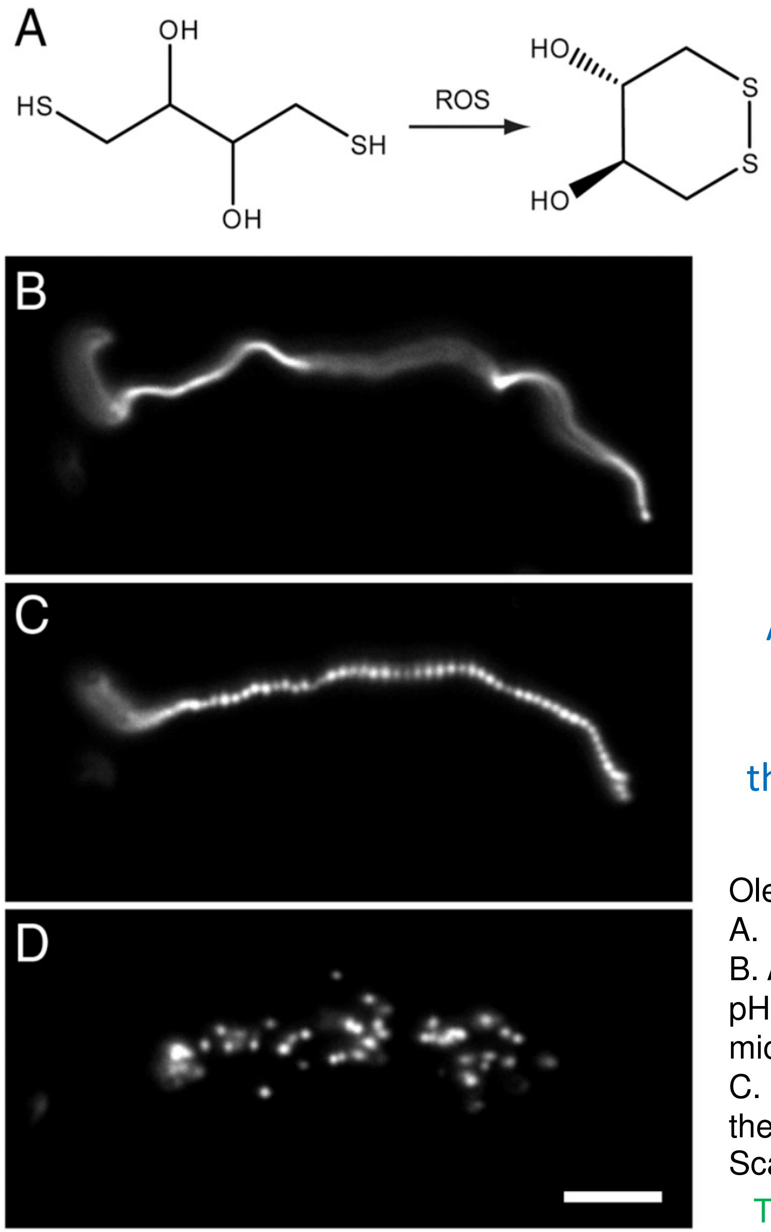

The illumination of filamentous fatty acid vesicles rapidly induces pearling and subsequent division in the presence of thiols.

Photochemically generated reactive oxygen species oxidize thiols to disulfide-containing compounds that associate with fatty acid membranes, inducing a change in surface tension and causing pearling and subsequent division.

Alternative route for the emergence of early self-replicating cell-like structures, particularly in thiol-rich surface environments.
The subsequent evolution of cellular metabolic processes controlling the thiol:disulfide redox state would have enabled autonomous cellular control of the timing of cell division, a major step in the origin of cellular life.

Oleate vesicle pearling and division.
A. Radical-mediated oxidation of DTT.
B. An oleate vesicle (containing 2 mM HPTS, in 0.2 M Na-glycinamide, pH 8.5, 10 mM DTT) 30 min after the addition of five equivalents of oleate micelles.
C. and D. Under intense illumination (for 2 s and 12 s, respectively), the long thread-like vesicle went through pearling and division
Scale bar, 10μm.

T. F. Zhu, K. Adamala, N. Zhang, J. W. Szostak *PNAS*, **2012**, doi:10.1073/pnas.1203212109

Photochemically driven protocell division

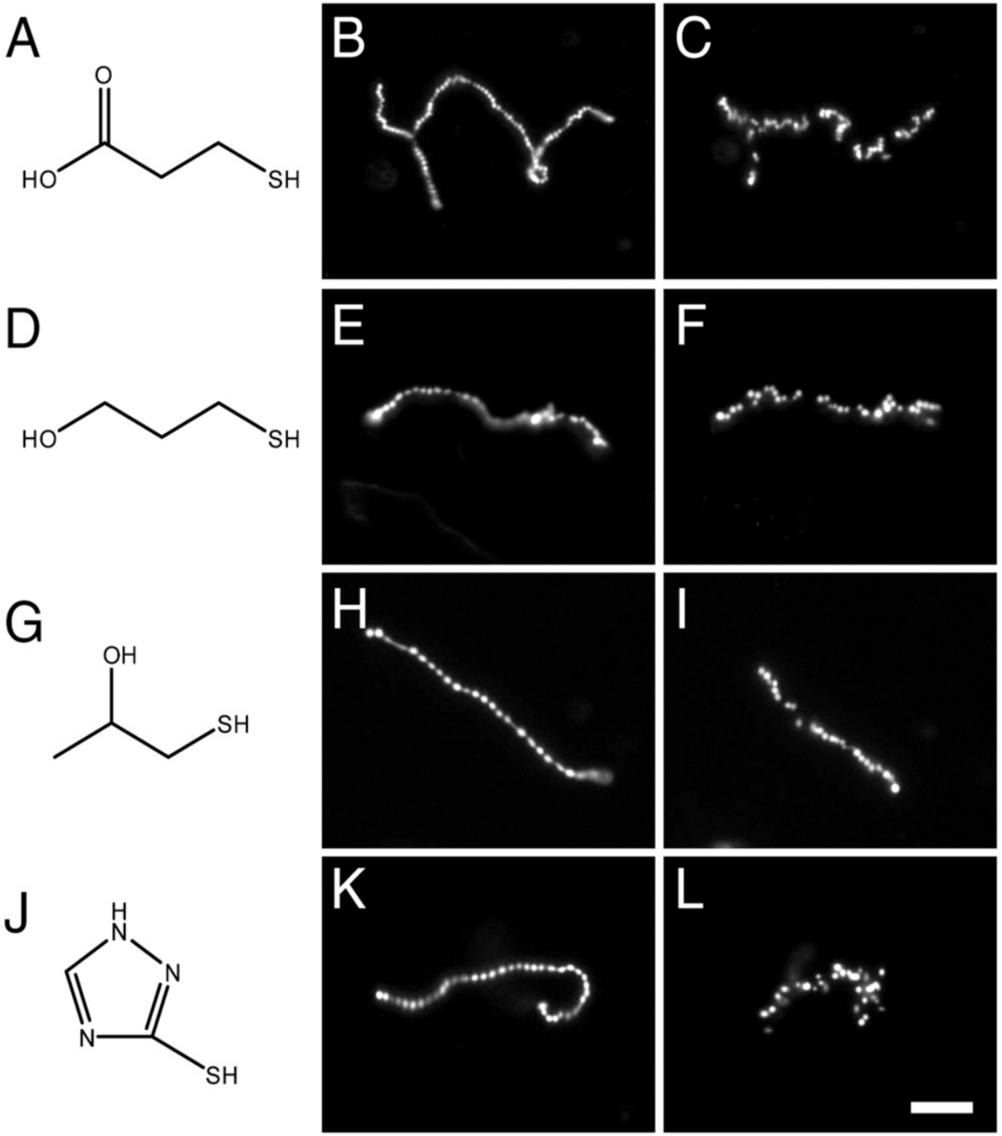

Oleate vesicle pearling and division with various thiols in the solution.

(A) 3-mercaptopropionic acid.
(B and C) An oleate vesicle (containing 2 mM HPTS, in 0.2 M Na-bicine, pH 8.5, 10 mM 3-mercaptopropionic acid, 30 min after the addition of five equivalents of oleatemicelles) went through pearling and division under intense illumination (for 3 s and 15 s, respectively).

(D) 3-mercapto-1-propanol.
(E and F) An oleate vesicle as above but in 50 mM 3-mercapto-1-propanol, went through pearling and division under intense illumination (for 2 s and 10 s, respectively).

(G) 1-mercapto-2-propanol.
(H and I) An oleate vesicle as above but in 50 mM 1-mercapto-2-propanol went through pearling and division under intense illumination (for 2 s and 9 s, respectively).

(J) 3-mercapto-1,2,4-triazole.
(K and L) An oleate vesicle as above but in 50 mM 3-mercapto-1,2,4-triazole went through pearling and division under intense illumination (for 3 s and 13 s, respectively).
Scale bar, 20 μm.

T. F. Zhu, K. Adamala, N. Zhang, J. W. Szostak *PNAS*, **2012**, doi:10.1073/pnas.1203212109

Noncovalent nucleotide association with membranes

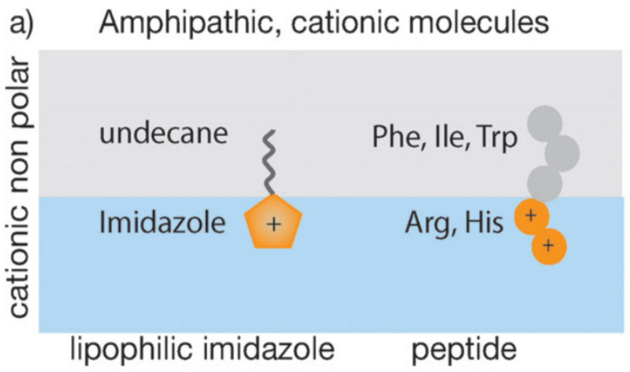

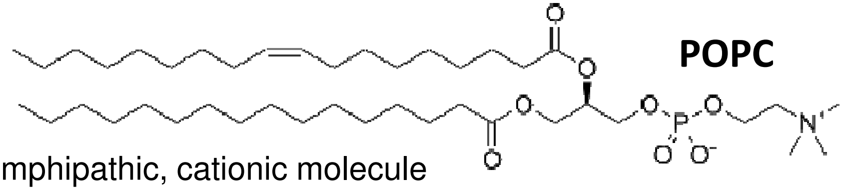

POPC

RNA localization with a model amphipathic, cationic molecule

a) Design of RNA-localizing molecules that include both nonpolar and cationic regions.
b) The change in zeta potential
c) Schematic of the FRET assay used to assess RNA localization to vesicle membranes
d) RNA (5’-FAM-U$_{15}$ and 5’-FAM-A$_{15}$) shows increasing localization to POPC membranes that contain increased amounts of undecylimidazole.

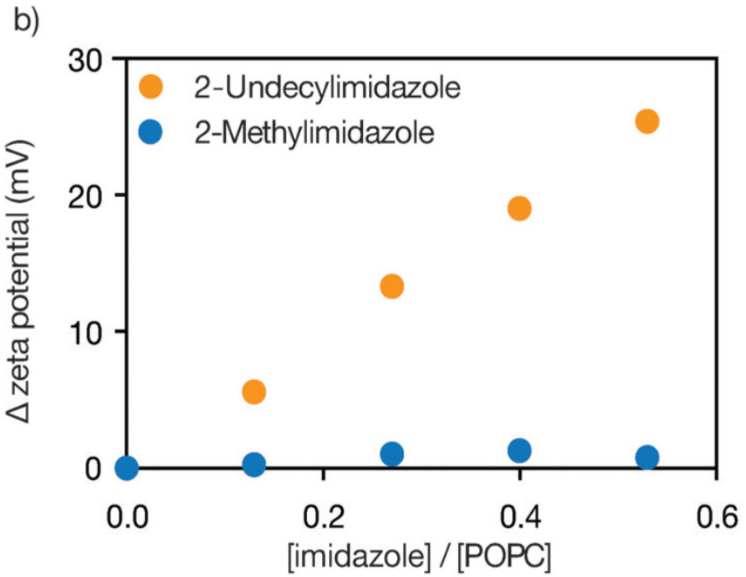

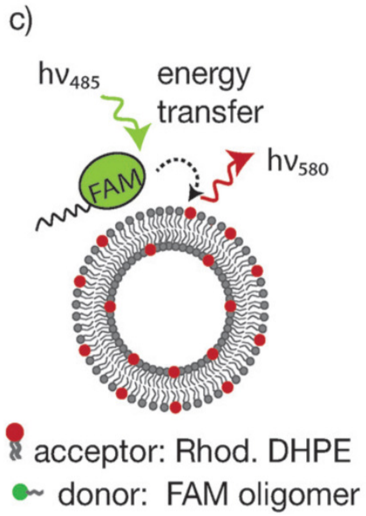

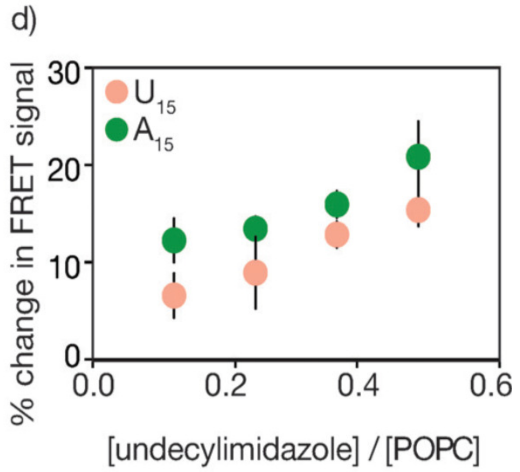

Neha P. Kamat, Sylvia Tobe, Ian T. Hill, and Jack W. Szostak *Angew. Chem. Int. Ed.* **2015**, *54*, 11735 –11739

Noncovalent nucleotide association with membranes

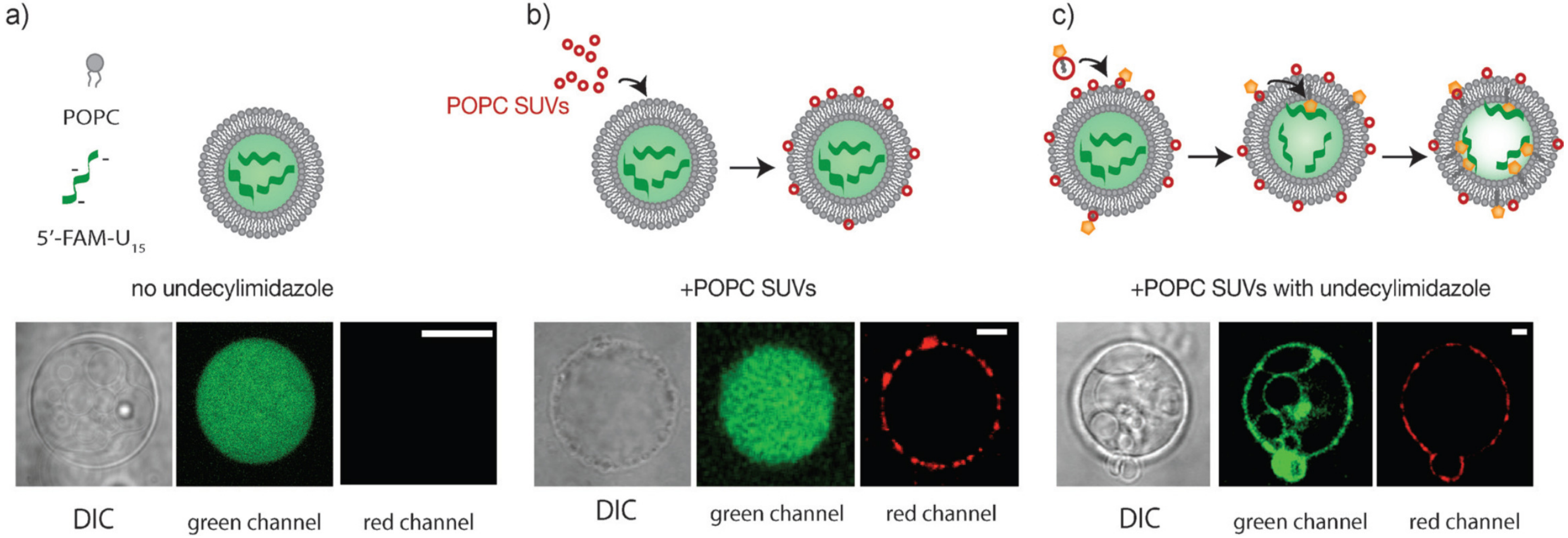

Microscopy of encapsulated RNA localization to POPC membranes with 2-undecylimidazole. Confocal images of 5’-FAM-U$_{15}$ RNA (green) association with giant POPC vesicles membranes in the presence of 2-undecylimidazole. Differential interference contrast (DIC) microscopy images are shown for each vesicle.

a) RNA appears uniformly distributed in the interior of POPC GUVs.
b) The addition of SUVs containing a rhodamine-labeled lipid (red) leads to SUV aggregation and association with the giant vesicle membranes, but RNA (green) remains uniformly encapsulated in the vesicle interior.
c) The addition of SUVs containing a rhodamine-labeled lipid (red) and 40 mol% 2-undecylimidazole leads to SUV association with vesicle membranes and RNA (green) localizes to the vesicle surface. The scale bar is 20 mm.

SUV – small unilamellar vescile ***GUV – giant unilamellar vescile (5-25 μm)***

Neha P. Kamat, Sylvia Tobe, Ian T. Hill, and Jack W. Szostak *Angew. Chem. Int. Ed.* **2015**, *54*, 11735 –11739

Noncovalent nucleotide association with membranes

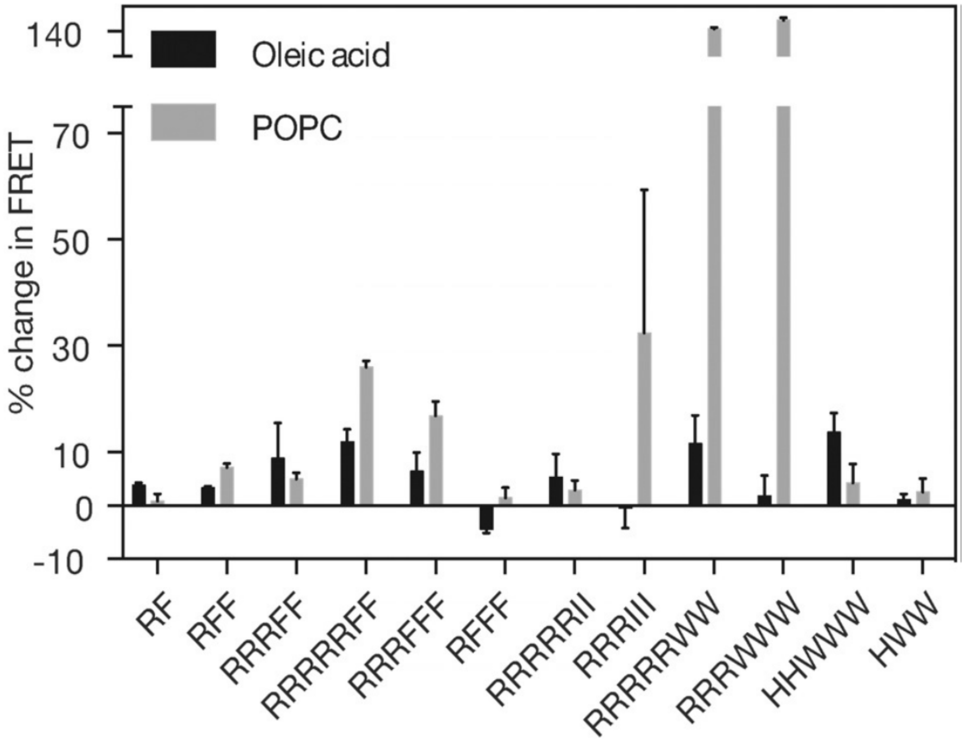

Peptide-induced RNA–membrane association. A FRET assay reports RNA localization (5’-FAM-U_{15}) to POPC and oleic acid membranes (7.5 mm) 10 h after the addition of 1 mm of various peptides to the vesicle solution at pH 8. Data is reported as a percentage change from control samples that lack peptide. n=4, error bars represent the standard error of the mean.

Neha P. Kamat, Sylvia Tobe, Ian T. Hill, and Jack W. Szostak *Angew. Chem. Int. Ed.* **2015**, *54*, 11735 –11739

Noncovalent nucleotide association with membranes

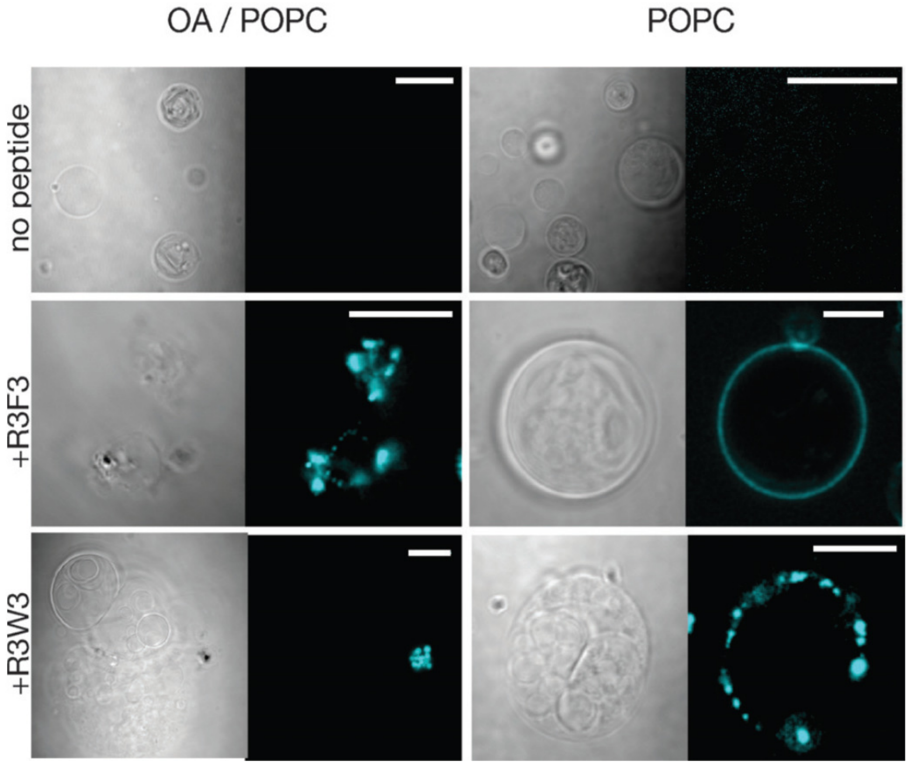

Microscopy of peptide-induced RNA–membrane association. Confocal images show RNA localization (5’-AlexaFluor647-labeled 15-mer, cyan) to the outside of oleic acid/POPC (90%/10%) and pure POPC membranes in the presence of R3F3 and R3W3 peptides. Control samples had no peptide added. For each image, the left panel shows the DIC image and the right panel shows AlexaFluor647 fluorescence. The scale bar is 20 mm.

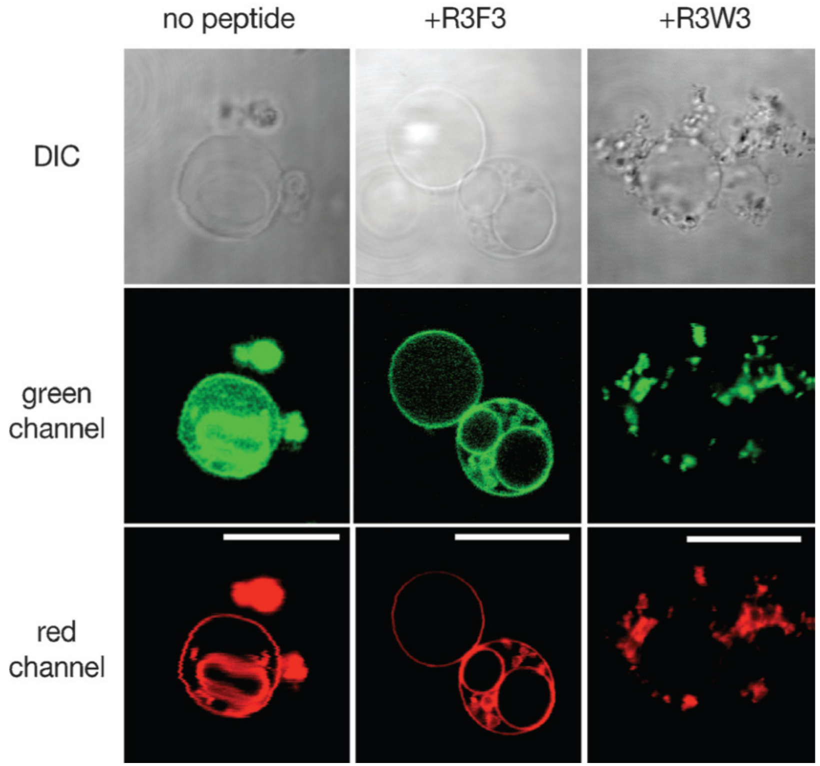

Microscopy of encapsulated RNA localization to POPC membranes with peptides. Confocal images show that RNA (5’-FAMU_{15}, green) encapsulated in POPC vesicles (containing a rhodaminelabeled lipid, red) becomes localized to the membrane of certain vesicles after an overnight incubation with R3F3 and R3W3 peptides. The scale bar is 20 mm.

Neha P. Kamat, Sylvia Tobe, Ian T. Hill, and Jack W. Szostak *Angew. Chem. Int. Ed.* **2015**, *54*, 11735 –11739

Phospholipids

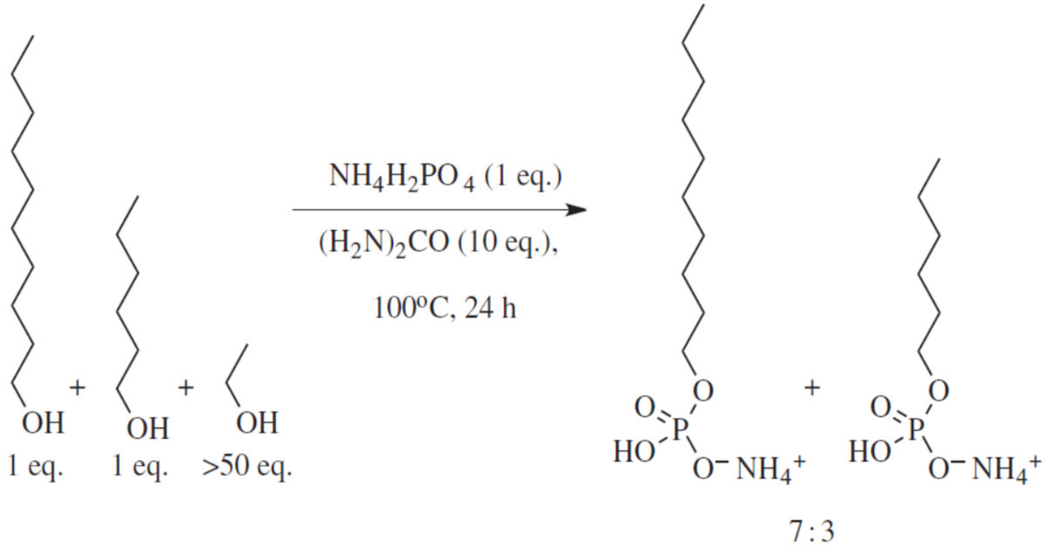

M. Powner, J. Sutherland *Phil. Trans. R. Soc. B* **2011**, *366*, 2870–2877

Phosphates

Source: Google Images

Schreibersite is generally a rare iron-nickel phosphide mineral, $(Fe,Ni)_3P$, though common in iron-nickel meteorites

Acidic schreibersite corrosion under anaerobic conditions (10% aq. HCl/N_2) → soluble forms of phosphorus

$$(Fe,Ni)_3P + HCl_{aq} \rightarrow H_2PO_3^{-} \rightarrow H_2P_2O_5^{2-}$$

T. P. Kee *et al.Geochimica et Cosmochimica Acta.* ***2013*** *109,* 90-112

Wikimedia , Butcherbird

slice of the Gebel Kamil Meteorite with schreibersite rimmed by kamacite

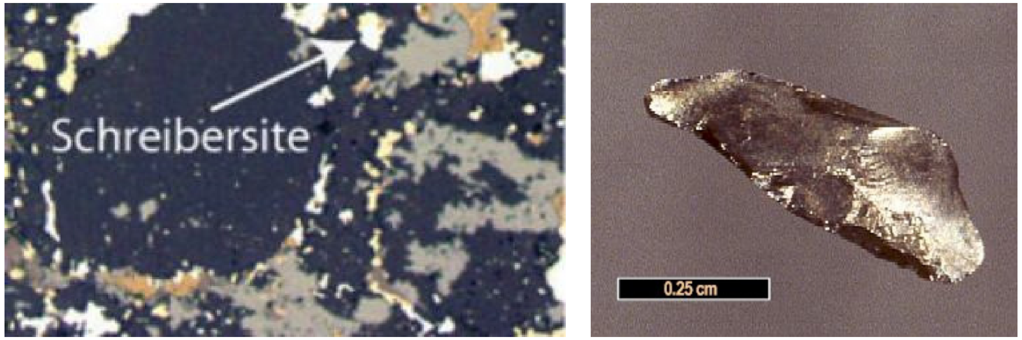

Virginia Smith, UA Lunar & Planetary Laboratory

Image of schreibersite grain present in a thin-section of the enstatite meteorite, KLE 98300.

Phosphates

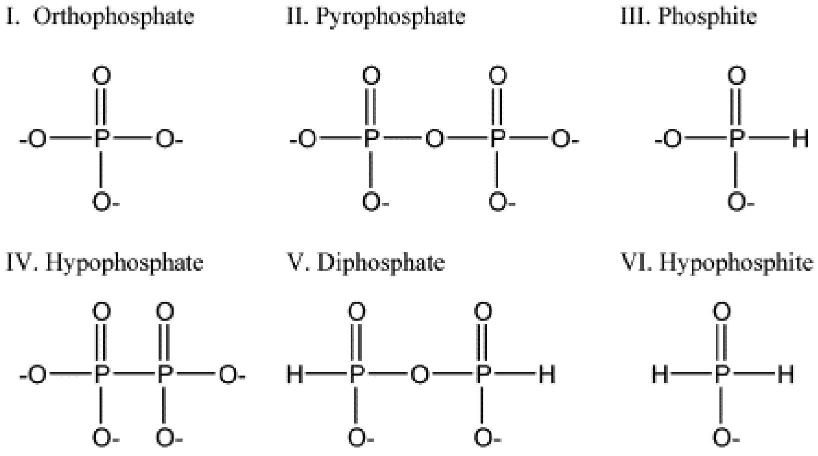

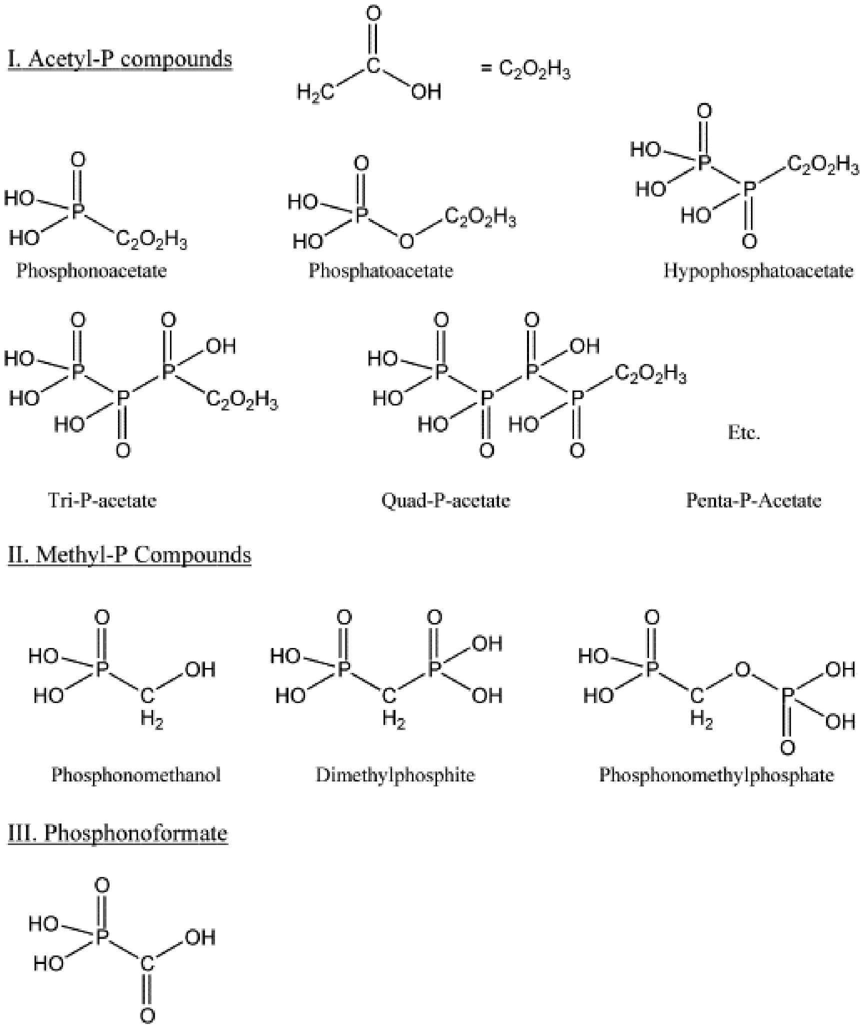

$$Fe_3P + 7H_2O \rightarrow Fe_3O_4 + H_3PO_3 + 5\tfrac{1}{2}H_2(g)$$

$$H_3PO_3 + H_2O \rightarrow H_3PO_4 + H_2(g)$$

$$2H_3PO_3 \rightarrow H_4P_2O_6 + H_2(g)$$

$$H_4P_2O_6 + H_2O \rightarrow H_4P_2O_7 + H_2(g)$$

$$H_4P_2O_7 + H_2O \rightarrow 2H_3PO_4$$

Radical pathway of the corrosion is suggested.
In presence of simple organic molecules (e.g. acetic acid)
organophosphorous compounds are detected

M. Pasek *et al.Geochimica et Cosmochimica Acta.* ***2007*** *71,* 1721-1736

Lipids - summary

Many amphiphilic organic compounds spontaneously form vesicles in water at sufficiently high concentrations

Current phospholipid membranes likely evolved late. Protocells probably encapsulated by fatty acids, fatty alcohols, prenyl oligomers, or phosphorylated alcohols

Phosphorus was accessible upon corrosion of meteorite materials and could be incorporated into lipids

The origin of small reactive intermediates


vivianite

Wikimedia , Carles Millan

Schreibersite $(Fe,Ni)_3P$, from iron-nickel meteorites: source of phosphorus, iron and nickel

Under more neutral conditions phosphates recombine with iron → $Fe_3(PO_4)_2$ (**vivianite**)

It should be re-solubilized to become accessible for following chemical transformations

HCN – the crucial reactive intermediate – burning of carbon-rich chondrite meteorites into redox-neutral atmosphere containing N_2 and water

$$Fe_3(PO_4)_2 + 18CN^-{}_{aq} \rightarrow 2PO_4^{3-} + 3[Fe(CN)_6]^{4-}$$

Two important functions: solubilization of phosphates and concentration of atmospheric HCN deposited as salts of mono- and divalent cations (Na, K, Mg, Ca)

Similar reactions take place with insoluble copper and nickel sulfides deposited by iron-nickel meteorite impacts (same occurence as schreibersite, rich mining sources of these metals until today)

$$NiS + H_2O + 6CN^- \rightarrow [Ni(CN)_6]^{4-} + HS^- + OH^-$$

$$Cu_2S + H_2O + 6CN^- \rightarrow 2[Cu(CN)_3]^{2-} + HS^- + OH^-$$

The origin of small reactive intermediates

Thermal decomposition of cyanoferrates (volcanic):

$$(Na,K)_4[Fe(CN)_6] \xrightarrow{700^oC} 4(\mathbf{Na/K})\mathbf{CN} + Fe(CN)_2$$

$$3Fe(CN)_2 \xrightarrow{700^oC} Fe_3C + 5C + 3N_2$$

$$Fe(CN)_2 \xrightarrow{700^oC} Fe + 2C + N_2$$

$$Ca_2[Fe(CN)_6] \xrightarrow{660^oC} 2Ca(CN)_2 + Fe(CN)_2$$

$$Ca(CN)_2 \xrightarrow{660^oC} \mathbf{CaNCN} + C \xrightleftharpoons{1000^oC} \mathbf{CaC_2} + N_2$$

$$Mg_2[Fe(CN)_6] \xrightarrow{315^oC} 2Mg(CN)_2 + Fe(CN)_2$$

$$Mg(CN)_2 \xrightarrow{395^oC} MgCN_2 + C$$

$$3MgCN_2 \xrightarrow{420^oC} \mathbf{Mg_3N_2} + 3C + 2N_2$$

$Cu_2S + H_2O + 6CN^- \rightarrow 2[Cu(CN)_3]^{2-} + HS^- + OH^-$

cyanocuprates and HS^- are delivered by this process

Photoredox cycle based on cyanocuprates may convert HCN into cyanogen

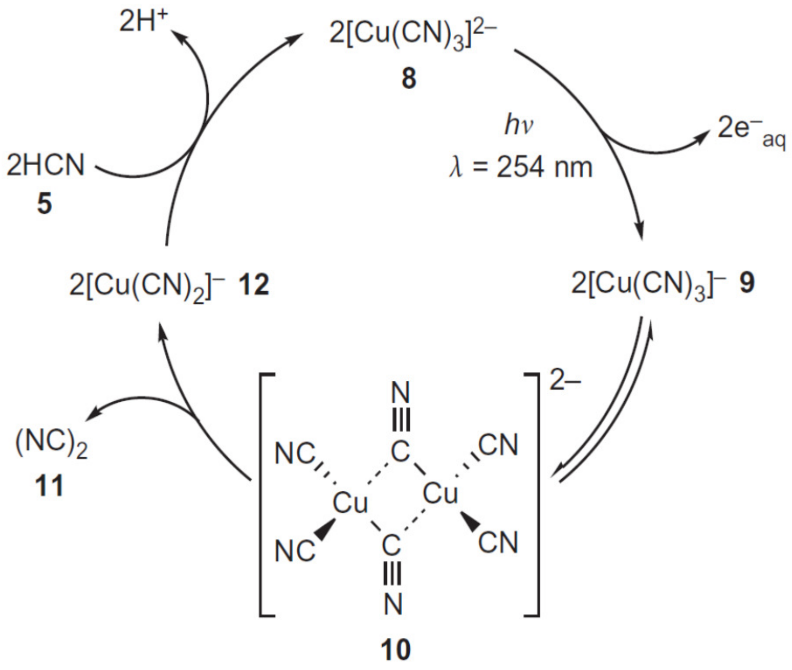

Action of water (bufferred to neutral or slightly acidic) on that mixture produced concentrated HCN solution + cyanamide (from CaNCN) + acetylene (from CaC_2) + ammonia (from Mg_3N_2)

Basic classes of biomolecules

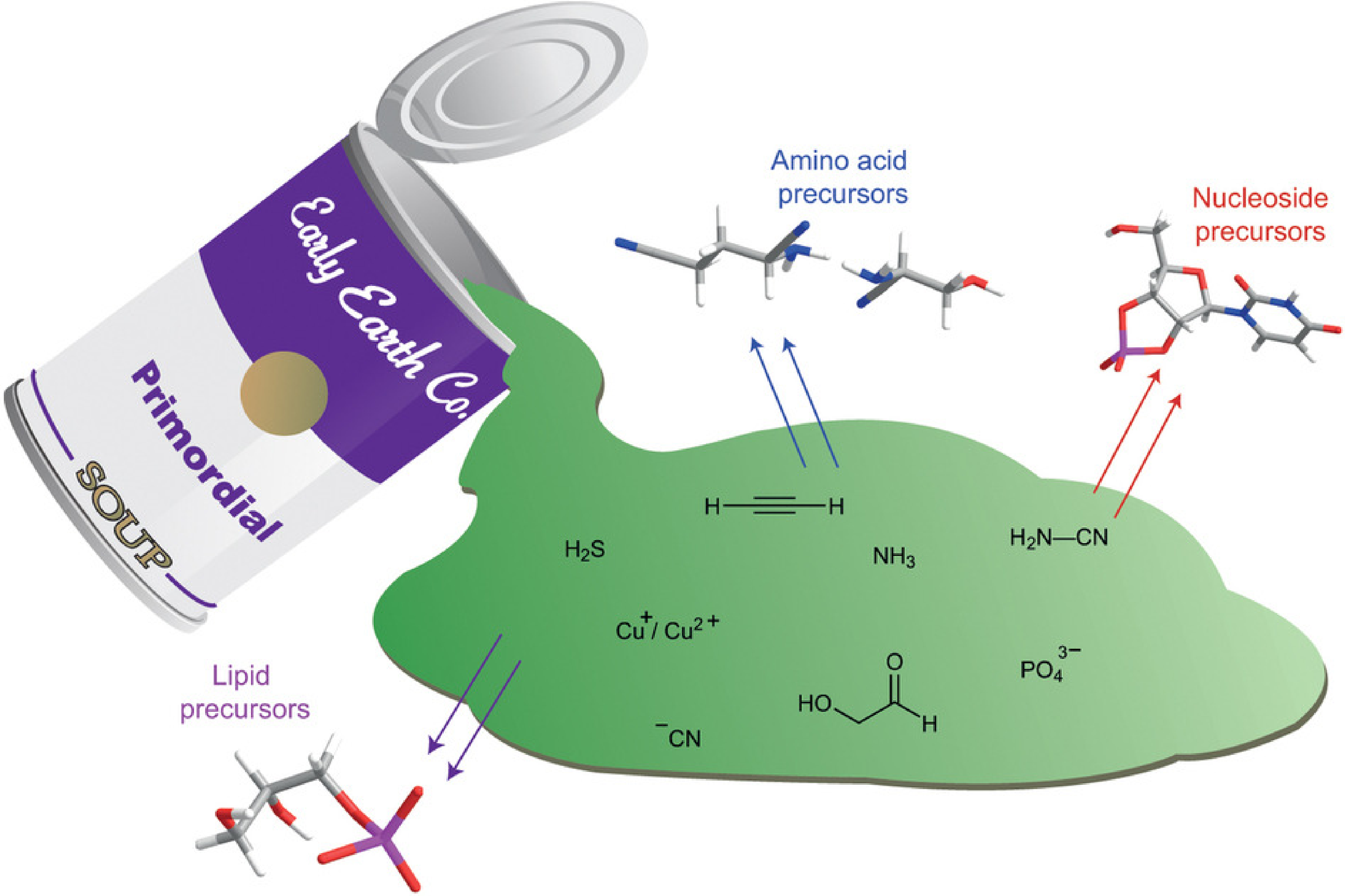

- Aminoacids
- Lipids
- **Carbohydrates (sugars)**
- **Nucleobases**
- **Nucleosides (sugar+nucleobase)**

Nucleotides - components

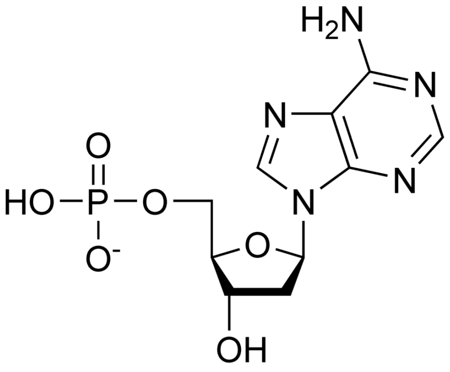

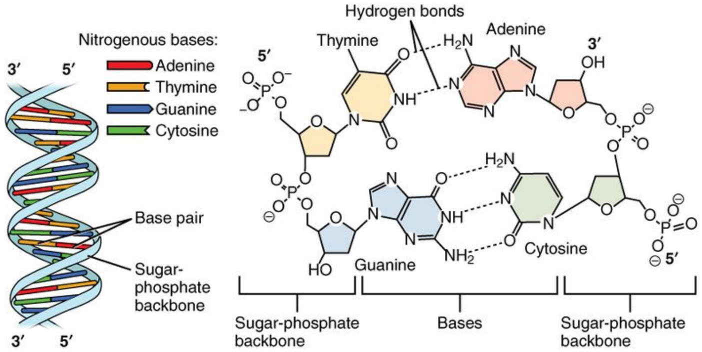

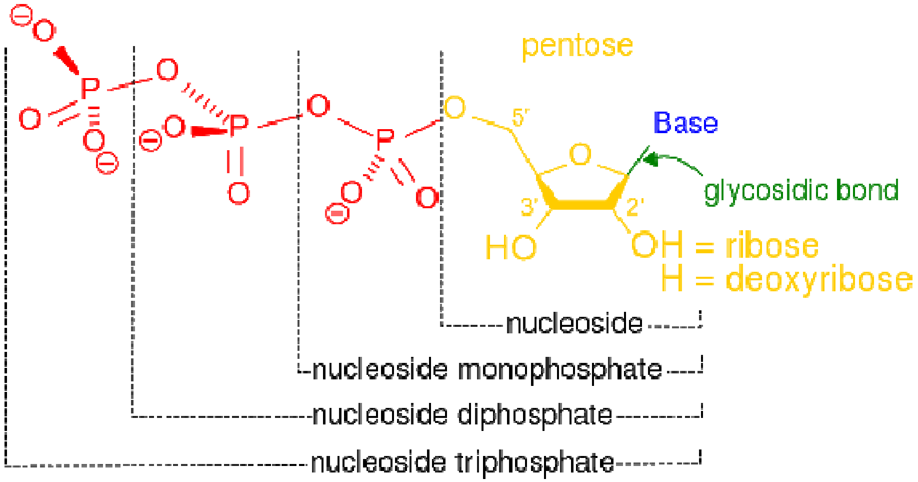

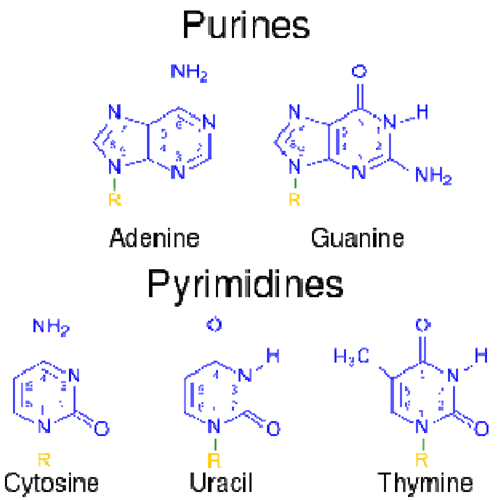

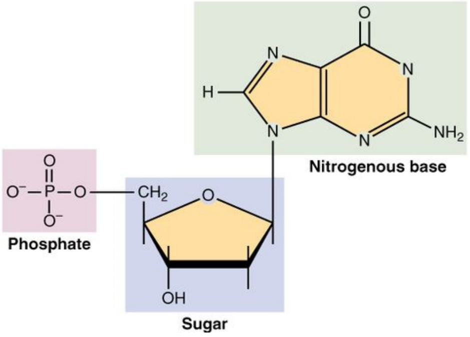

Phosphates and the prebiotic synthesis of oligonucleotides

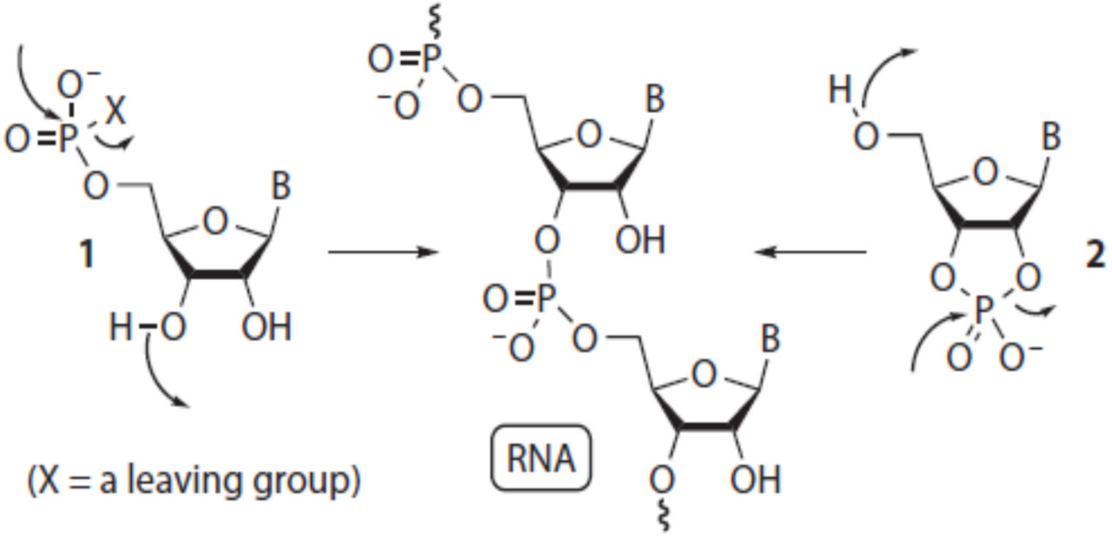

Activated ribonucleotides in the potentially prebiotic assembly of RNA. Potential P–O bond forming polymerization chemistry is indicated by the curved arrows.

Phosphorylation reagents

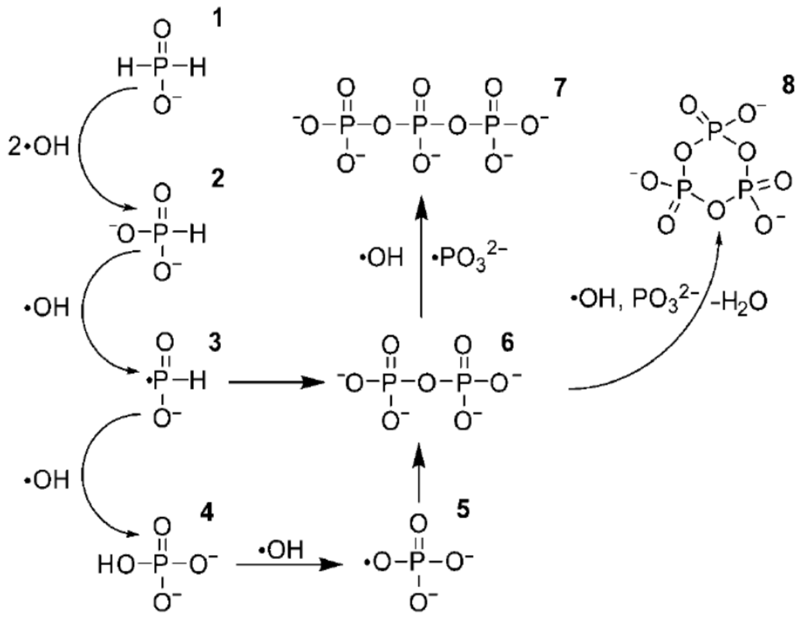

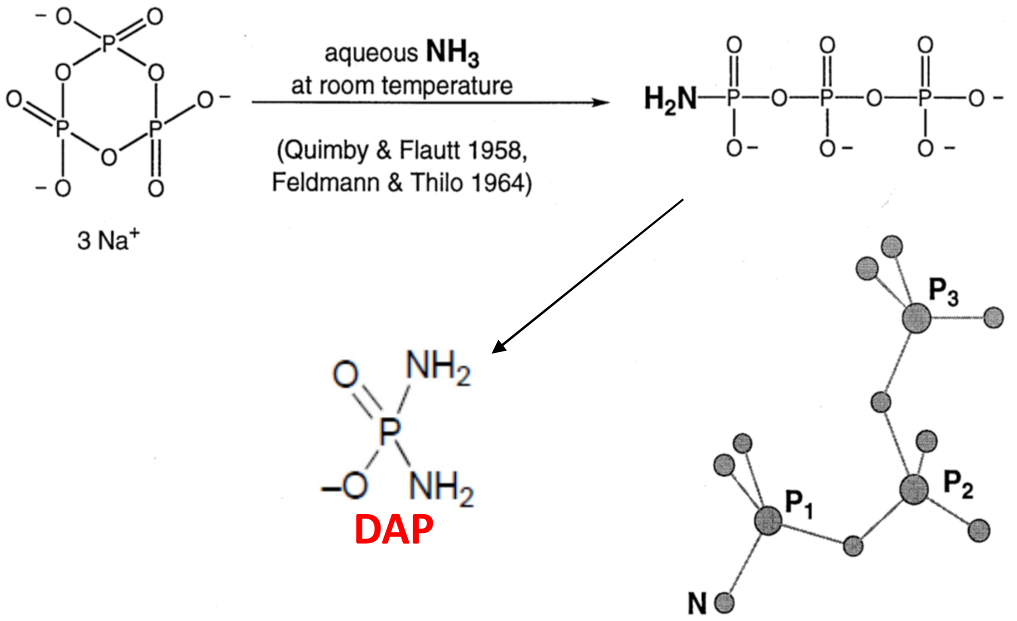

x-ray structure of $K_4(P_3O_9NH_2)$ (Hilmer, 1965)

M. A. Pasek, *et al. Angew. Chem. Int. Ed.* **2008**, *47*, 7918-7920 A. Eschenmoser, *et al. Orig. Life Evol. Biosph.* **1999**, *29*, 333-354

Phosphorylation reagents

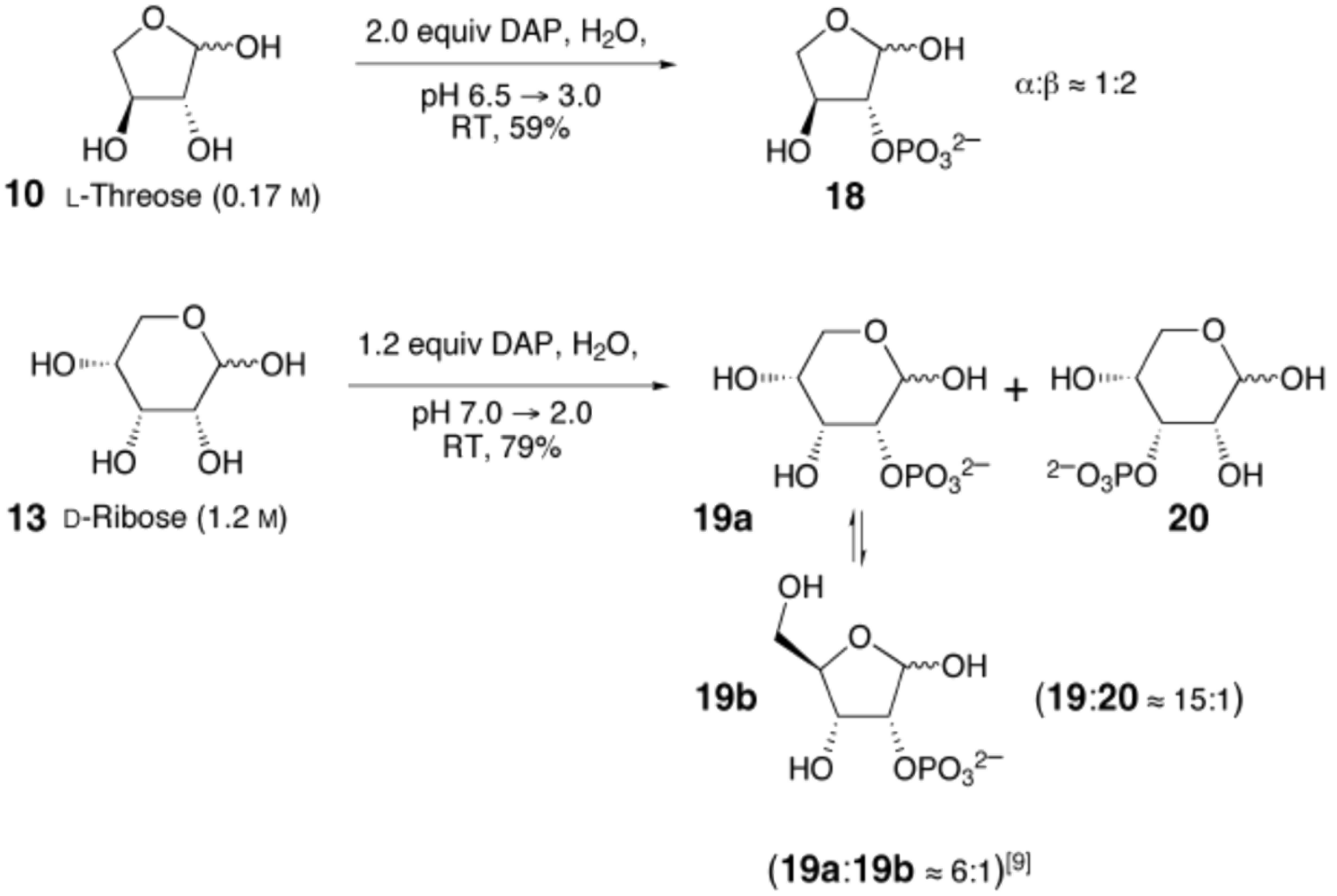

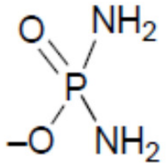

DAP

M. A. Pasek, *et al. Angew. Chem. Int. Ed.* **2008**, *47*, 7918-7920 A. Eschenmoser, *et al. Orig. Life Evol. Biosph.* **1999**, *29*, 333-354

Phosphorylation of sugars

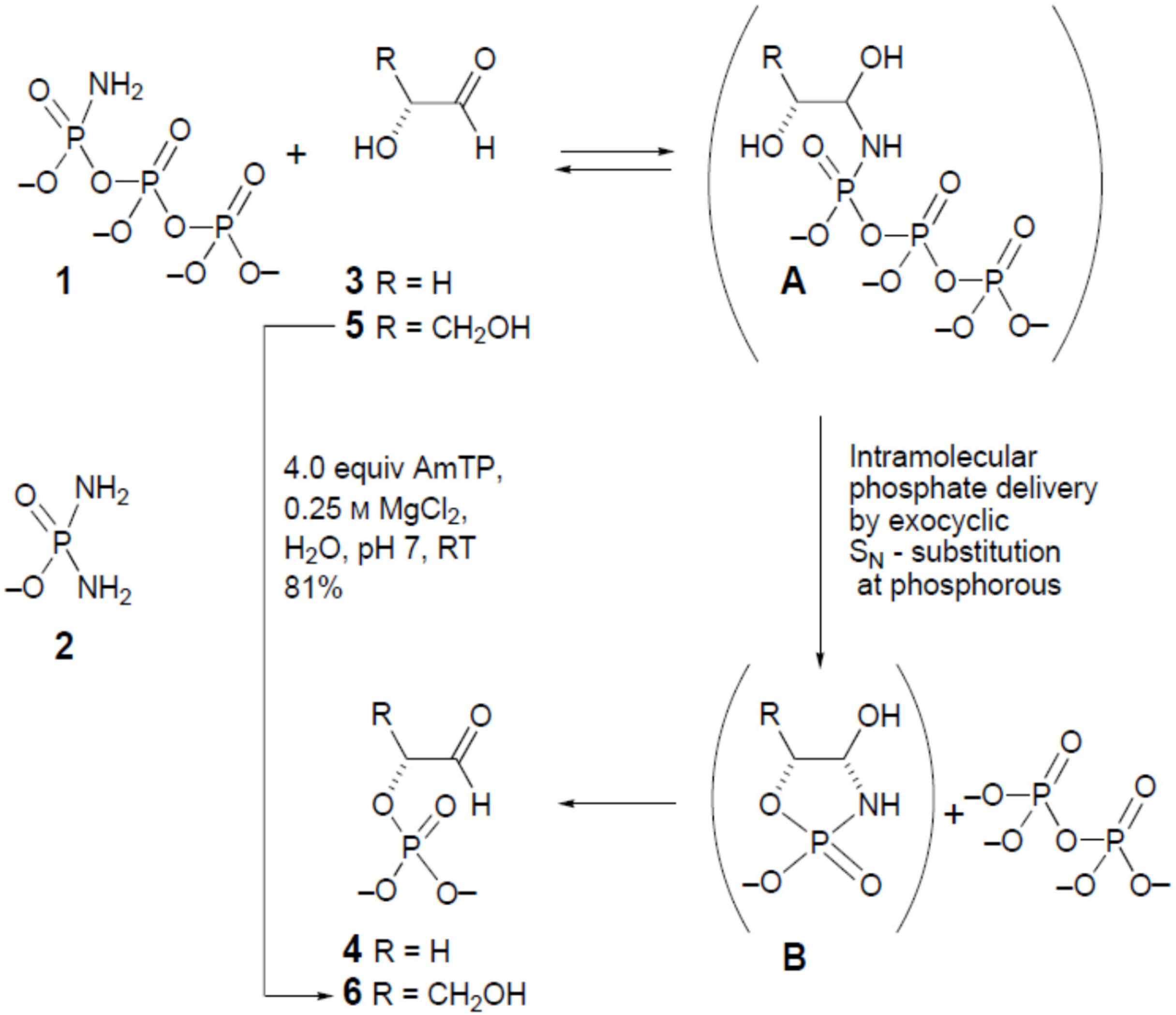

A. Eschenmoser, *et al. Angew. Chem. Int. Ed.* **2000**, *39*, 2281-2285

Phosphorylation of sugars

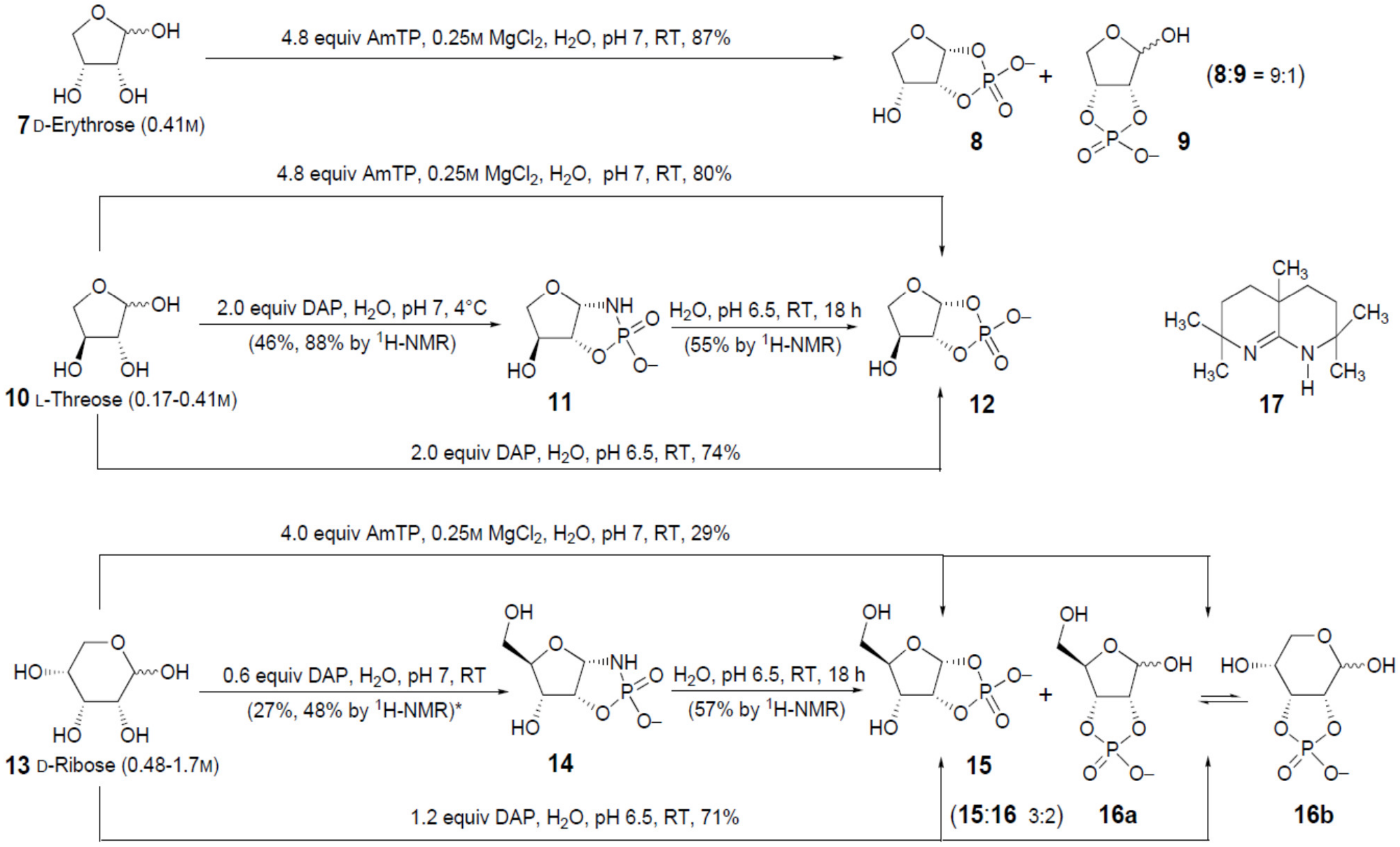

A. Eschenmoser, *et al. Angew. Chem. Int. Ed.* **2000**, *39*, 2281-2285

Nucleosides - nucleobases + sugars

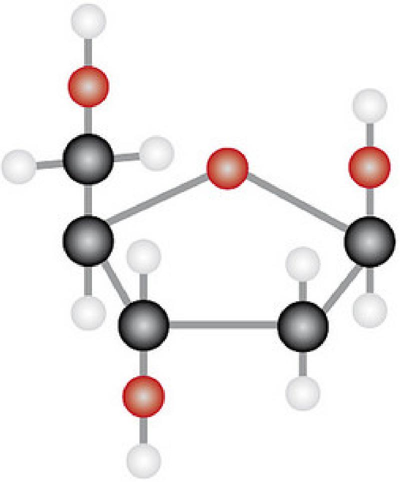

Deoxyribose
used in DNA backbone

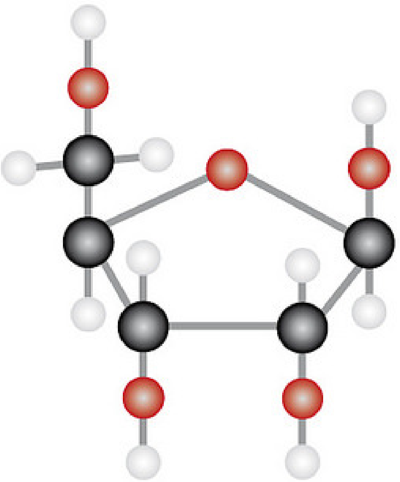

Ribose
used in RNA backbone

Key
○ Hydrogen
● Oxygen
● Carbon

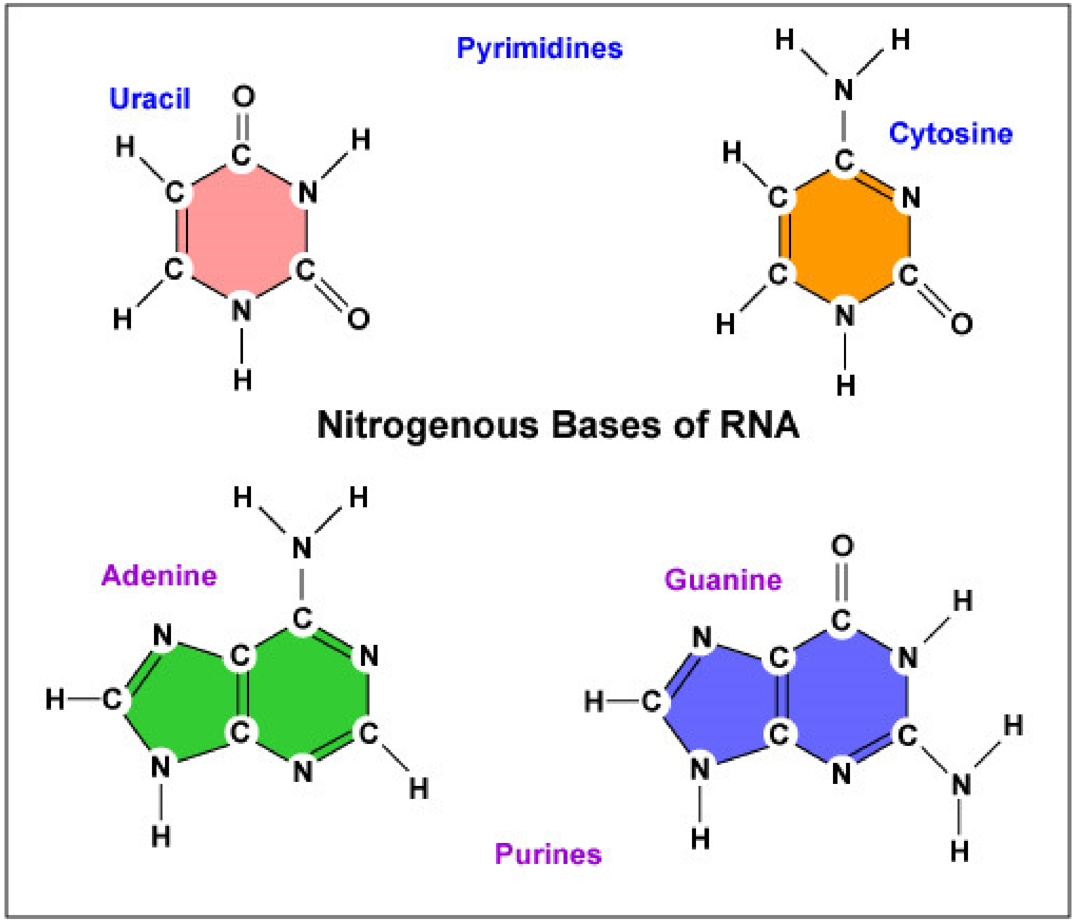

Carbohydrates

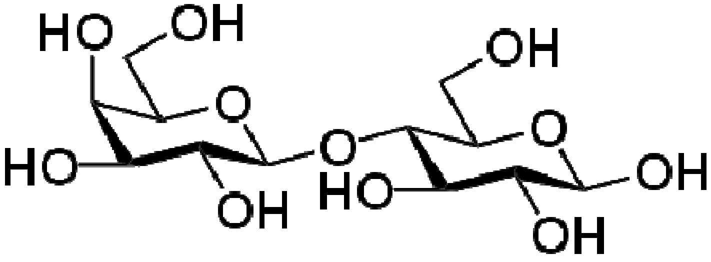

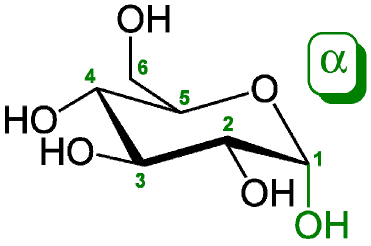

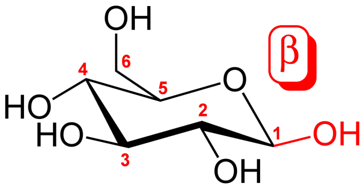

Formose reaction

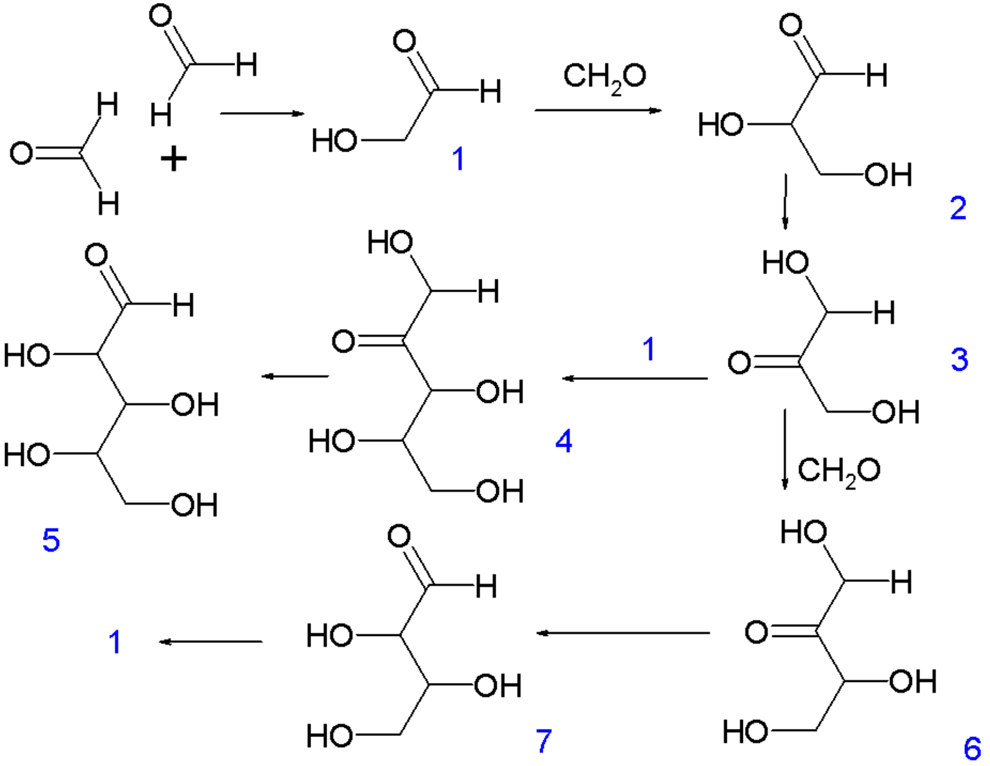

Alexander Butlerov (1828-1886)
St. Petersburg, Kazan, Russia

Ronald Breslow (1931-)
Columbia University, USA

The reaction begins with two formaldehyde molecules condensing to make glycolaldehyde **1** which further reacts in an aldol reaction with another equivalent of formaldehyde to make glyceraldehyde **2**. An aldose-ketose isomerization of **2** forms dihydroxyacetone **3** which can react with **1** to form ribulose **4**, and through another isomerization ribose **5**. Molecule **3** also can react with formaldehyde to produce tetrulose **6** and then aldoltetrose **7**. Molecule **7** can split into **2** in a retro-aldol reaction.

Formaldehyde condensation

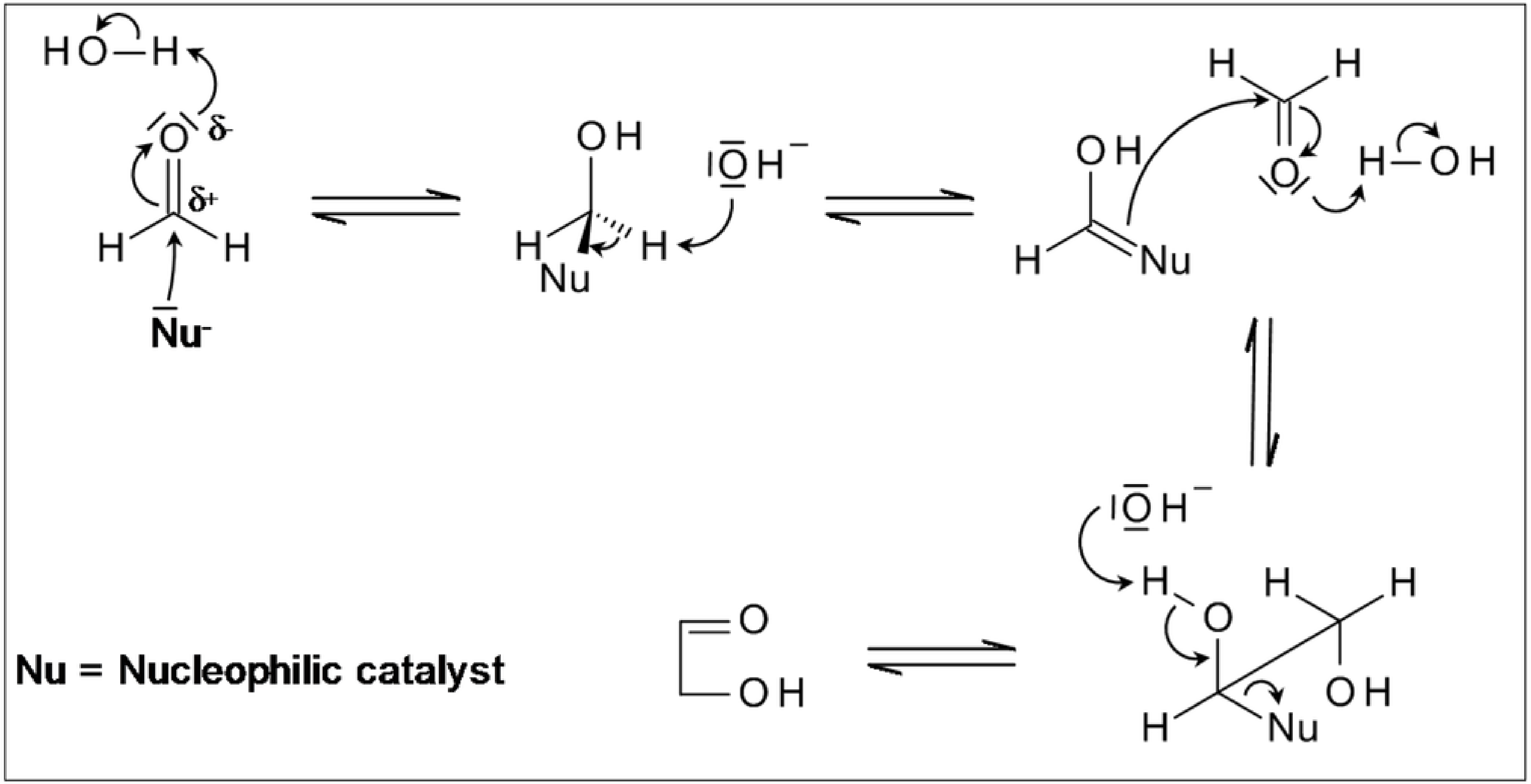

Nu = Nucleophilic catalyst

Aldol reaction

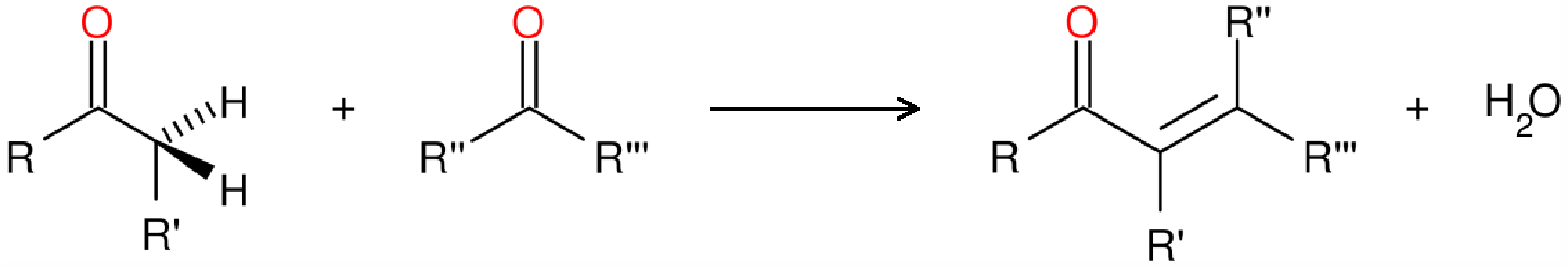

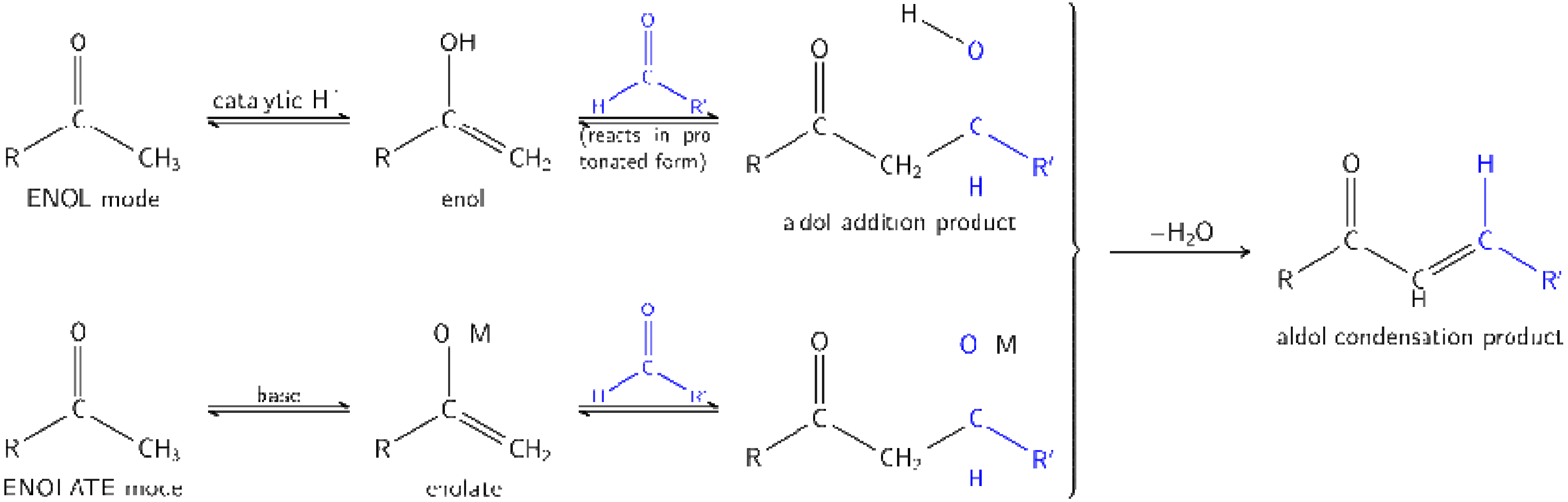

Aldol reaction

Base catalyzed aldol reaction (shown using $^{-}OCH_3$ as base)

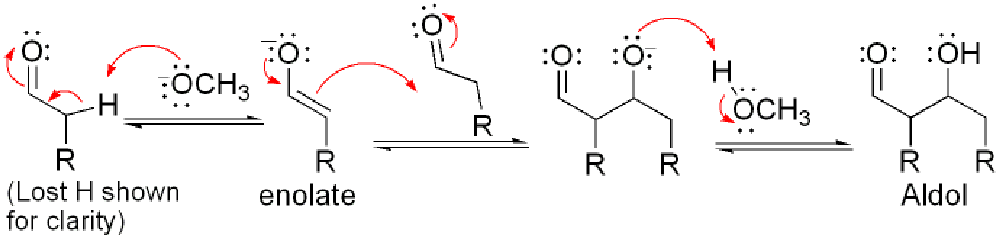

Acid catalyzed aldol reaction

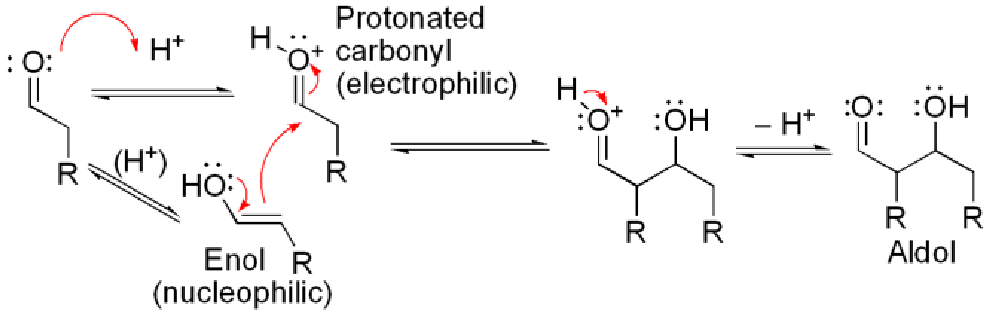

Base catalyzed dehydration (sometimes written as a single step)

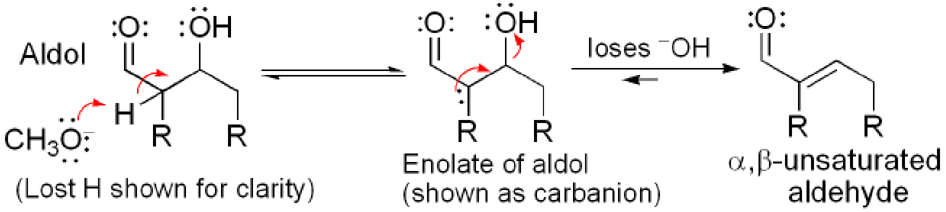

Acid catalyzed dehydration

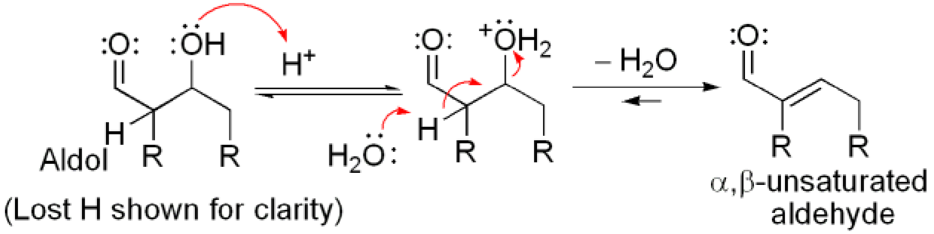

Reversible process

→ retro-aldol reaction

Acid catalyzed aldol reaction

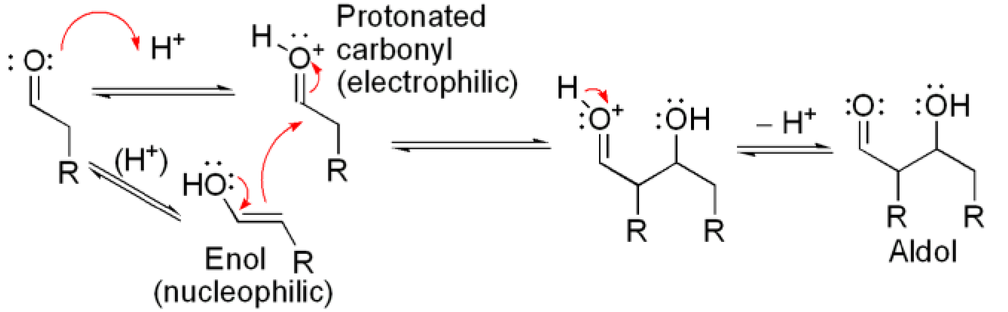

Formose reaction as an autocatalytic process

Formose reaction starts in concentrated alkaline aqueous solutions of formaldehyde
alkali are typically calcium, magnesium or lead

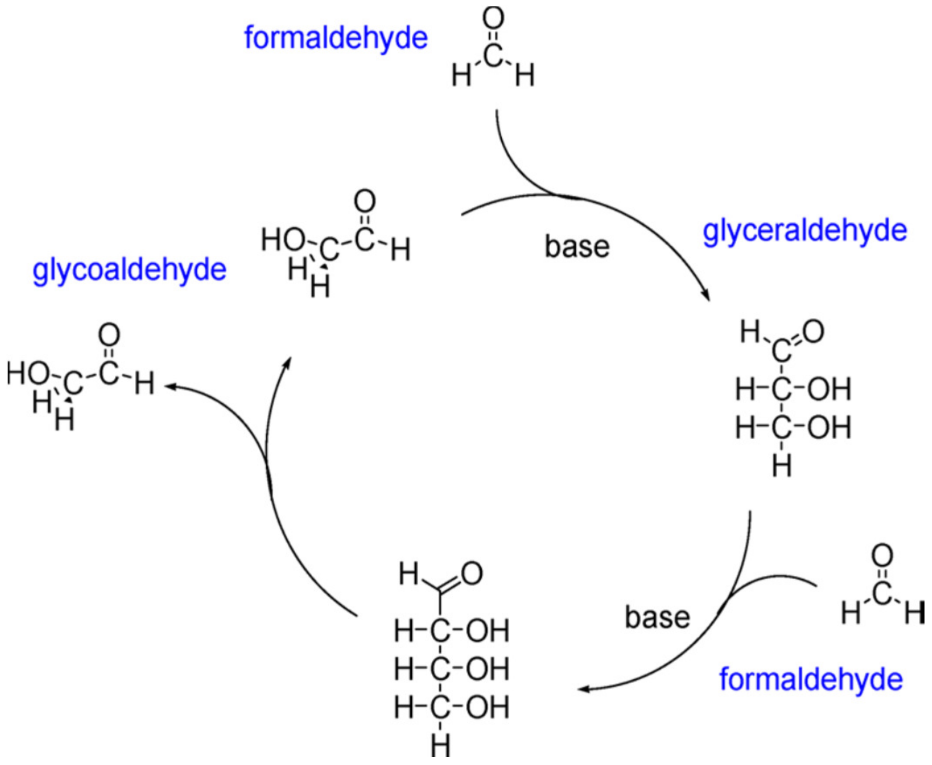

Detailed conditions for the formose reaction

Formose reaction starts in concentrated alkaline aqueous solutions of formaldehyde alkali are typically calcium, magnesium or lead

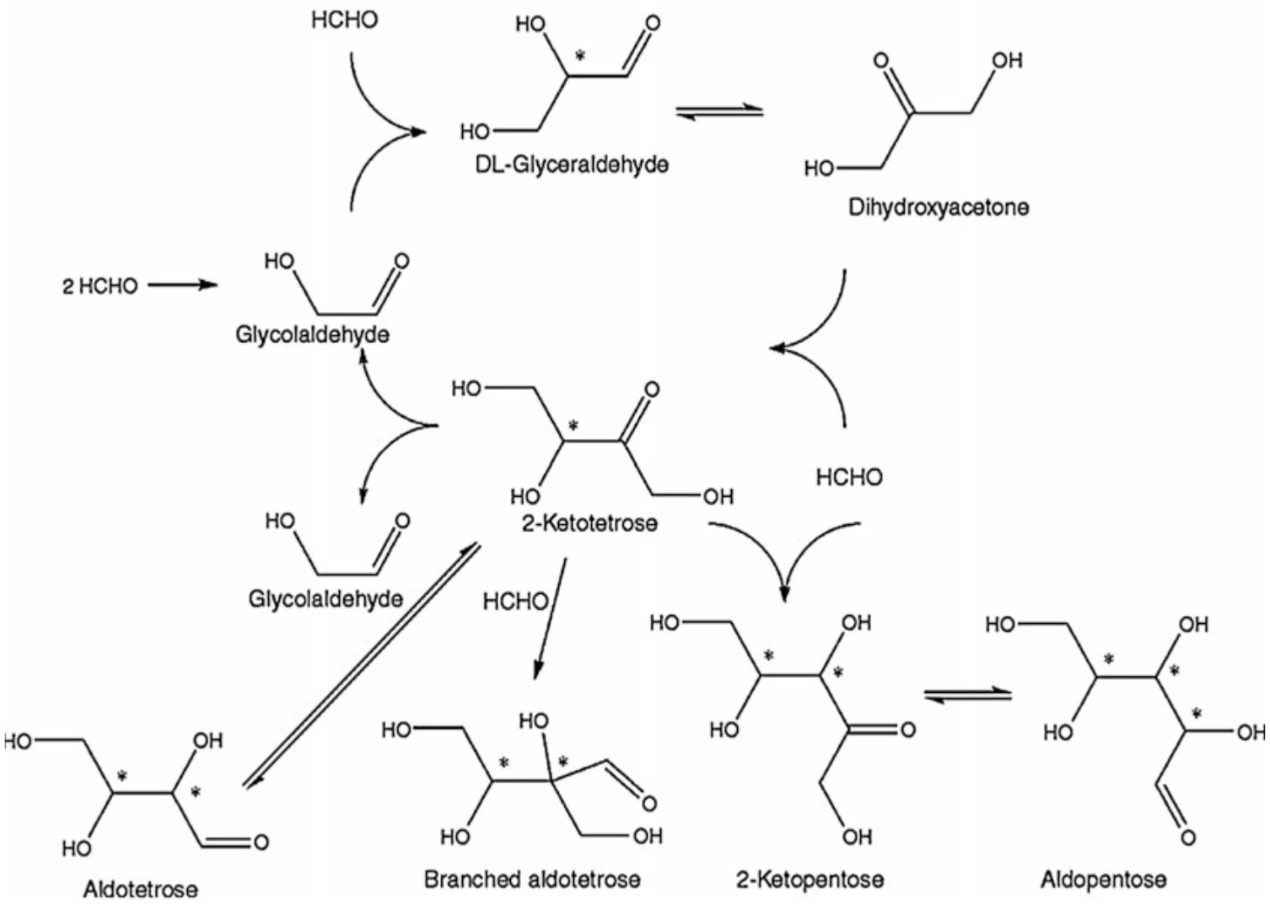

Aldose-ketose isomerization

Lobry de Bruyn(–Alberda)-van Ekenstein transformation

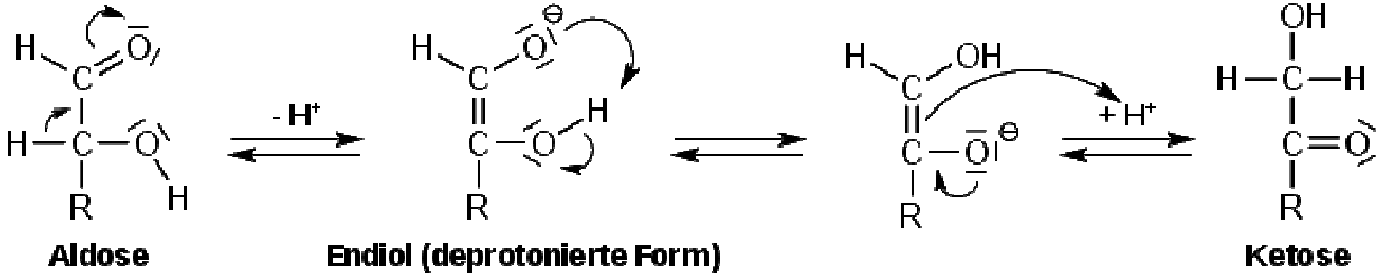

Formose reaction – substrate modifications

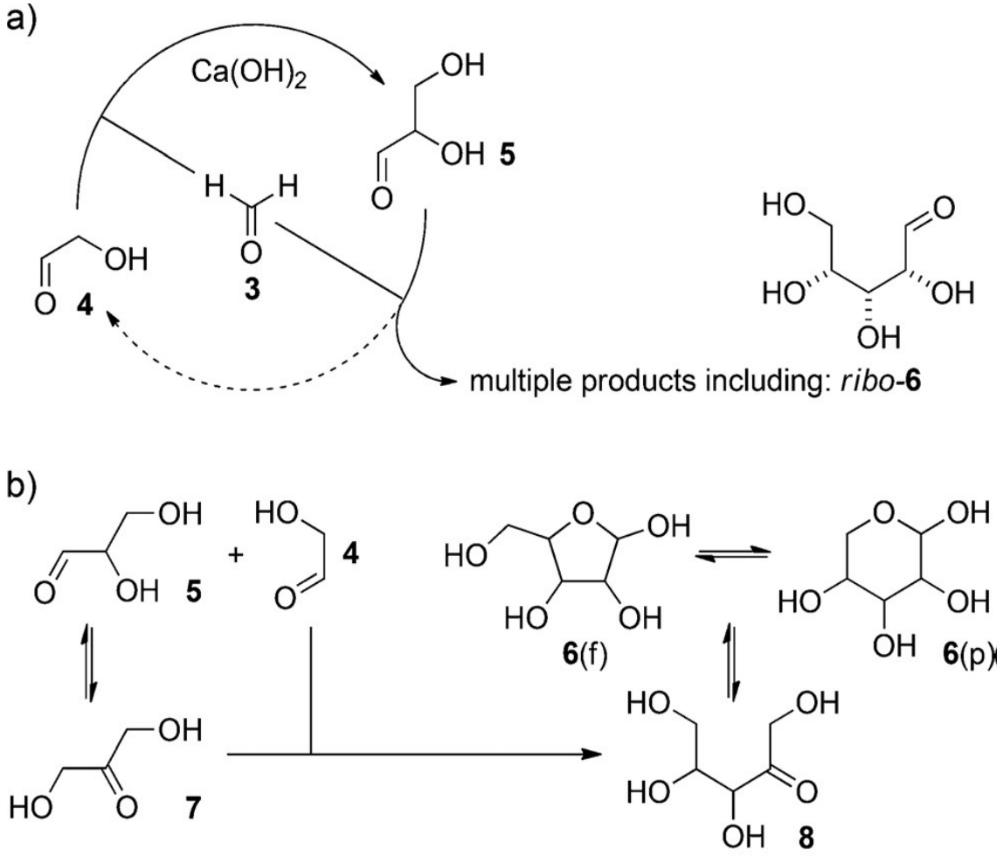

Formose reaction – substrate modifications

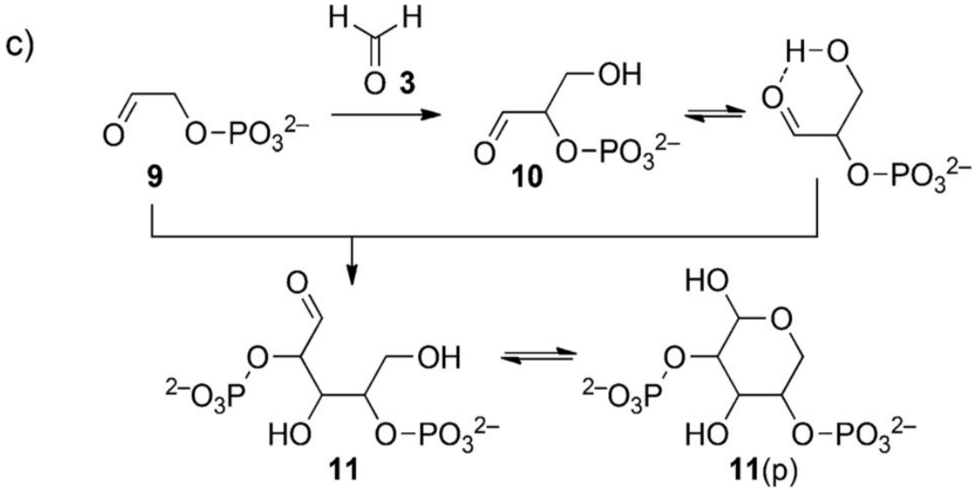

Formose reaction under standard basic catalysis

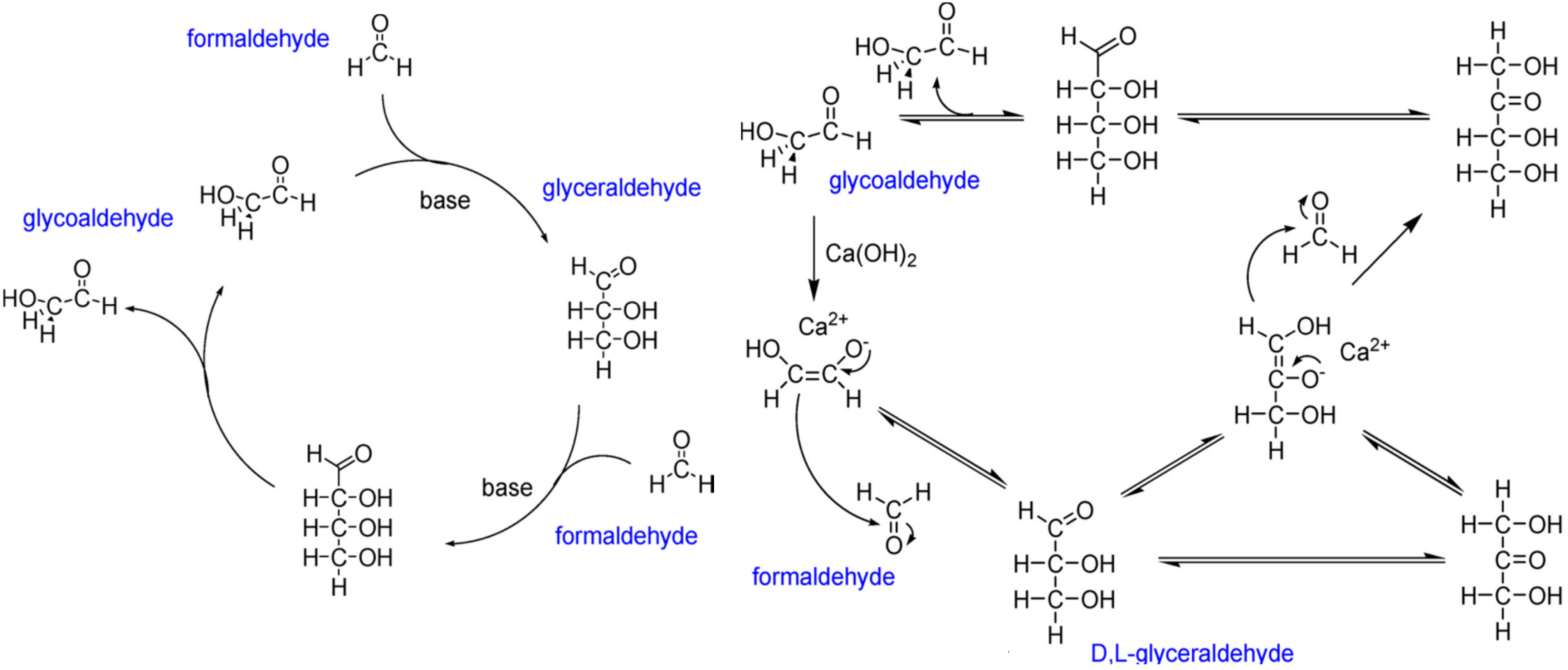

Escosura

Formose reaction in presence of borates

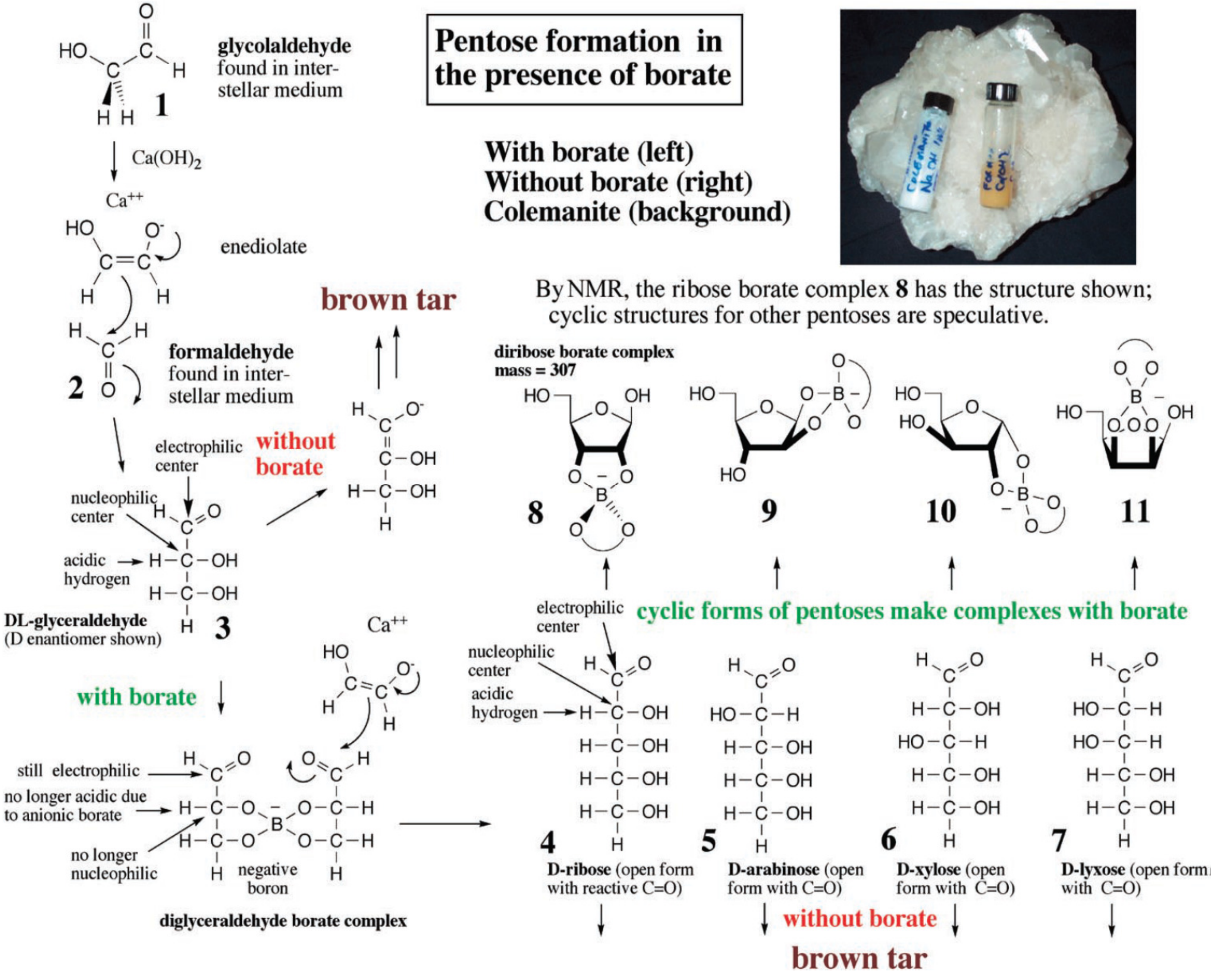

Pentose formation in the presence of borate

With borate (left)
Without borate (right)
Colemanite (background)

By NMR, the ribose borate complex **8** has the structure shown; cyclic structures for other pentoses are speculative.

A. Ricardo, M. A. Carrigan, A. N. Olcott, S. A. Benner *Science* **2004**, *303*, 196

Formose reaction in presence of borates

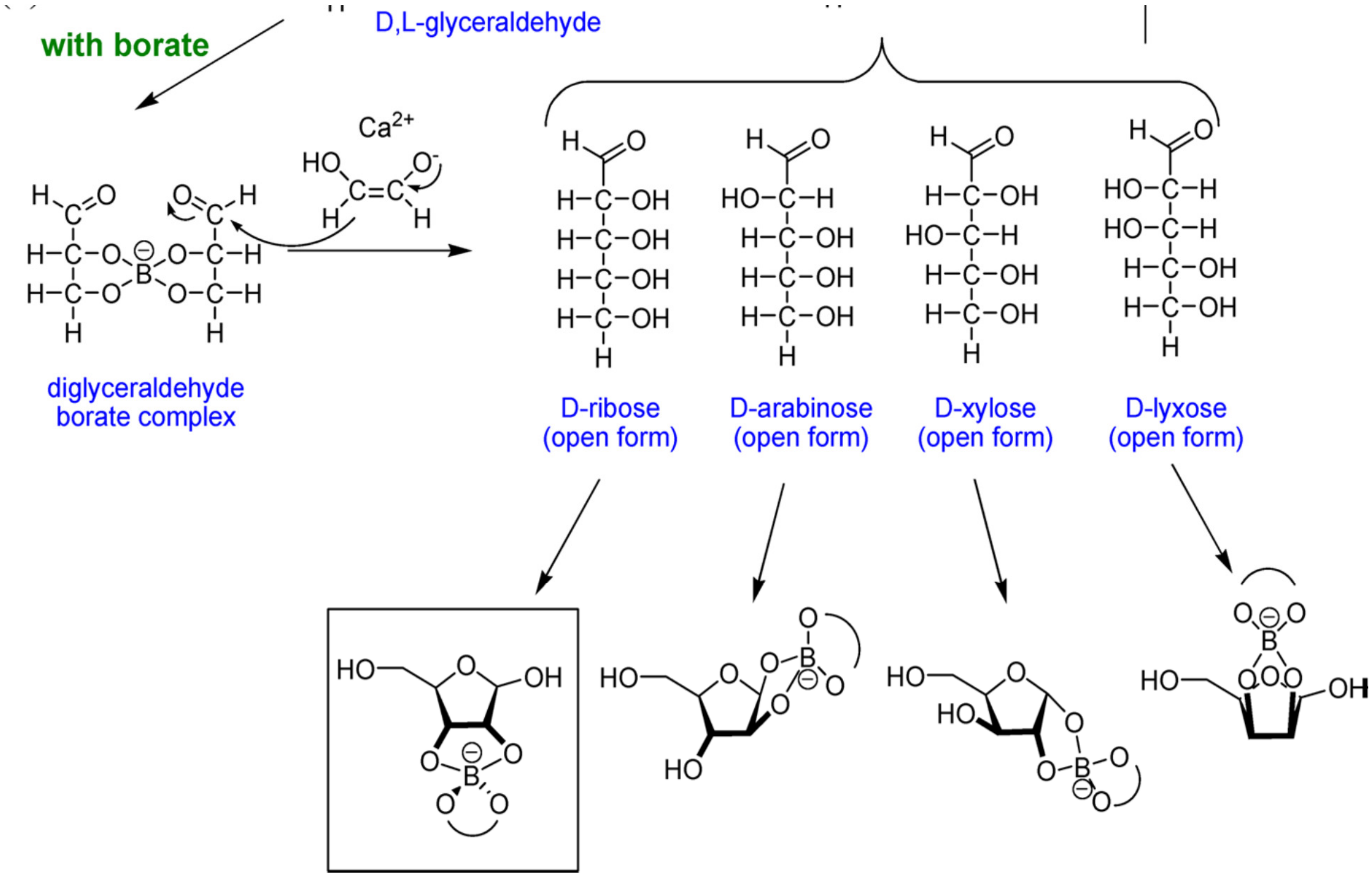

Escosura

Interstellar origin of carbohydrates

Simulations of photo- and thermochemistry of interstellar ice (silicate/carbon grains surrounded by ice H_2O, CH_3OH and NH_3) exposed on UV light, low pressure (10^{-7} bar) and temperature (78K) delivers a mixture of sugars

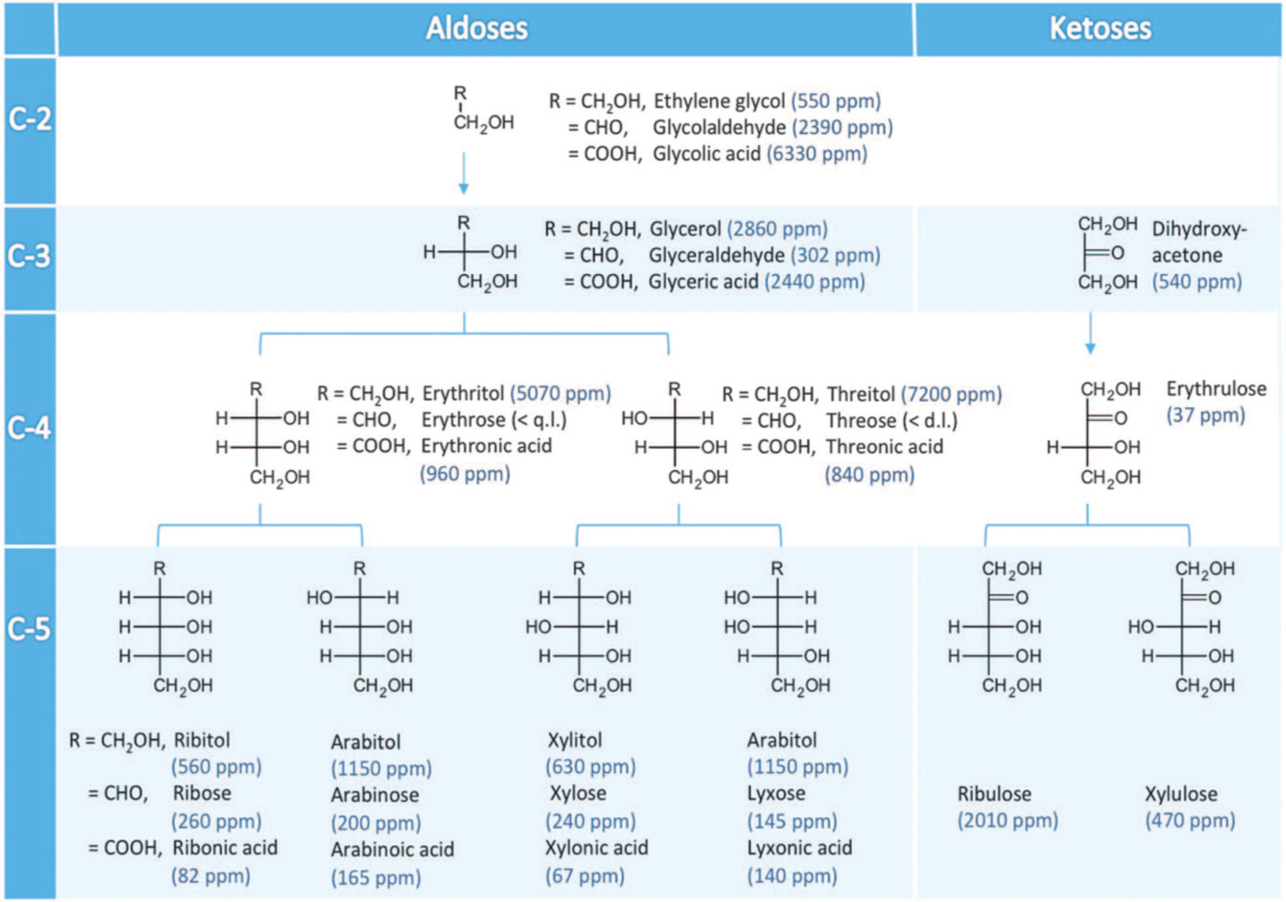

U. Meierhenrich, *et al. Science* **2016**, *352(6282)*, 208-212

Interstellar origin of carbohydrates

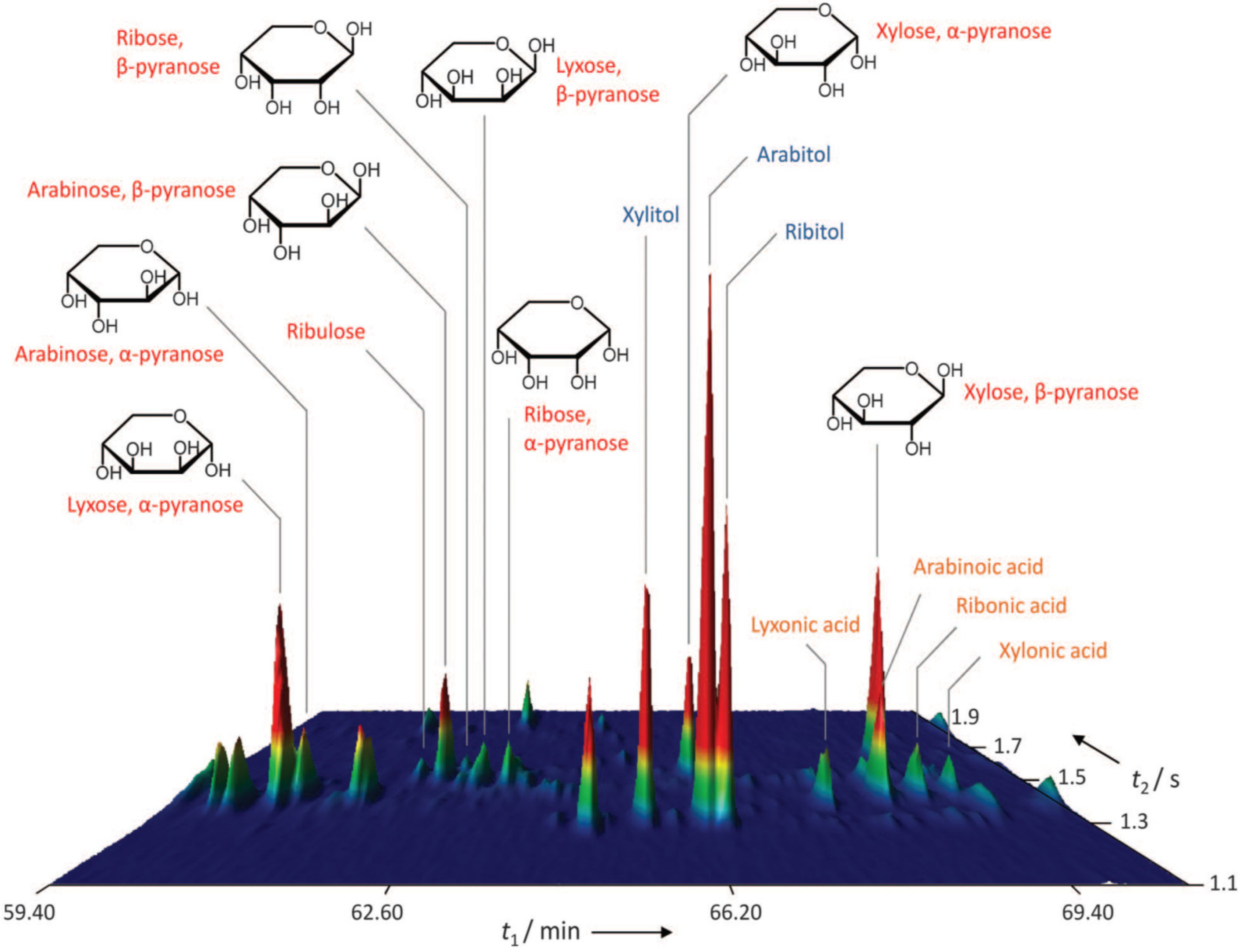

U. Meierhenrich, *et al. Science* **2016**, *352(6282)*, 208-212

Prebiotically plausible alternatives to formose process

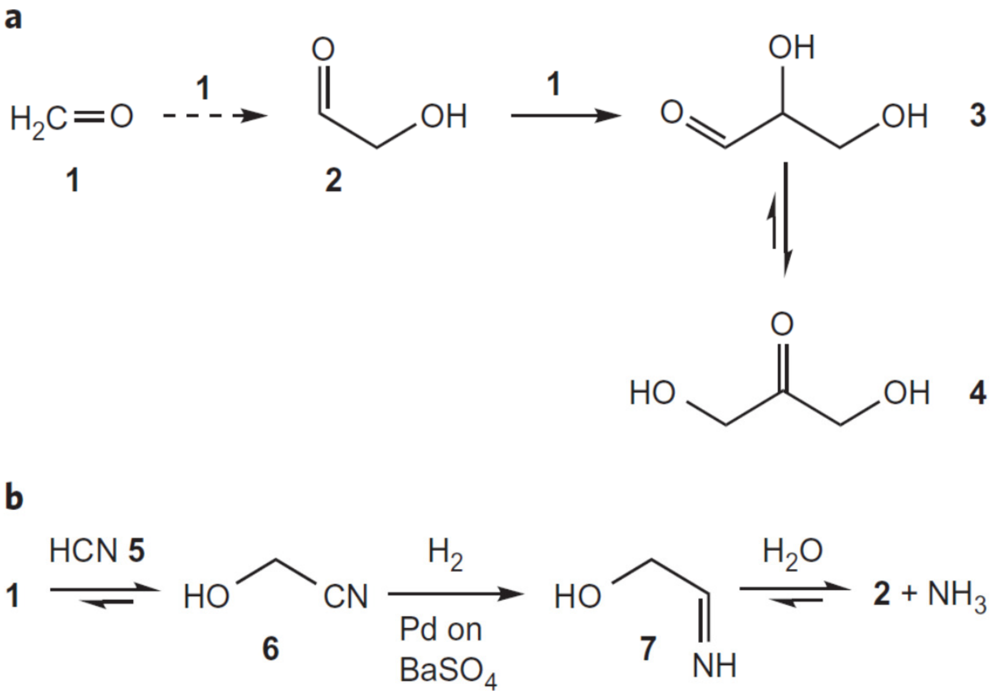

Homologation routes to simple sugars from formaldehyde **1**.
a, Direct homologation of formaldehyde **1** is problematic, because the first dimerization step (dashed) requires umpolung, and because the trimer is more stable as the ketose **4** than the aldose **3** under conditions where **3** can be formed from **1** and **2**. b, Kiliani–Fischer homologation of **1** in conventional synthetic chemistry involves favourable formation of the cyanohydrin **6** by reaction of **1** with hydrogen cyanide **5**, followed by the selective reduction of **6** using very specific conditions.

Kiliani-Fischer homologation

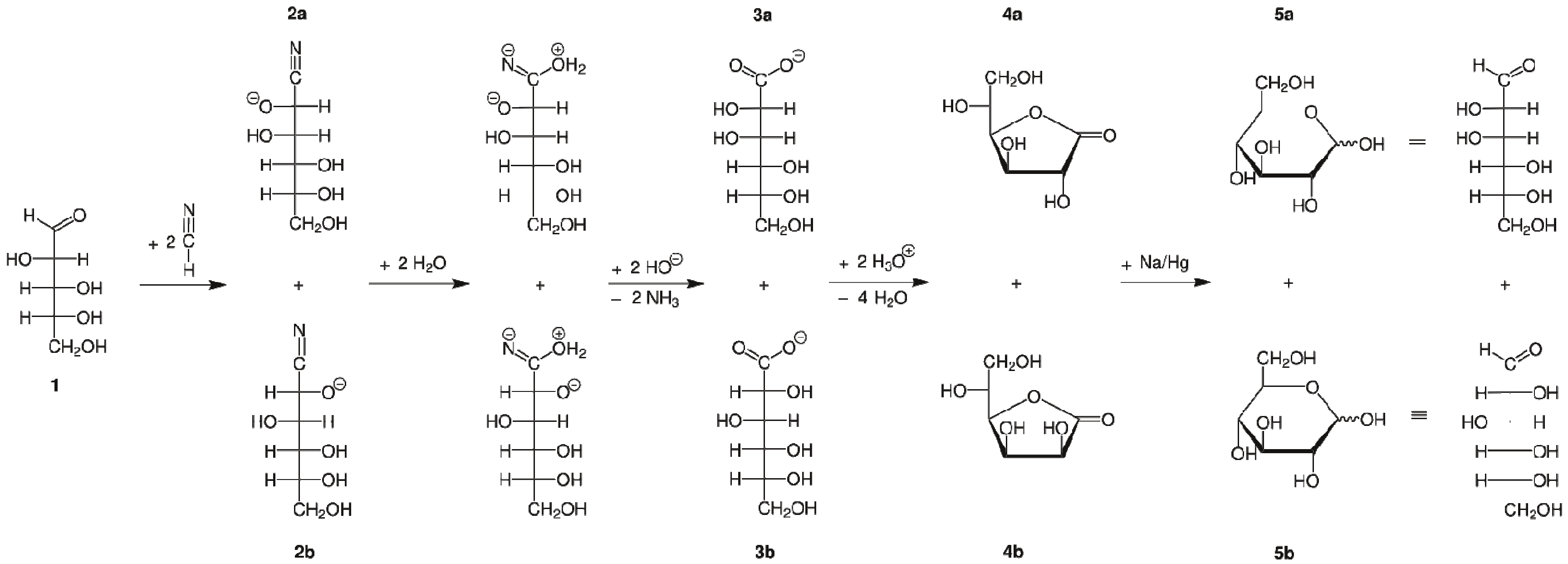

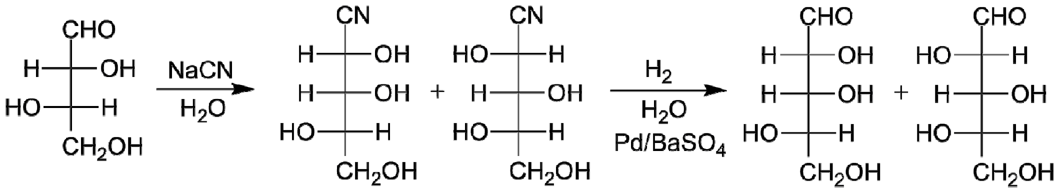

Cyanosulfidic chemistry for the Kiliani-Fischer homologation

$Cu_2S + H_2O + 6CN^- \rightarrow 2[Cu(CN)_3]^{2-} + HS^- + OH^-$

Photoredox cycle based on cyanocuprates may convert HCN into cyanogen

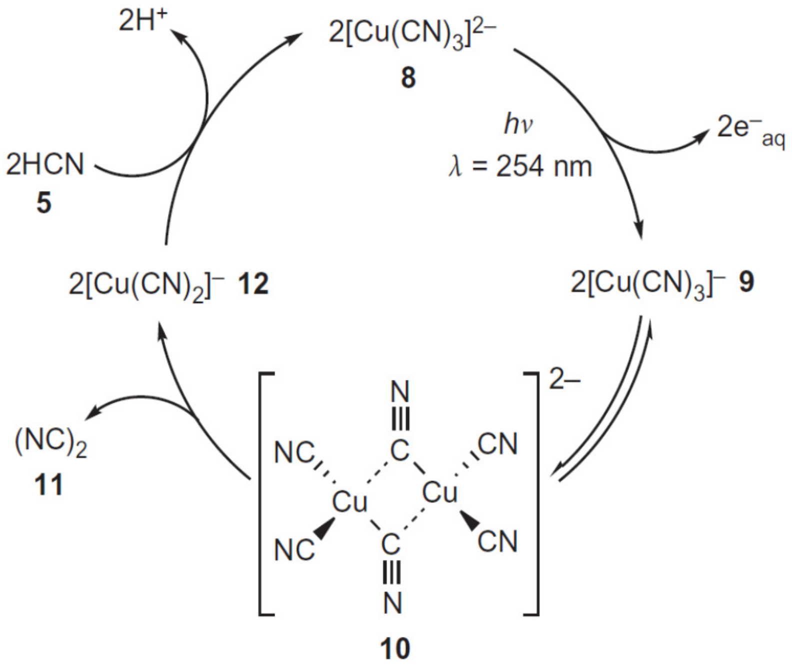

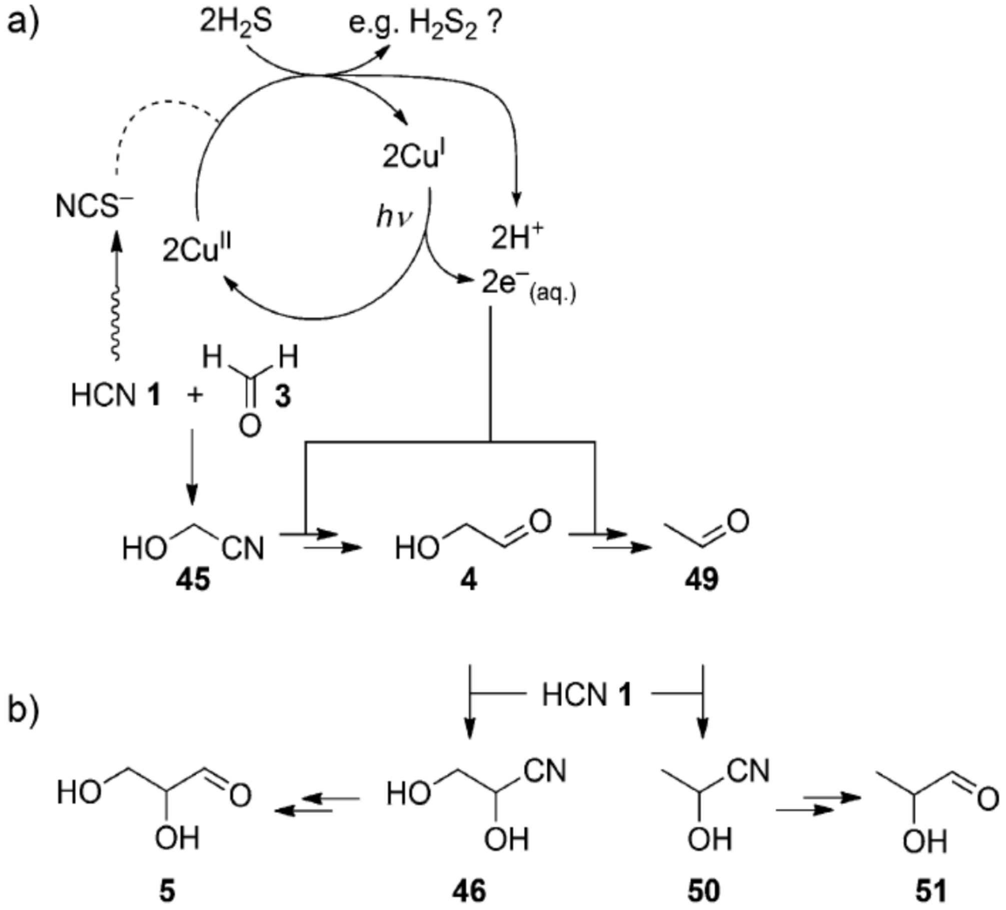

Cyanosulfidic chemistry for the Kiliani-Fischer homologation

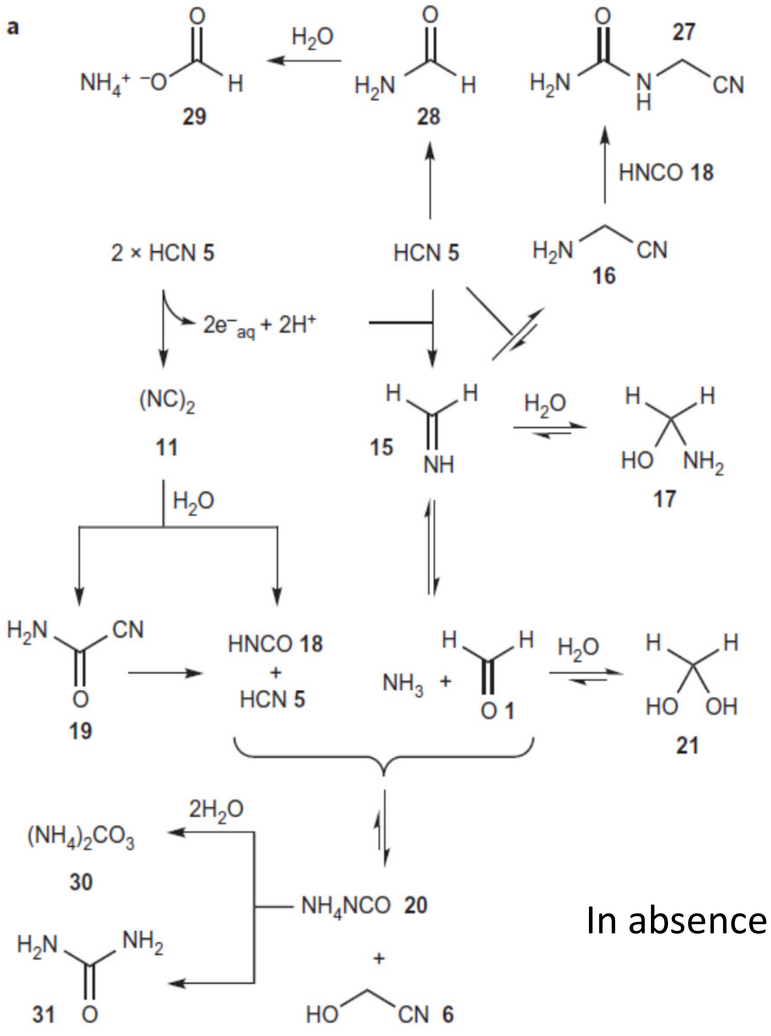

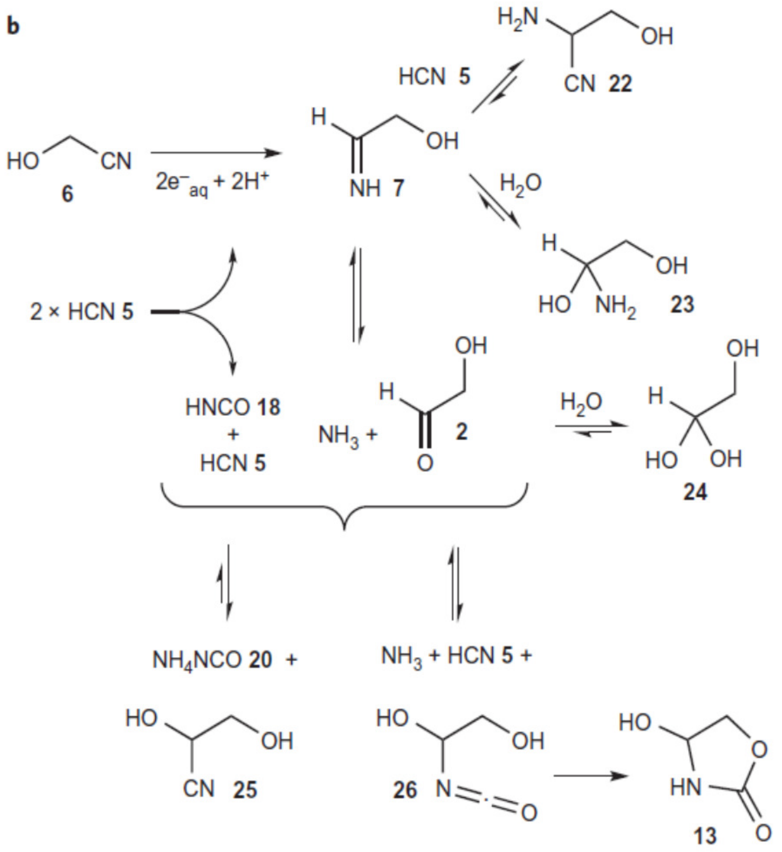

In absence of HS^- glycolaldehyde **2** ends up mainly as a cyclic derivative **13**

Cyanosulfidic chemistry for the Kiliani-Fischer homologation

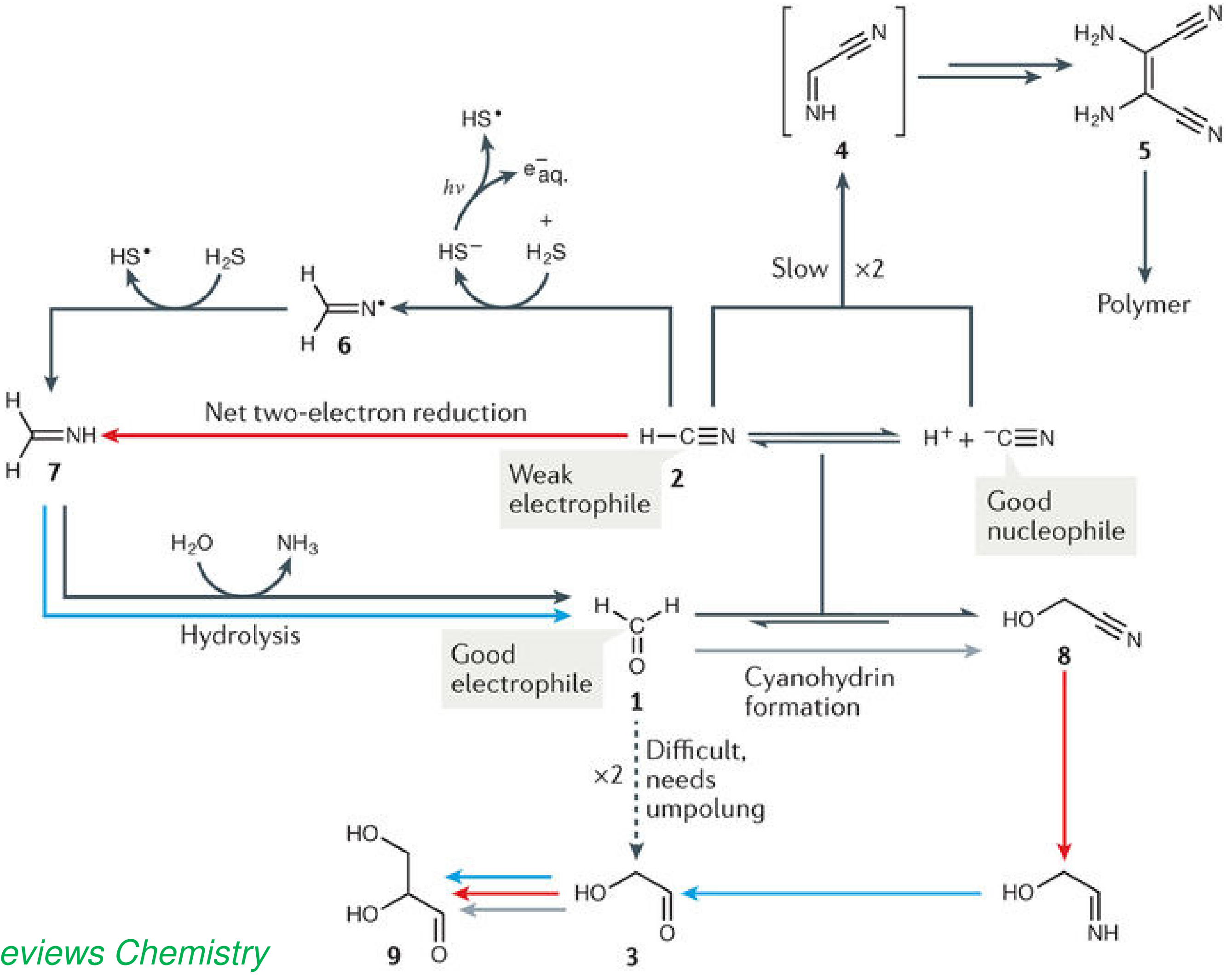

Nature Reviews | **Chemistry**

J. Sutherland, *Nature Reviews Chemistry*
2017, *1*, Article 0012, doi:10.1038/s41570-016-0012

Carbohydrates - summary

Formose reaction gives access to numerous C_2-C_5 and higher carbohydrates, but is difficult to direct towards particular outcome, and ultimately turns into polymeric tar if overcooked

In presence of borates, the formose reaction tends to deliver protected pentoses in high yields and stable form

Although formaldehyde is the simplest starting material, the reaction is autocatalytic in glycolaldehyde and without it long incubation period is required

Carbohydrate synthesis can also occur under simulated extraterrestrial conditions – by UV-light irradiation of cometary ice

Alternative prebiotic synthesis of simple carbohydrates involves Kiliani-Fischer homologation process based on HCN in presence of copper ions and hydrosulfides – all accessible by the meteorite-derived cyanide-metal chemistry

The same type of chemistry can also deliver a set of reactive intermediates like cyanogen, acetylene, ammonia, and activated forms of phosphate – the latest can derivatize sugars and, after redox processes, deliver numerous building blocks present in currently known metabolic cycles

Nucleotide polymerization

Regioselective formation of 3’-5’ phosphodiester bonds between nucleotides

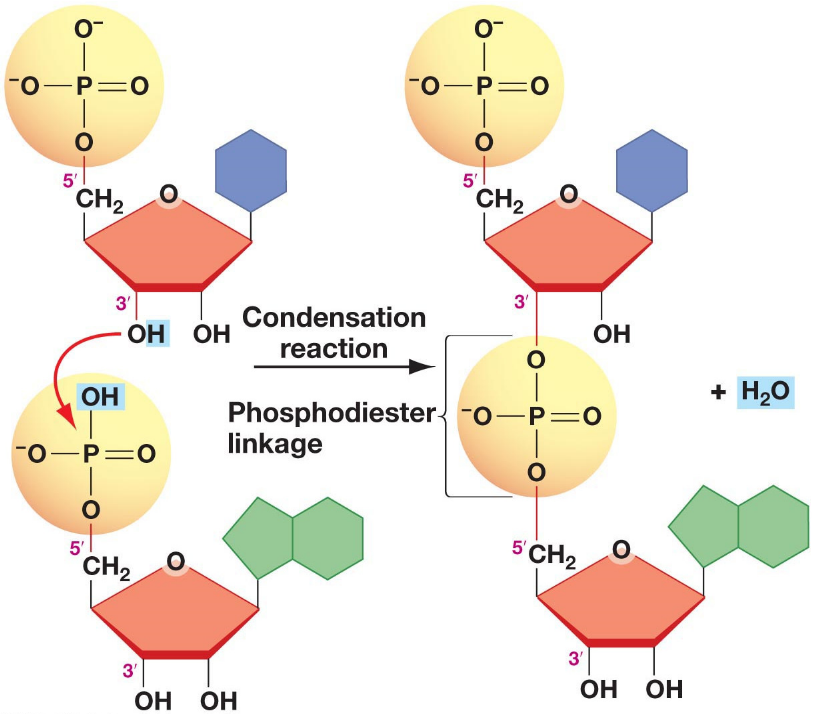

RNA oligomers – prebiotic disconnections

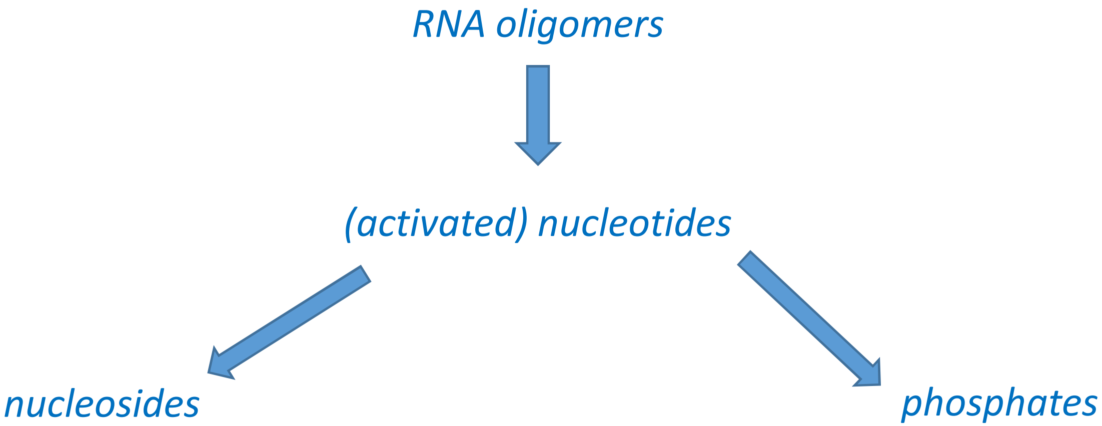
RNA oligomers

(activated) nucleotides

nucleosides

phosphates

Nucleosides - nucleobases + sugars

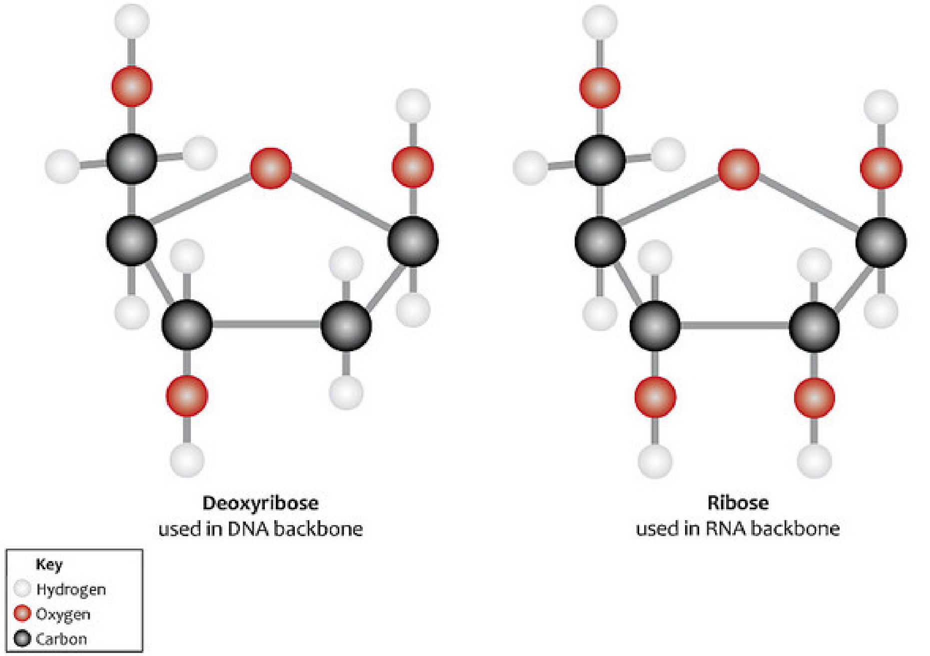

Deoxyribose
used in DNA backbone

Ribose
used in RNA backbone

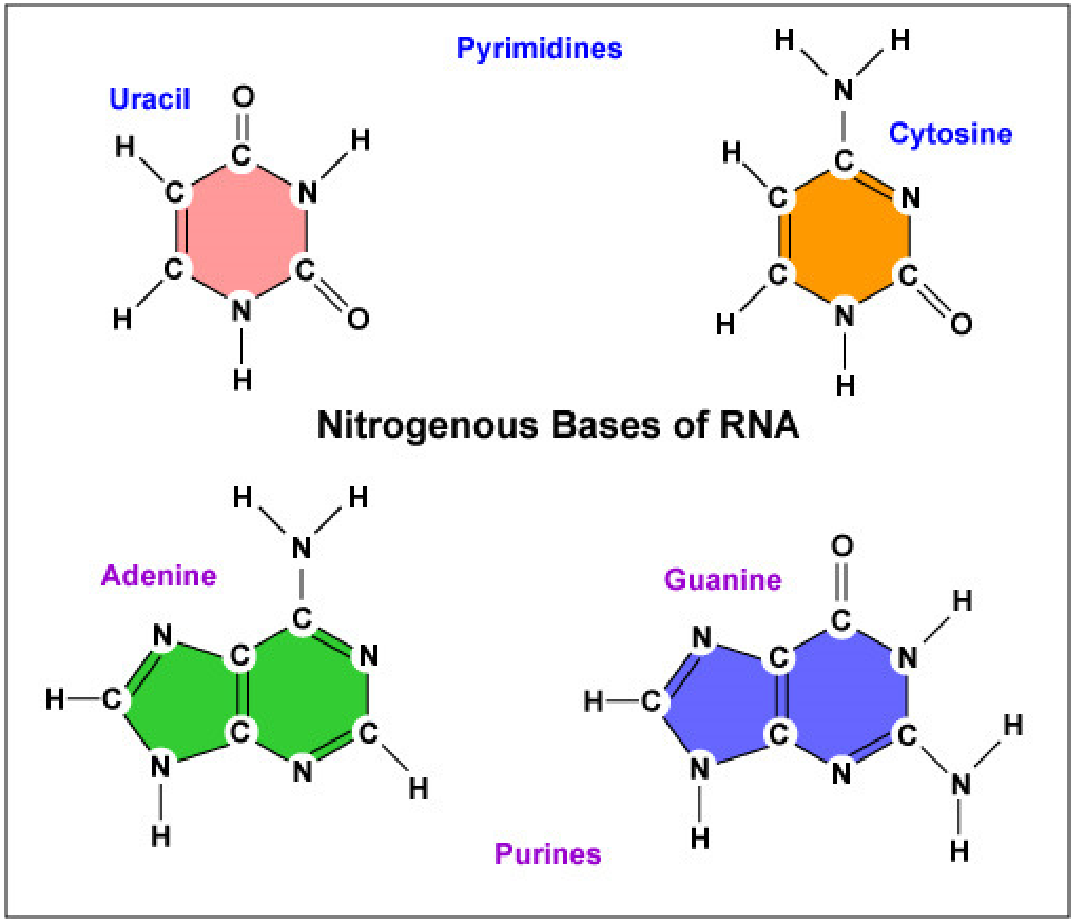

Since 1950's – assumed separate synthesis of sugars and nucleobases, followed by regio- and diastereoselective glycosidation → monomeric nucleosides

RNA oligomers – prebiotic disconnections

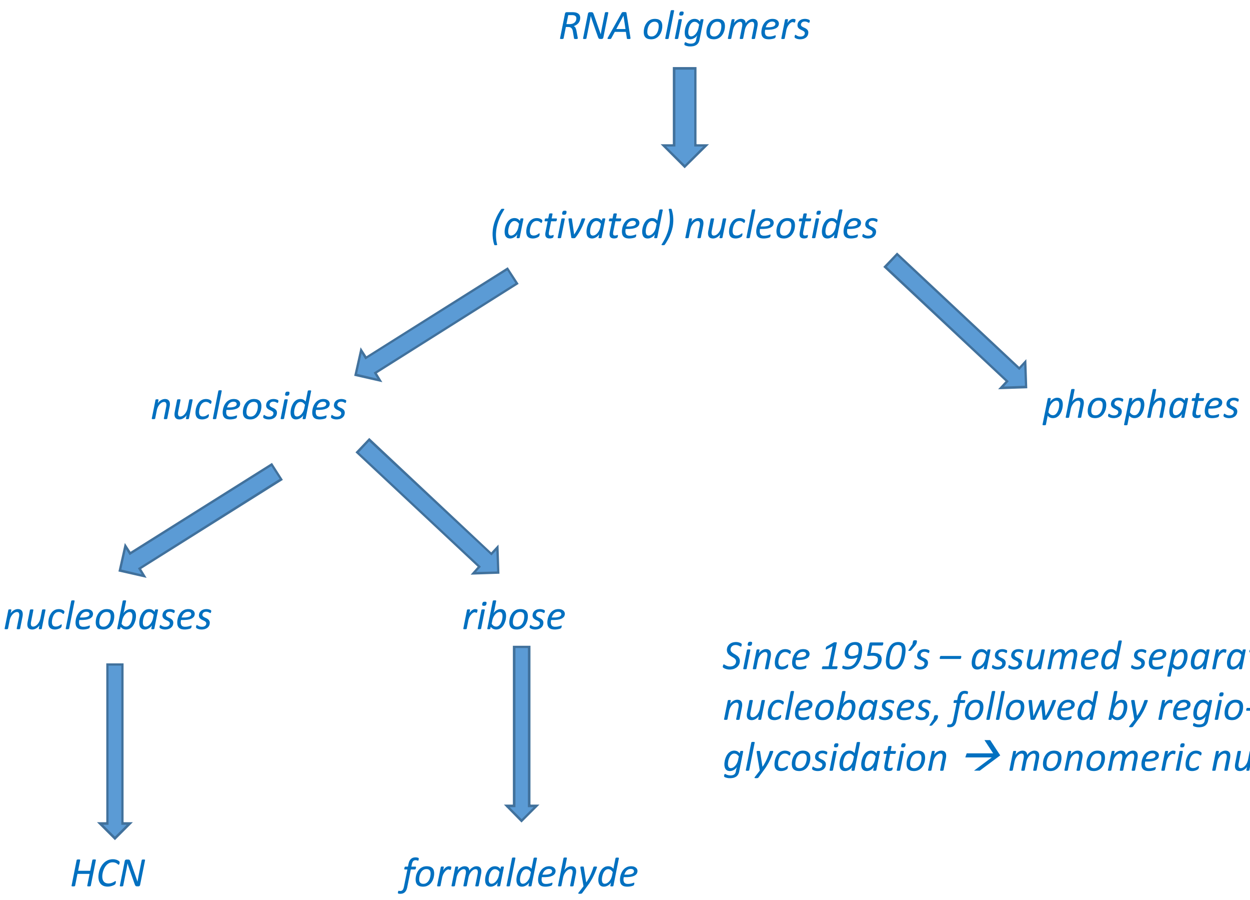

RNA oligomers

(activated) nucleotides

nucleosides

phosphates

nucleobases

ribose

HCN

formaldehyde

Since 1950's – assumed separate synthesis of sugars and nucleobases, followed by regio- and diastereoselective glycosidation → monomeric nucleotides

Literature sources

J. Oro, *Biochem. Biophys. Res. Commun.* **1960**, *2*, 407–412.

J. D. Sutherland, *Cold Spring Harbor Perspect. Biol.* **2010**, 2, a005439.

M. W. Powner, B. Gerland, J. D. Sutherland, *Nature* **2009**, *459*, 239–242

J. D. Sutherland, *Angew. Chem. Int. Ed.* **2016**, *55*, 104-121.

B. H. Patel, C. Percivalle, D. J. Ritson, C. D. Duffy, J. D. Sutherland, *Nat. Chem*. **2015**, *7*, 301–307.

J. D. Sutherland, *et al. Nat. Chem*. **2013**, *5*, 383–389.

L. E. Orgel, *Crit. Rev. Biochem. Mol. Biol.* **2004**, *39*, 99-123.

Powner, M. W.; Sutherland, J. D.; Szostak, J. W. *J. Am. Chem. Soc.* **2010**, *132*, 16677

T. Carell, *Nature* **2016**, *352(6287)*, 833-836

Prebiotic synthesis of nucleobases

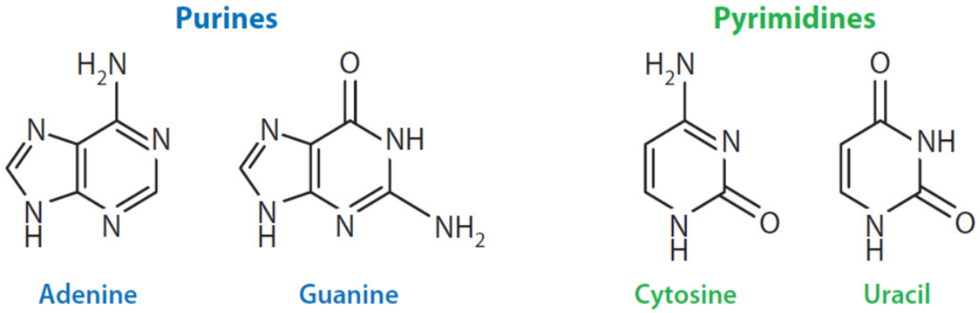

Prebiotic synthesis of adenine – the pentamer of HCN!

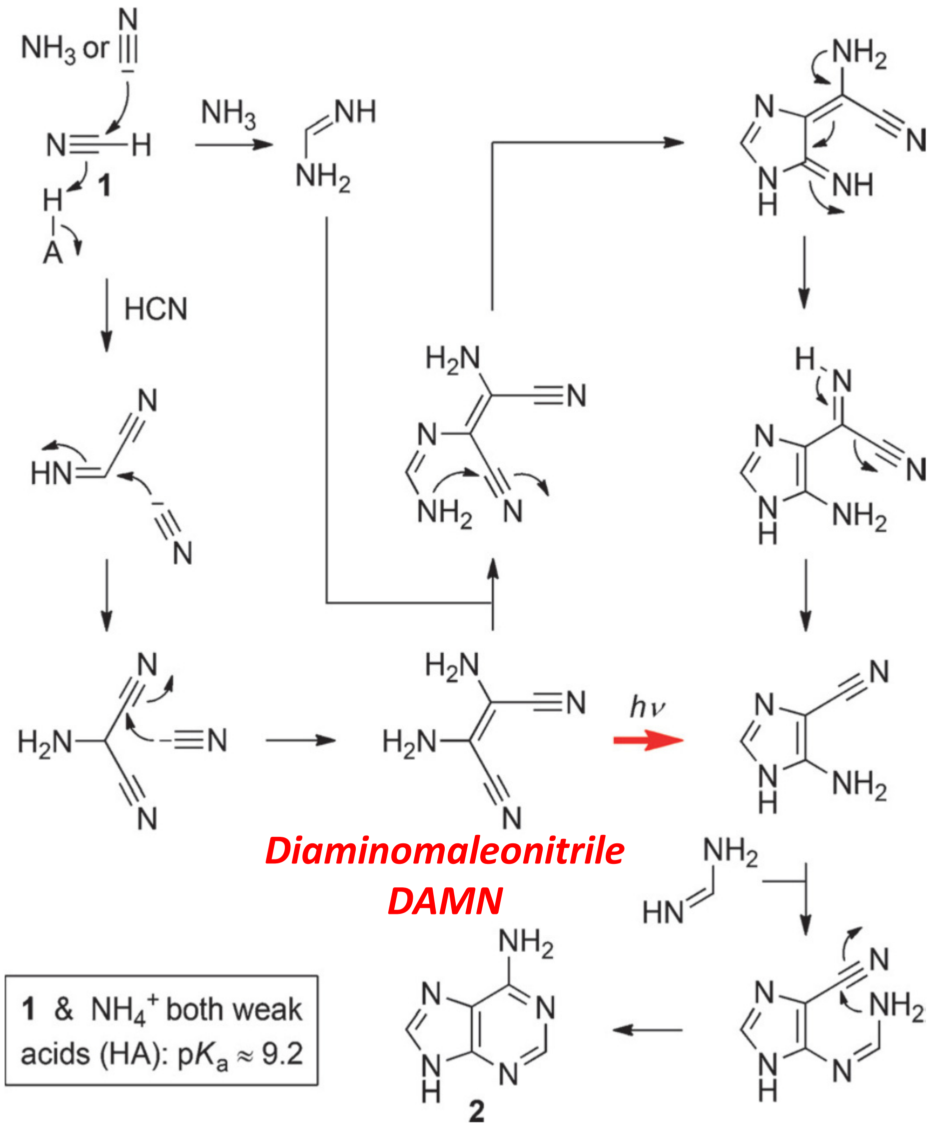

Diaminomaleonitrile DAMN

1960 - Oró's synthesis of adenine **2** from hydrogen cyanide **1** and ammonia (general acid–base catalysis, presumed to operate in most steps, is only shown once).

Heating ammonium cyanide at 70°C for a few days
→ 0.5% adenine

Heating HCN with liquid ammonia in a sealed tube → 20% adenine

The photochemical shortcut discovered by Ferris and Orgel is shown by the red arrow.

Optimized yields – up to 20% for adenine, 3% for guanine

Eutectic freezing (-20°C) increases the yield of DAMN formation by concentrating HCN between pure ice crystals

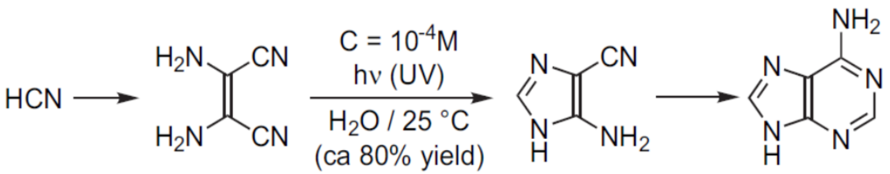

J. Oro *Biochem. Biophys. Res. Commun.* **1960**, *2*, 407.

J. P. Ferris, L. E. Orgel, *J. Am. Chem. Soc.* **1966**, *88*, 1074

Prebiotic synthesis of purines

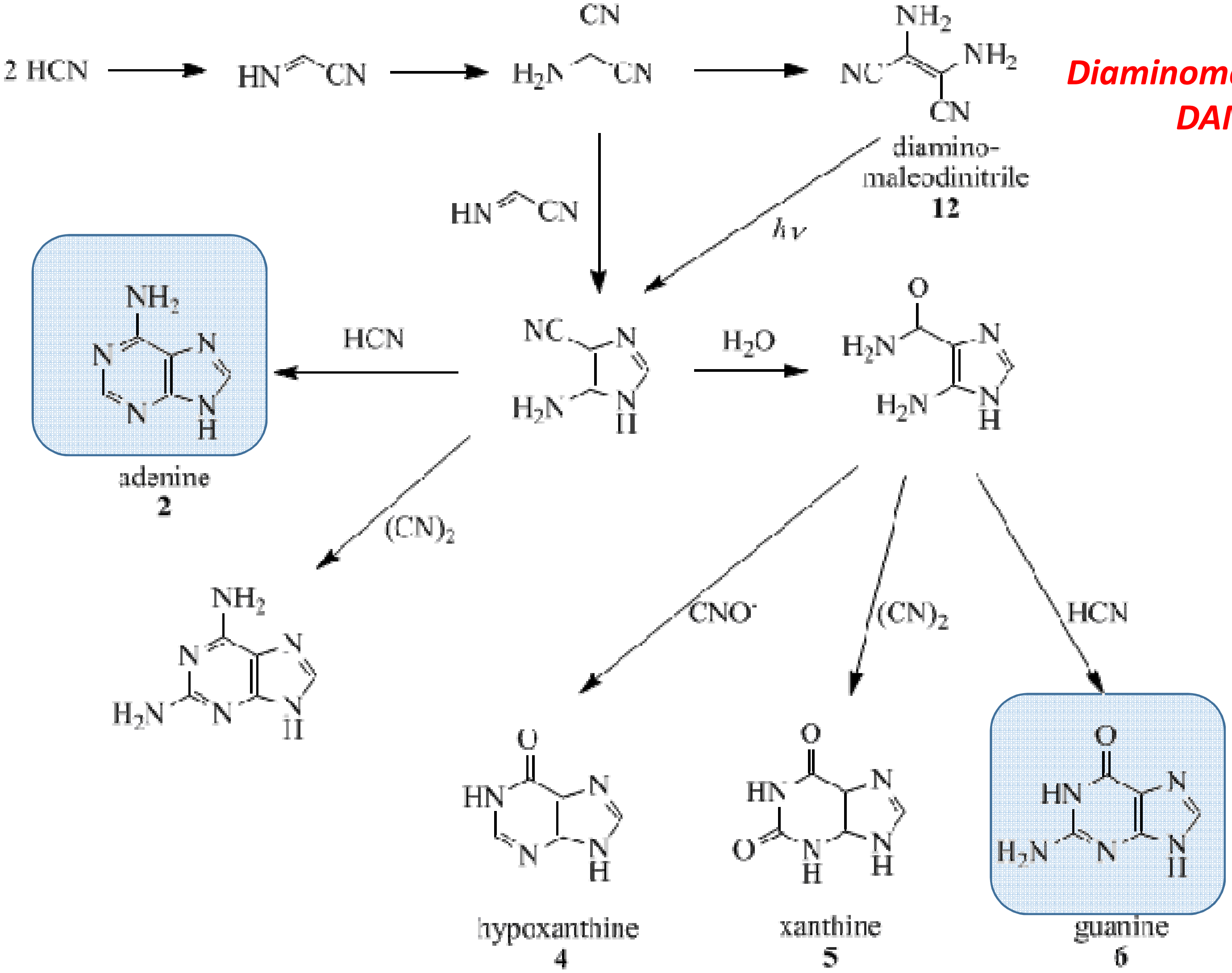

Diaminomaleonitrile
DAMN

Prebiotic synthesis of pyrimidines

Cyanoacetylene is a major product of electric discharges in the mixture of nitrogen and methane

Cyanoacetylene can be hydrolysed to cyanoacetaldehyde. That compound can condense with urea to form cytosine

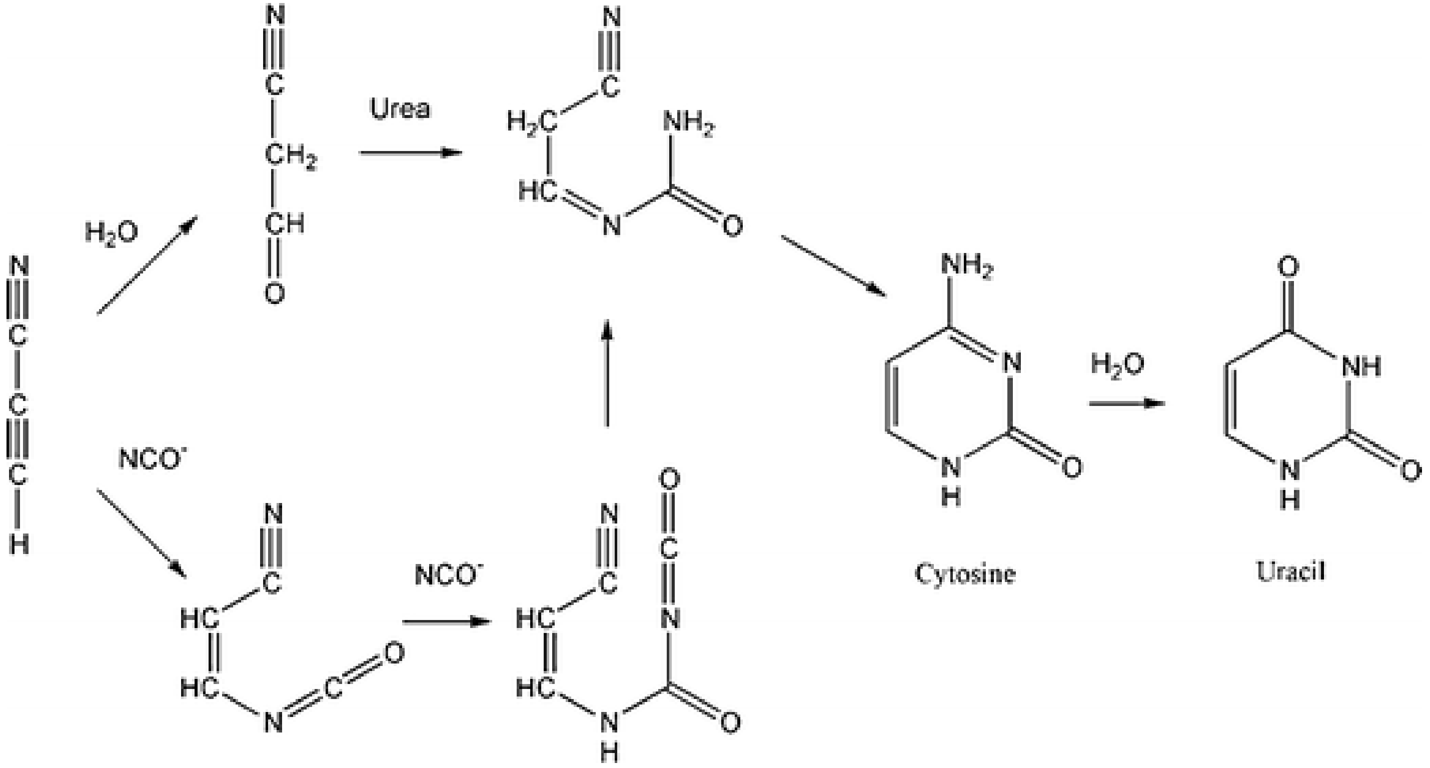

Cyanoacetylene incubated with saturated solution of urea yields up to 50% **cytosine**.
Other methods typically yield up to 5% cytosine.It is further converted to uracil by hydrolysis.

R. Shapiro PNAS **1999**, *96,* 4396-4401

Prebiotic synthesis of nucleosides, nucleotides and RNA

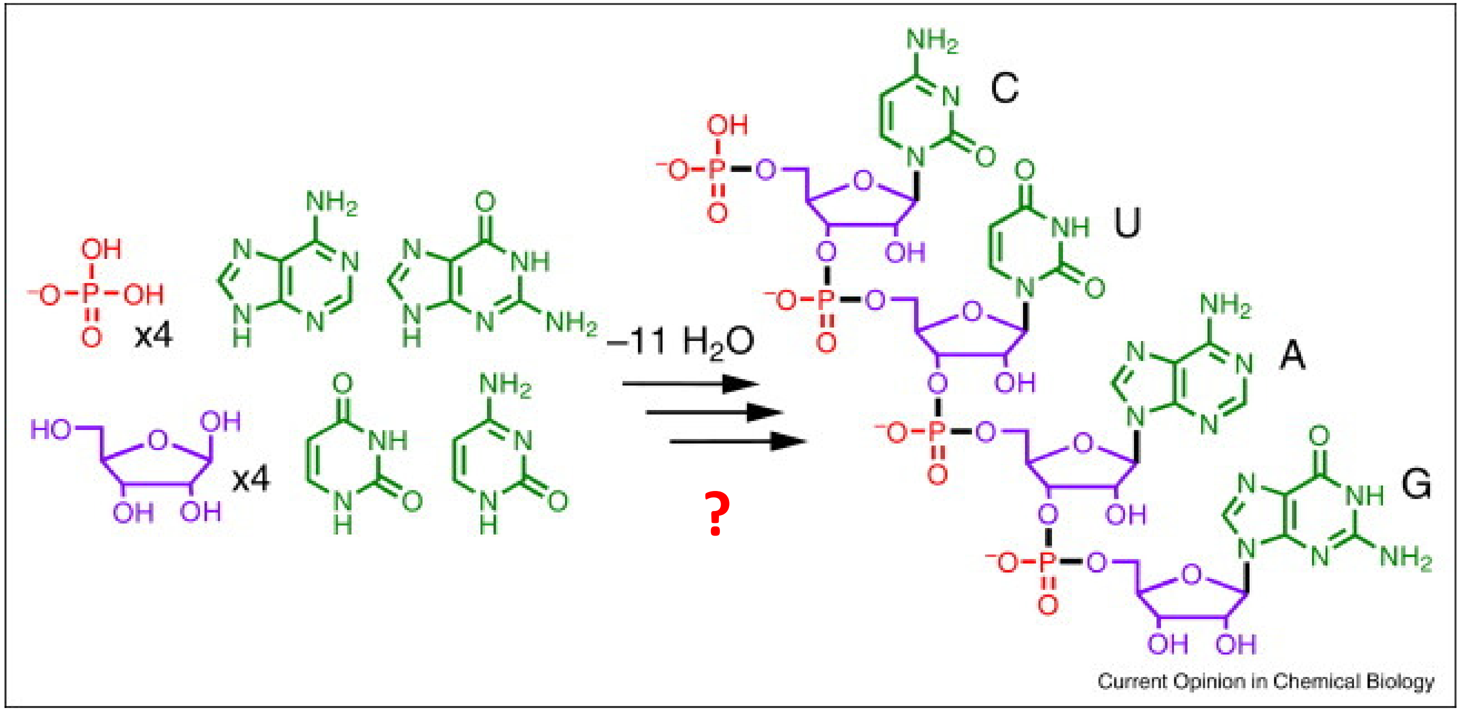

Current Opinion in Chemical Biology

Prebiotic synthesis of nucleosides

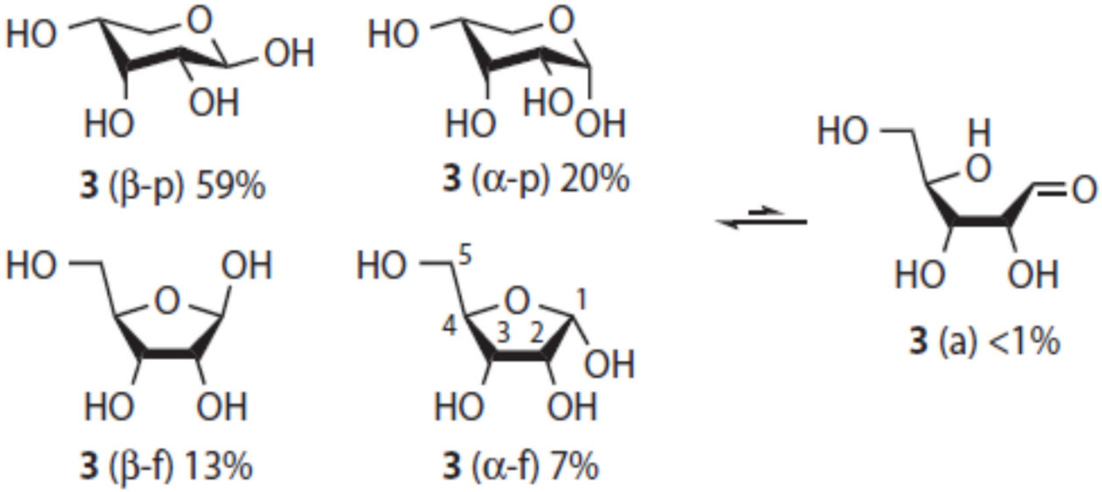

The difficulties of assembling beta-ribonucleosides by nucleobase ribosylation:

The many different forms of ribose **3** adopted in aqueous solution. The pyranose (p) and furanose (f) forms interconvert via the open-chain aldehyde (a), which is also in equilibrium with an open-chain aldehyde hydrate (not shown).

Prebiotic synthesis of nucleosides

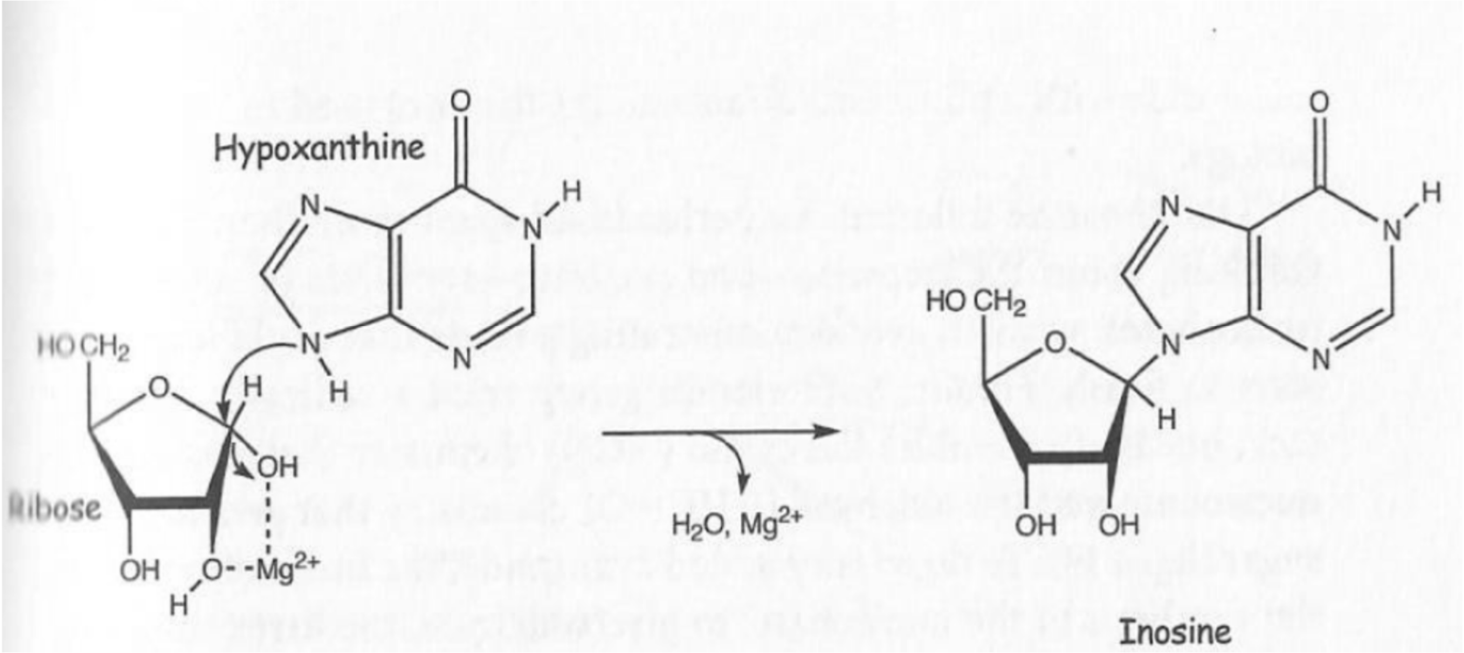

Heating purines with ribose and magnesium salts yields beta-nucleosides, although with low yields
β-inosine – 8%, β-adenosine – 4%, β-guanosine – 9%
Other isomers (e.g. alpha-glycosides) also present.

W. Fuller, R. Sanchez, L. Orgel *J. Mol. Biol.* **1972**, *67, 25-33*

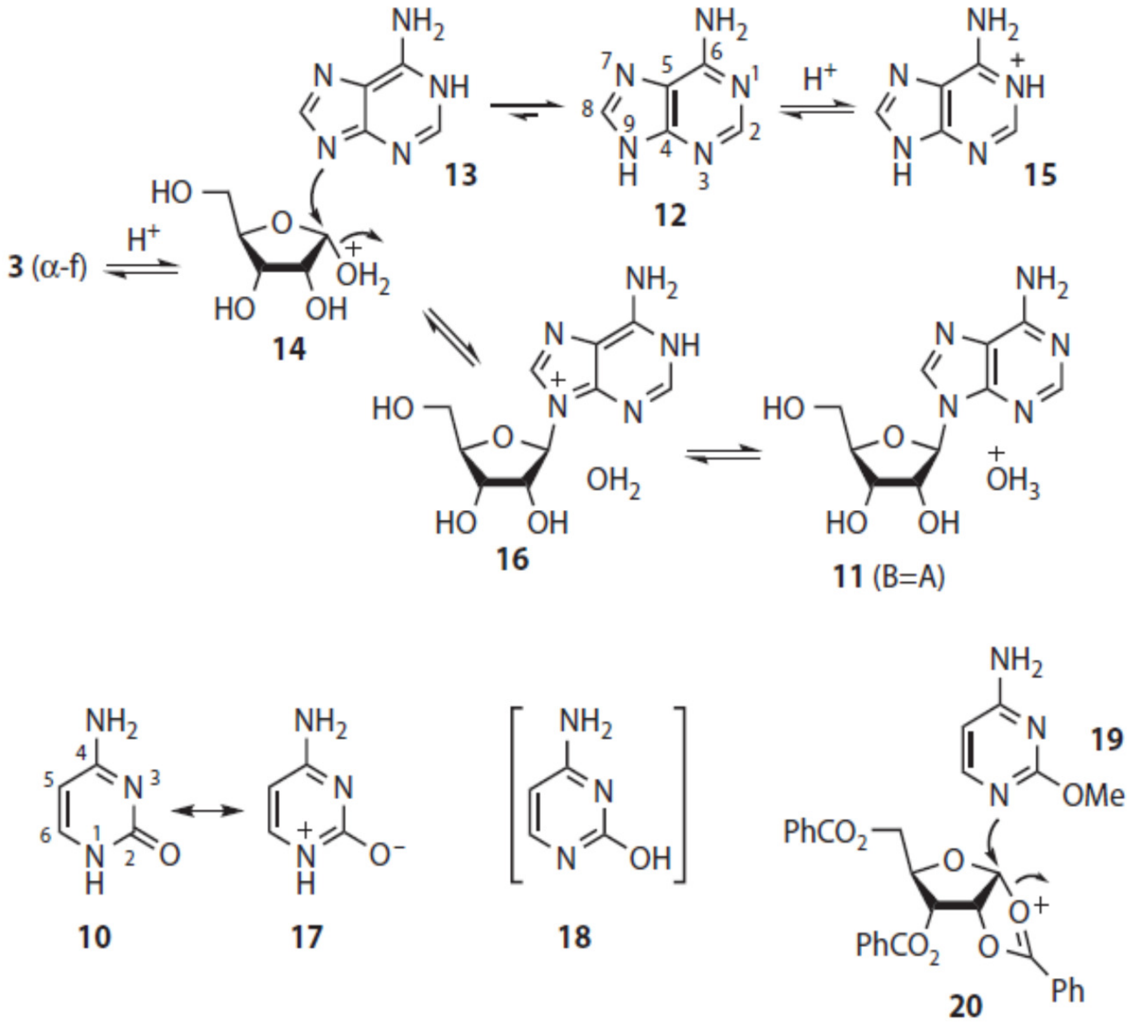

Adenine tautomerism and the ribosylation step necessary to make the adenosine **11** thought to be needed for RNA assembly. The low abundance of the reactive entities **13** and **14** is partly responsible for the low yield of **11**. The reason for the lower nucleophilicity of *N1* of the pyrimidines, and the conventional synthetic chemist's solution to the problems of ribosylation.

Prebiotic synthesis of pyrimidine nucleosides

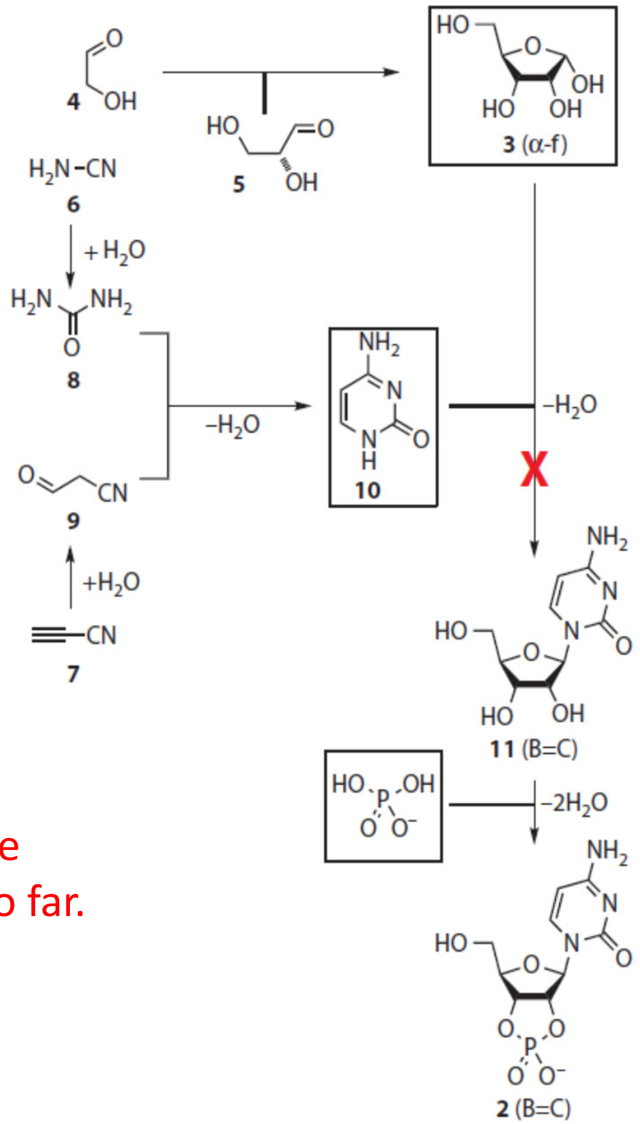

No direct synthesis of pyrimidine nucleosides from ribose reported so far.